CHARACTERIZATION OF MOLECULAR SIEVES BY N-HEXANE CRACKING

BY

ABDULKAREEM MODUPE MELAIYE

A Thesis Presented to the

DEANSHIP OF GRADUATE STUDIES

KING FAHD UNIVERSITY OF PETROLEUM & MINERALS

DHAHRAN, SAUDI ARABIA

In Partial Fulfillment of the
Requirements for the Degree of

MASTER OF SCIENCE

In

CHEMISTRY

DECEMBER 1999

ProQuest Information and Learning Company
300 North Zeeb Road
P.O. Box 1346
Ann Arbor, MI 48106-1346

KING FAHD UNIVERSITY OF PETROLEUM AND MINERALS

Dhahran 31261, SAUDI ARABIA

DEANSHIP OF GRADUATE STUDIES

This thesis, written by **Abdulkareem Modupe Melaiye** under the supervision of his thesis advisor and approved by his Thesis committee, has been presented to and accepted by the Deanship of Graduate Studies, in partial fulfillment of the degree of MASTER OF SCIENCE IN CHEMISTRY.

Thesis Committee

Dr. Sami A. I. Barri
Chairman

Dr. Abdul-Rahman A. Al-Arfaj
Member

Dr. Adnan M. Al-Amer
Member

Dr. Assad A. Al-Thukair
Department Chairman

Dr. Abdullah M. Al-Shehri
Dean of Graduate Studies

Dedicated to

My Parents,

Brothers and Sisters

ACKNOWLEDGMENT

Praise is to Allah the Almighty, the all knowing, and the all wise for making it possible for me to accomplish this work successfully.

I wish to express my unreserved appreciation to Dr. Sami A. I. Barri, who served as my thesis advisor. The completion of this work is credited to his un-flinching support, and priceless ideas. I wish to also thank my thesis committee members, Dr. Abdul-Rahman Al-Arfaj and Dr. Adnan Jarallah for their constructive contribution towards the success of the work. Last but not the list is Dr Pasl Abdul-Jalil whom I'm indebted to for his sincere help and un-quantifiable support.

My sincere appreciation to the following friends for their kindness and encouragement in the course of this work, Bashir A., Al-Amin Adhab, Abdullameed B, Dr G. Oloriegbe, Abdulkareem B. A, Dr. J. A. Odogba, Yushau B, Shuiab B. G, Abdul-Baasit S, Adewusi S, Shazali A, Yunus U, Tijani J, Sulyman A, Nasir T, I.D Kasumu, Kamarudeen A, Ayinde T, Abiola T, Suleiman Edah, Zakari H, Saeed A, Ali El-Rayees, AbdulAziz S, Mazahr M. H, Adeleke H, Izzat K, Shuaib B.G, Hammawa H, Uwais B, Dr Umar Y, and finally, King Fahd University of Petroleum and Minerals for the assistantship and support towards completing the program.

TABLE OF CONTENTS

LIST OF TABLES

LIST OF FIGURES

ABSTRACT

NAME: **Abdulkareem M. Melaiye**

TITLE: **Characterization of Molecular Sieves by n-Hexane cracking**

MAJOR FIELD: **Chemistry**

DATE: **December, 1999**

Molecular sieves of the types ZSM-5, Theta-1, and the mesoporus MCM-41 were synthesized using hydrothermal methods. The Si/Al ratio of ZSM-5 and Theta-1 was 50, whereas the composition of the MCM-41 was varied from SiO_2/Al_2O_3 ratio of 4.7 to a ratio of 20.5. The samples were characterized by powder x-ray diffraction, ICP-AES, and magic angle solid-state nuclear magnetic resonance.

The *n*-hexane cracking activities of the samples were determined using a fixed bed system in a micro-reactor system. The catalytic activity of the MCM-41 was extremely low compared with the microporus molecular sieves, possibly due to the low acid strength of the catalytic sites. The most active catalyst for hexane cracking was ZSM-5 due to the extensive bimolecular cracking activity in the channel intersections. In case of the Theta-1, most of the activity was via mono-molecular protolytic cracking mechanism because of the 1-D channel system provided by the structure of this molecular sieve. The two main parameters that affected the activity and the mechanism involved were the catalyst structure and the cracking temperature. In spacious pore structure and at relatively low temperature, bimoluclar cracking was favored.

The cracking activity of ZSM-5 and Theta-1 are far higher than that of the MCM-41 mesoporous materials, because of the strong interaction of the reactants with the surface of the channel system due to the "nest effect".

MASTER OF SCIENCE DEGREE

KING FAHD UNIVERSITY OF PETROLEUM AND MINERALS
DHAHRAN, SAUDI ARABIA

الخلاصة

عنوان الرسالة : تشخيص و تقيم حفزي لمواد بلوريه بواسطة قوة
النشاط في تكسير الهكسان العادي

التخصص : الكيمياء

تاريخ الشهادة: ديسمبر ١٩٩٩

تم تصنيع مواد بلورية ذات تركيب Thetal-1 ,ZSM-5 و MCM-41 لتبلور الحراري المائي . كانت نسبةبطريقة ا تساوي ٥٠. بينما تراوحت النسبة ZSM-5 و Thetal- 1 في Si/Al تم تشخيص المواد بواسطة حيود .MCM-41 في مادة 20.5- بين ٤,٧ والطنين النووي المغناطيسي للمواد ICP-AES الأشعة السينية و الصلبة.

تم قياس قوة النشاط في تكسير الهكسان العادي بواسطة مفاعل ذو السرير الثابت. قوة نشاط بلورات MCM-41 كانت قليلة جدا بالمقارنة مع المواد الأخرى ربما بسبب ضعف قوة الأماكن الحمضية في البلورات . أكثر قوة نشاط كانت للمحفز ZSM-5 بسبب كثرة التكسير ثنائي الجزيئات في تقاطع القنوات. في حالة المحفز Thetal-1 كانت معظم النشاطية عن طريق التكسير أحادي الجزيء بسبب القنوات ذو البعد الواحد في هذا المحفز. البناء البلوري وميكانيكية ودرجة الحرارة عاملان مهمان يؤثران في قوة النشاط التكسير. في القنوات الواسعة ودرجة الحرارة المنخفضة يكون التكسير ثنائي الجزيئات هو المفضل.

قوة التكسير في MCM-41 أكثر بكثير من مواد ZSM-5 و Theta-1 بسبب التفاعل بين المواد المتفاعلة وسطح القنوات بسبب ما يسمى "بعامل العش".

درجة الماجستير في العلوم

جامعة الملك فهد للبترول والمعادن
الظهران - المملكة العربية السعودية

ديسمبر ١٩٩٩

CHAPTER 1

INTRODUCTION

Mcbain in 1932 coined the term "Molecular Sieve" to describe a class of materials that exhibited selective adsorption properties on components of a mixture on the basis of molecular size and shape.[1] This is exemplified by the large family of aluminosilicate known as zeolites and its zeotypes.

Aluminosilicate are crystalline inorganic polymers, having framework that contain Silicon (Si) and Aluminum (Al) atoms bridged by oxygen (O), [(Si + Al)/O = ½]. The primary building block of the aluminosilicate structure is a tetrahedron of four oxygen atoms surrounding a central Si^{4+} and Al^{3+} ion to form SiO_4^{4-} and AlO_4^{5-} respectively. These are connected through their corners of shared oxygen atoms to form a wide range of small secondary building units, and eventually polyhedral units, which further connect to form the infinitely extended framework of the various specific structures with channels and cavities of discrete size. Different combination of the same secondary building unit may give numerous distinctive aluminosilicate structures. SiO_2 is neutral, but substitution of Si^{4+} for Al^{3+} results in a single net negative charge on the framework, which is compensated by an exchangeable "non-framework" cation (examples; Na^+, H^+, R_4N^+, Mg^{2+}) that is located in the pores or cavities of the structure. The

frameworks are so porous that their interstices hold not only the cations needed to neutralize the anionic framework charge but also large amount of water. Due to the crystalline form of aluminosilicate, the pores are as regular as the positions of the lattice atoms forming their walls, and they are of molecular dimensions.[2] The additions and removal of guest molecules can be fully reversible.

Aluminosilicate belong to a widely used family of inorganic solid catalysts in the industries as heterogeneous catalyst, with pore dimensions in both the microporous (small and medium pores < 20Å) and mesoporous range (20Å - 500Å). Its first commercial application as a cracking catalyst was in 1959.[3] The size of the aluminosilicate pore openings is determined by the number of tetrahedral units –or alternatively, oxygen atoms required to form the pore, and the nature of the cations present in or at the mouth of the pore. The protonated form of aluminosilicate materials are acidic, and referred to as Bronsted acid sites, being cations balancing the framework anionic charge. These are responsible for most of the cracking activity of the catalyst on hydrocarbons. The catalytic cracking of hydrocarbons is a key step in the production of transportation fuels from crude oil.

Considerable work has been carried out in order to evaluate the mechanism of reaction involved, assess the acid strength and activity of solid inorganic acid catalyst, using information of the product distributions and selectivity of the cracked paraffin.

Small hydrocarbons such as *n*-propane, *n*-butane, *n*-pentane, 3-methylpentane, *n*-hexane, and *n*-heptane are often used as reactants due to the limited number of

possible reactions and products inherent in the catalytic cracking process of these compounds. Criteria such as the paraffin/olefin ratio [4-10], cracking mechanism ratio (CMR) [11], constrain index, α-test [12,13] and β-test [14,15] has been implored to explain the predominant mechanism involved in the course of paraffin cracking reactions. And how other factors such as the structure of the catalyst effect the catalytic cracking activity, product distribution and selectivity.

It is generally accepted that cracking reactions of *n*-hexane over ZSM-5, Zeolite Y, Mordenite, and Ferrierite proceed through two routes. Namely, the protolytic monomolecular cracking route, which involves penta-coordinated carbonium ion formed upon protonation of paraffin on the Bronsted acid sites of a solid inorganic acid catalyst. This is analogous to reactions occurring in liquid super acid reported by Olah.[16,17] The second route is the classical bimolecular carbenium ion reaction route, which involves the reaction between carbenium ions adsorbed on the conjugate base site of bronsted acid site and paraffin.

The protolytic monomolecular mechanism, serves as the initiation step in *n*-hexane cracking reaction, by the formation of a carbonium ion on the bronsted acid sites, which subsequently decomposes into an adsorbed carbenium ion and lower paraffin or hydrogen. Stronger acid sites have been attributed to the determinitive reactions of the monomolecular process. Typical products obtained through this route are methane, ethane, ethene, and hydrogen at high temperatures.[18-20]

The propagation steps involve the adsorbed carbenium ion, which undergo hydride transfer, isomerization, and β-scission. This second step of reaction is

attributed to the basis of the bimolecular carbenium ion mechanism, which account for the characteristic products obtained such as propene and isobutane.[16-19, 21-24)]

The termination reaction, involve desorption of the surface carbenium ions to form olefins by dehydrogenation, or β-scission. The two routes have been considered as an integrated part of a chain mechanism required for catalytic cracking of paraffin over the aluminosilicate molecular sieves tested. [25,26)]
Catalytic cracking may have reached a technological maturity, however the understanding of the fundamentals and quantification of its elementary process are still advancing.

The present study is aimed towards contributing to the existing literatures on the characterization of molecular sieves using *n*-hexane. It involves the synthesis and characterization of various molecular sieves with widely varying properties covering the medium pore structures such as ZSM-5 and Theta-1, and mesoporous structures such as MCM-41. These structures have been characterized by a number of analytical techniques and were tested as catalysts for the n-hexane cracking reaction. The hydrocracking pattern was analyzed and corrected with the physiochemical properties of the catalysts.

1. 1 BACKGROUND

1. 1. 1 ALUMINOSILICATE MOLECULAR SIEVES

MICROPOROUS CATALYST

The term "zeolite" is derived from two Greek words meaning "to boil" and "a stone".[27] It has been studied by mineralogists for two and a quarter centuries with the first member stilbite discovered in 1756 by Cronstedt.

Zeolites or aluminosilicate materials may conveniently be divided into one-dimensional (1D), two dimensional (2D), or three-dimensional (3D) pore structures. Zeolites with more than one pore system are classified according to their largest accessible pore. The commonly lumped classes of zeolites used in catalytic applications are based on their pore sizes and structures such as the:

Small pore size (example: Erionite): having 6, 8 number of tetrahedral units, with a maximum free diameter of 4.3Å and 2-dimensional channel system.

Medium pore size (example: ZSM-5, synthetic ferrierite): ZSM-5 has 2-D 10 tetrahedral unit (10-T-rings) interconnected giving effectively 3-D medium pore channel system with a maximum free diameter of 6Å. Ferrierite has 10-T-ring channel intersecting 8-T-ring channel.

Large pore size (example: Mordenite, Faujasite - linde type X and Y); with 1D and 3D- channels system respectively, and 12 number of tetrahedral unit, with maximum free diameter of 8Å.[3]

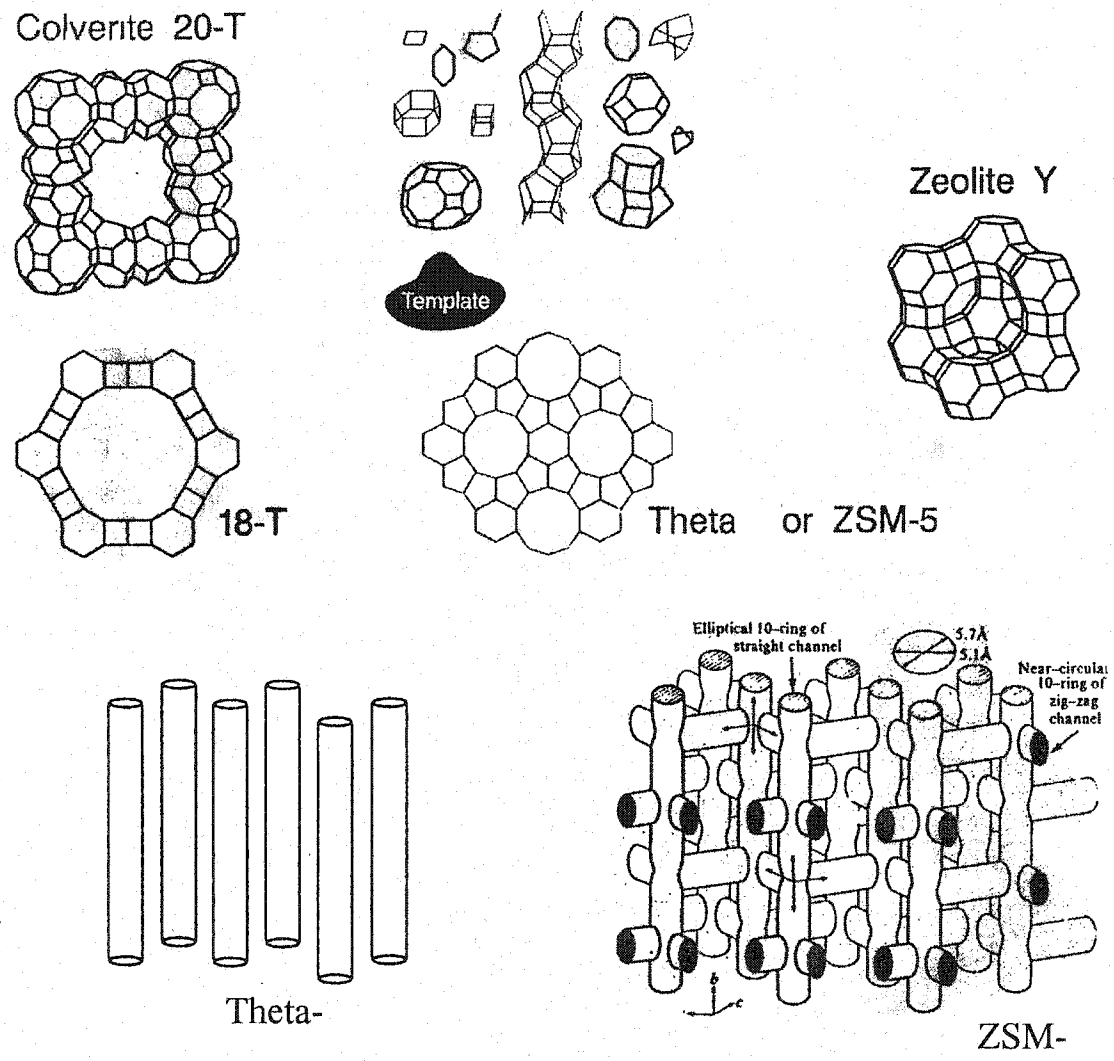

Figure 1.1 showing some zeolite structures and channels.

Although over 150 different zeolite structures have been identified, only about 15 are used commercially. The application of zeolites as catalyst for oil refining, petrochemistry and organic synthesis in the production of fine and specialty chemicals is related to the specific features of these materials as follows:

- They have very high surface area and adsorption capacity.
- The adsorption properties of the zeolites can be controlled and varied from hydrophobic to hydrophilic type.
- Active sites such as acid sites can be generated in the framework and their strength/concentration can be tailored for a particular application.
- The pore sizes and channels cavities are in the range typical of many molecules of interest (5–12Å), with a strong electric field existing in the micropores alongside an electronic confinement of the guest molecules.
- The intricate channels structure of the zeolites allows it to present different types of shape selectivity for product, intermediate, and reactant, which can be used to direct a given catalytic reaction towards the desired product by avoiding undesired side reaction.
- High thermal and hydrothermal stability.[28-30]

A representative empirical formula for a zeolite is written as:

$$M_{2/n}O.Al_2O_3.xSiO_2.yH_2O$$

Where ***M*** represent the exchangeable cations, which are generally from group I or II ions, although other metals, non-metal and organic cations may also be used to balance the framework. ***n*** represents the cation valence, which are present either during synthesis or through post synthesis ion exchange. ***x*** value is greater or

equal to 2, according to Lowenstein's rule.[31] y represent the water molecules contained in the zeolite voids.

Much of the pre-1960 synthetic zeolite chemistry sought to mimic the geochemical environment of the known mineral forms, and was thought it required temperature range of 200-400 °C with several tens of atmospheric water pressure. Not until 1957 did chemist begin to successfully synthesize zeolite at low temperature (< 100 °C). [32] Most synthetic zeolites are thermodynamically metastable products in their preferred synthesis conditions. They are prepared under controlled conditions of temperature, pressure, and time, with specific reactants and physical reaction environments, particularly ones that control levels of homogenization and nucleation conditions. For example, agitation or mixing during crystallization of a preparation may enhance the "collision breeding" of nuclei of a desirable product or undesirable crystallization of an impurity phase. Many zeolites synthesized yield two or more crystalline phases with un-reacted gel components. Much development work is aimed at the process and compositional control needed to produce a reaction window, where a single-phase, fully crystallized product may be isolated. The process of synthesis required reactive forms of silica, alumina, templates, distilled water and a basic medium. These ingredients are blended together in the required amounts to form a homogeneous gel or slurry, which is then aged under the desired conditions. Reactants may be added, and mixed sequentially, simultaneously, or in a variety of "in line" homogenizers. However, the mixing mode or sequence of adding reactants may affect the structure of the resultant gel. Therefore, the rate of

reaction, crystallization, and even the nature of the final product, including not just crystal size or shape, but the nature and level of impurities, might result in an entirely different product. [32] The synthesis process, are usually batch systems run under one of the following conditions:

Temperature range 90-100 °C, at one atmospheric pressure (1 atm.), and pH>10.

Temperature range 140-180 °C, autogenous water pressure (5-10 atm) and pH>10.

Temperature range 100-180 °C, with water plus "amine" autogenous pressure, and pH>10. [32]

Acidic form of zeolites is classified according to their silicon to aluminum (Si/Al) ratio. A ratio of (Si/Al) greater than 10 is considered as high silica materials, with relatively high stability of framework in acid, low stability in base, low concentration of acid groups, resulting in high acid strength. A ratio of (2-5) is intermediate, while (1-1.5) is low with relatively low stability of framework, low stability in acid, high stability in base, and high concentration of acid groups with moderate acid strength.[21]

MESOPOROUS

Recently, a new family of mesoporous crystalline silicate and aluminosilicate designated M41S has been discovered by Kresge et al, researchers at Mobil Oil Company.[33 -35] They used a new concept in the synthesis of porous material in which the templating agent is no longer a single, solvated, organic molecule or metal ion, but rather a self assembled molecular array. These lead to mesoporous structures with adjustable pore sizes between 15 Å and greater than

100Å. These compounds named MCM (where MCM stands for Mobil's composition of matter) possess an ordered hexagonal arrangement (MCM-41), cubic (MCM-48), and laminar (MCM-50) arrays, which can be visualized by a transmission electron microscope.[36,37] They possess long range order with surface area above 700 m^2g^{-1}.[34-40] The pore sizes combined with the acidic properties, depends on the nature of template and synthesis conditions used, over a range of Si/Al ratio as framework.

Different synthesis procedure have been proposed in the literature to synthesize silicate and aluminosilicate mesostructure in alkaline conditions, using sol-gel process disclosed by Kresege et al.[37] Several factors have been found to play a vital role in determining the final structure of as-synthesize mesoporous material and its average pore size, as mentioned in the next page. In a typical synthesis condition, Busio et al [79] synthesized 12 samples of aluminosilicate MCM 41 with the hydrogel having a pH range of 13 – 14, and varied ratio of silica to aluminate ranging from 12 – 200, at a reaction condition of 110 °C for seven days without stirring. The source of aluminate was sodium-aluminate, Ludox HS 40 was the silica source, while cetyltrimethylammonium bromide as surfactant, and tetramethylammonium hydroxide as an auxillary ion and alkaline source. The as-synthesized material showed complete incorporation of tetrahedral coordination of Al [IV] in the framework with a single peak observed near 50 ppm of ^{27}Al NMR spectra. But upon calcination at 540 °C for 1 hour in flowing N_2 gas followed by 6 hours in air, the extra-framework Al [VI] species was observed with a peak near 0 ppm of the spectra. A general rule proposed is that the pore volume

and the average pore size, decreased when SiO_2/Al_2O_3 in the gel decreased from 32 down to 8. Thus, the presence of the inter-channel hydroxyl groups associated with Al $^{(IV)}$ a four coordinated framework atoms gives the mesoporous material its Bronsted acidity and catalytic activity.[5]

M41S formation was found to differ from that of normal zeolite crystallization principally in its timing. The templates used were quaternary ammonium ions $C_nH_{2n+1}(CH_3)_3N^+$, with different alkyl chain lengths (n = 8, 9, 10, 12, 14, 16), which are also useful as surfactants in detergents. These ions are known to form micelles in aqueous solutions. The template molecules is assumed to be ordered (see figure1.1) in the aqueous gel during crystallization, and the silicate or aluminosilicate solution present between the "walls" of the porous solid.

According to the templating mechanism, the alkyl chain length *n* influences the pore size of the MCM-41 material by exhibiting different X-ray diffraction lines (d_{100}). Another way to alter the pore size is the addition of "auxillary" template molecules also called "expanders" such as mesitylene.[33-37] These substances can dissolve into the hydrophobic region of the surfactant micelles, whereupon the micelle diameter and the pore size increases. An inverse relationship exist -

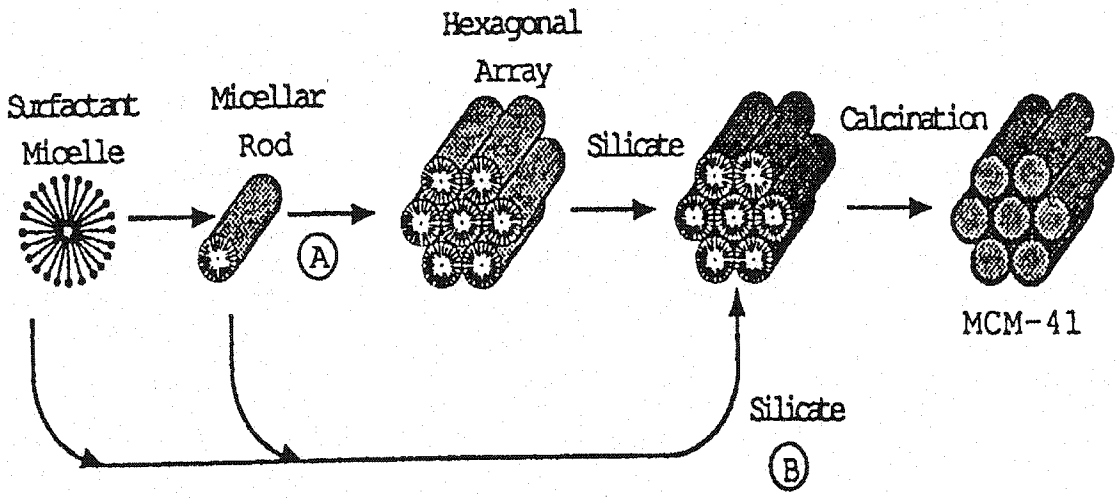

Figure 1.2 Possible Mechanistic Pathways for the Formation of MCM-41: **A**. Liquid Crystal Phase Initiated, and **B**. Silicated Anion Initiated.[33]

between the diameter of the micellar template and the wall thickness of the pore. Thus, decreasing the template diameter leads to thicker walls. This templating chemistry gives the opportunity to produce "tailor –made" mesoporous solids. Varied surfactant to silicon ratio result in four categories of M41S materials; Sur/Si < 1 has hexagonal array of uniform pores (MCM-41), Sur/Si = 1-1.5 with cubic array (MCM 48), Sur/Si = 1.2-2.0 gives lamillar array, and finally Sur/Si = 2 forming cubic octamer, which is thermally unstable. Investigation of the crystallization process of microporous zeolite-type compounds, have shown that the "best" (that is, the most strongly structure directing) templates are rigid organic molecules stiffened by the presence of one or more ring system. However, due to the potential flexibility of micellar arrangements, the order in the walls of the mesoporous materials is possibly less strict than in convectional zeolites. Mesoporous molecular sieves has been found useful as support for producing carriers on which catalytically active phases such as heteropoly acids, amines, transition metal complexes and oxides, hydrogenation, hydrodesulfurization, hydrodenitrogenation, and oxidation function.[29] Besides its characteristics as support, the possibility of generating Bronsted acid sites on the surface of mesoporous structures due to the presence of Al^{IV} in the framework, enhances its acid catalyzed properties, and in addition grafting of transition metals gives it a catalytic redox properties to produce monofunctional acid as well as acid/metal oxide bifunctional catalyst. [29]

1. 1. 2 BRŐNSTED ACID SITES

The number and strength of the acid sites are complex functions of the nature and concentration of tetrahedral trivalent X groups, their location, and the nature and concentration of exchangeable cations that are present.[3] In the case of aluminosilicate, the active sites are provided by the imbalance in between the silicon and aluminum ions in the framework. Each aluminum atom contained within the framework structure induces a potential acid site.[41] Classical Bronsted and Lewis models of acidity have been used to classify the active acid sites in zeolite. Bronsted acidity occurs in the zeolites when the cations balancing the framework anionic charges are protons. Lewis acid sites occur when a trigonally coordinated aluminum atom is electron deficient and can accept an electron pair, thus behaving as a Lewis acid. Acidic zeolite is produce by replacing the cations present in the as-synthesized form with protons. When the as-synthesized form is calcined in air at high temperature (550 ^{o}C) for a period of time, the organic cations undergo combustion, and a mixture of alkali cations and some protons is left behind. The remaining alkali cations is then removed through ion exchange treatments, which is normally done with an aqueous ammonium salt to produce the ammonium ion form. The final step involves thermal treatment at 773 K, which decomposes the ammonium cations there by releasing ammonia gas and leaving behind protons as counter-ions to the zeolite framework.[42] see figure 1.2. The aluminum site with its associated silanol bridged (Si-O^{-}H^{+}-Al) is the classical Bronsted acid.[43] The Bronsted site has been proposed to exist in equilibrium with trigonally coordinated aluminum, which in turn constitute a Lewis acid (electron

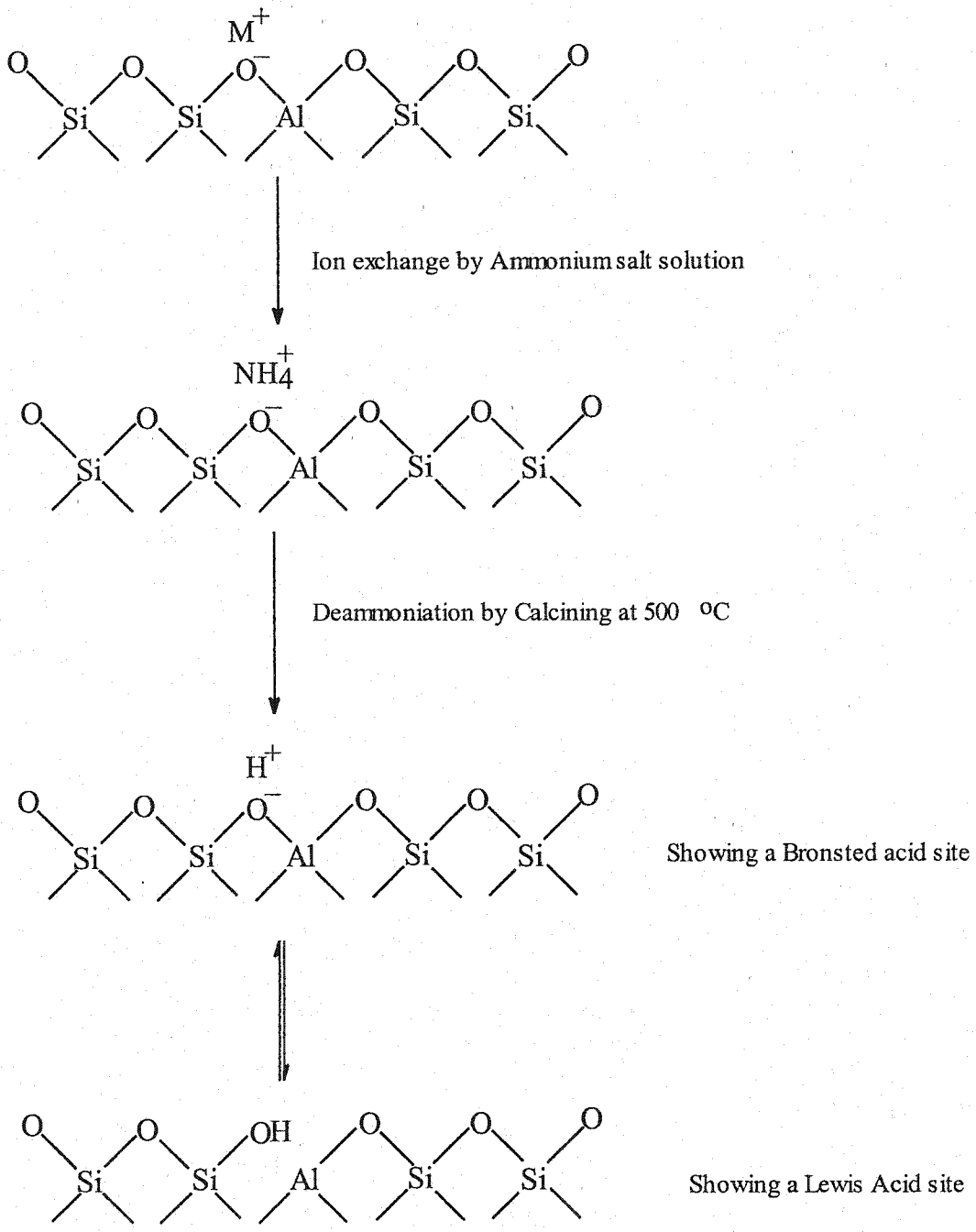

Figure 1.3, Diagram showing steps of Protonation of a synthesized aluminosilicate framework.

donor) site.[43] The proton is acidic through the interaction between the unshared pair of electrons on the oxygen atom and the unoccupied orbital of the aluminum atom, which weakens the bond between the oxygen atom and the proton coordinated to it so that the proton has donor (Bronsted) acidity. [44-45]

The temperature of calcination is important due to its effect on the acid density distribution and catalytic properties of the zeolite.[46] The severity of the thermal treatment could affect the zeolite through dehydroxylation (loss of structural water from the lattice). This leads to a drastic change in the proton acidity, and steaming which is caused by the generation of H_2O as a result of combustion of the trapped organic amine in air. Both effects are accompanied by the loss of aluminum from the crystal lattice, this leads to the decrease of the acidity of the zeolite.[47] Progressive dealumination occurs with the severity and duration of the thermal treatment [48], which is accompanied by a partial loss of crystallinity and the formation of various aluminum containing species in the intracrystalline pores, and an increase in the surface concentration of aluminum on the crystal.[47] The various aluminum containing cations and neutral species produced as a result of the thermal treatment, are found to occupy the pores and channels of the molecular sieve catalyst. It has been proposed that some of these cations interact with neighboring basic oxygen of the zeolite lattice to induce a more active catalytic site. The cation-oxygen pair is thought to act as a Lewis acid-base ion pair.[48] In other instances, hydrated metal cations were found to produce new types of proton (Bronsted) acid sites, though none were found to have a stronger Bronsted acidity than the acid bridged hydroxyls.[49] The removal of the

aluminum from the lattice has been claimed to produce a "nest" of four Si-O-H silanols.[50] These hydroxyl groups along with the terminal silanols (on the external surface of the crystal are reported to give rise to the "weak " acid sites characterized by infrared (IR) spectroscopy.[51] Bronsted acidity can be defined in terms of a reactant or probe molecule, which act as a proton acceptor. Adsorption of reactant or product molecules prior to its desorption influence the acidity of the catalyst. A relatively strong base such as ammonia drives the acid equilibrium towards the Bronsted acid configuration. Moreover, the more polarizable the adsorbed molecule, the greater is the Bronsted acid strength.

1.1.3 Nature of Aluminosilicate Catalyst on Paraffin Cracking

The reactivity and selectivity of molecular sieve zeolites as catalysts are determined by two main factors, the nature of active sites (particularly acidic sites) and the topology (cavities, channels, pores etc).

The cracking of hydrocarbons on acid catalysts is a long established and critically important industrial process. Developed in the 1930s, catalytic cracking quickly replaced thermal cracking in the commercial production of motor fuels. Since then, cracking technology has undergone much major improvement, both in reactor configuration and in catalyst formulation. Although, many of the research has been largely empirical in nature, and has been very successful in terms of the technological advances achieved to date. However, it has left a gap in the understanding of the fundamental processes underlying the conversion of petroleum distillates into internal combustion engine fuel.[52] Thus, significant

future improvements in catalytic cracking technology will require major advances in the fundamental understanding of the chemical mechanisms involved in cracking reaction.

1. 1. 4 Evidence of Protolysis on Bronsted acid sites of Alumino-silicate acid Catalyst

In 1933, Gayer [53] was perharps the first to propose that cracking proceeds on acid surfaces containing protons. Years later, most of the subsequent literatures describe catalytic cracking in terms of a "β-cracking" ionic mechanism.[54-58] There has been clear evidence for the participation of Bronsted sites in cracking reactions [59,60] by subjecting a catalyst to pretreatment temperature above 500 °C, resulting in a loss of cracking activity for linear paraffin. Olah's work with liquid Bronsted super-acids, [63-65] has demonstrated beyond question that alkanes undergo protolytic cleavage with the general electrophilic reactivity of C-C and C-H bonds. Ethane was the simplest alkane subjected to test with a product selectivity of 15:1 ratio methane to hydrogen. Generally, the reactivity towards protolytic cleavage of paraffin by Bronsted acid in both homogeneous and heterogeneous catalytic cracking reactions are in the order of $R_3C\text{-}H > C\text{-}C > R_2HC\text{-}H > RH_2C\text{-}H$ [16,66-68].

It has been convincingly shown that a penta-coordinated carbonium ion can be formed on alkane by protonation, if a sufficiently strong Bronsted proton is available.[69] However, Lewis acid sites has been suspected to interact inductively with Bronsted sites on zeolites to increase the acid strength and produce sites with

a Bronsted acidity high enough to be comparable to that of liquid superacids. The lewis sites has also been ascribed to that of enhancing the formation of aromatics and coke during cracking reaction by a separate process, but do not contribute to cracking selectivity by processes independent of the presence of Bronsted sites.

It is now widely accepted that the initiating event in the cracking of paraffin is the protolysis of feed molecule by a strong Bronsted acid on the catalyst surface. [24] This is represented generally as:

$$C_nH_{2(n+1)} + H^+S^- \longrightarrow C_nH^+_{2(n+1)+1}S^- \rightarrow C_iH_{2i+2} + C_{n-i}H^+_{2(n-i)+1}S^-$$

Were S^- is the conjugate base site of the aluminosilicate framework of the catalyst. The intermediate step in the above process is the formation of a carbonium ion, which permits paraffin and a carbenium ion to form by the dissociation of this transitional species. Further more, the acid strength of a catalyst is found to play a critical role in determining the degree of stability of hydrocarbon ions, their residence time on the surface of the catalyst and the type of reaction the ion will undergo. A strongly acidic catalyst is known to encourage hydrogen transfer reactions and coke formations. [70]

1.1. 5 Evidence of Carbenium ion in Catalytic Cracking

Carbenium (then known as carbonium ions)[54] ions have long been acknowledged to form on the surfaces of solid acid catalysts as essential intermediates of cracking reactions. [71] Direct physical evidence was obtained from spectroscopy data of adsorbed molecules, with the spectral studies showing the presence of hydrocarbon ions on cracking catalyst.[72,73] An example is the

comparison of the spectrum of triphenylmethane on silica – alumina catalyst [74] with the known spectrum of the triphenycarbenium ions, is as a consequence of chemisorption of a hydrocarbon on the surface of a cracking catalyst. However, it has been demonstrated by observation that the carbenium ions do not form covalent surface- to – carbon bonds, since the surface bonding does not destroy the resonance system responsible for the stability and characteristic spectra of the carbenium ions.[75]

1. 1. 6 Shape Selectivity

Topology of the catalyst imposes stereoselectivity or shape selectivity that plays a very important role in molecular sieve catalysis.[16] Highly crystalline and regular channel structures are among the principle features that molecular sieves used as catalyst over other materials.

There are three types of shape selectivity these are reactant shape selectivity, product shape selectivity and transition – state shape selectivity. The reactant shape selectivity results from the limited diffusivity of some of the reactants, which cannot effectively enter and diffuse through the pores/channels of the catalyst. Product shape selectivity occurs when slowly diffusing product molecules cannot rapidly escape from the channels of the catalyst, and thus undergo secondary reactions. Restricted transition – state shape selectivity is a kinetic effect arising from the local environment around the active site. An example is the differences between the cracking rates of n-hexane and 3-methylpentane (3-MP) in zeolite MFI, which are related to the differences in the

dimensions of the transition – state complexes formed during cracking of the two compounds. It has been suggested that the transition – state formed upon 3-MP cracking is bulkier, and sterically more hindered than the one formed upon n-hexane. [76] As a result the cracking rate for n-hexane is higher than 3-MP, with zeolite MFI at standard test conditions. [77,78]

1. 1. 7 Characterization of Catalyst by different test reaction using alkane cracking

Small hydrocarbon molecules have been used to study the catalytic cracking process of a catalyst. This is due to the advantage of having limited number of possible reactions (and products) which can be studied with ease, as compared to large hydrocarbon molecules with complexities inherent in the cracking reactions and products.

Propane cracking; Propane conversion over H-ZSM-5 catalyst has been studied by Ono et al [4] at low conversion (<5%) with methane and ethene found to be the major products of the reaction. The result obtained shows that the main reaction involved the decomposition of propane into methane and ethyl ion ($C_2H_5^+$) via the attack of a proton (Bronsted acid) on the C-C bond of propane, rather than on any of the C-H bonds, while the ethyl ion formed desorbs as ethene. However, at higher conversion the reaction yield more propene and less methane. It was inferred that product olefins principally ethene must have been involved in secondary reaction with propyl carbenium ion formed on Bronsted acid sites, resulting in larger carbenium ion which eventually β-crack or cyclize.

This processes or mechanism might explain the observed formation of benzene, toluene, and xylene as part of the reaction products at higher conversions.

n-Butane cracking: Both propane and n-butane contain only primary and secondary hydrogen atoms. Ono et al also studied n-butane conversion over H-ZSM-5 [4] at low conversion, with the main products of reaction found to be methane, ethane, propane, butanes and hydrogen. The products obtained have been explained by reaction involving penta-coordinated carbonium ion intermediates of the feed formed at the Bronsted acid sites by a process of protolysis. At higher conversions, the selectivity decreases for methane, ethane and hydrogen formation with higher yield of propane. Propane formation was postulated to be by hydride transfer from the feed molecule to a propyl carbenium ion or disproportion reaction of ethyl ions with the feed. Desau and Haag calculated that the hydride transfer mechanism accounts for 40 % of the reaction undergone by butane at higher conversion.[4]

n-Pentane cracking: Hall and co-workers also studied the catalytic cracking of n-pentane [4] over HY zeolites, with methane and propane obtained as major initial products of the reaction (protolysis), while hydrogen and methane were the dominat products obtained for iso-butane cracking. From the major initial products obtained for n-pentane cracking, it was concluded that the carbenium ions left on the surface of the catalyst can be isomerize to form t-butyl and isopropyl ions which then undergo a chain of consecutive reactions, involving at each step the displacement of the surface species by a hydride transfer from the feed. The termination of the above process is by decomposition of the carbenium

ion into a pristine Bronsted acid site and the corresponding alkene. The molecular chain length of n-pentane is such that β-scission of the parent carbenium ion makes the chain transfer process a more important component of the overall conversion mechanism.

n-Heptane cracking: Corma et al [4] worked on n-heptane cracking, and according to established theory on n-heptane cracking, the following monomolecular cracking reactions should be involved;

$$nC_7H_{14} \longrightarrow C_3H_6 + C_4H_{10} \text{ OR } C_3H_8 + C_4H_8$$

$$nC_7H_{14} \longrightarrow C_2H_4 + C_5H_{12} \text{ OR } C_2H_6 + C_5H_{10}$$

Thus ethane, propane, butane, and pentane are expected to be the primary products of the cracking process, with the initial ratio of C_2:C_5 and C_3:C_4 should be equal to 1, while the overall paraffin to olefin ratio should also be unity. In practice, not one of the above mentioned expectation was fulfilled. The presence of C_6 molecules in the primary products complicated matters, while C_1 was found only as a secondary product. The ratio of C_5:C_2 and C_3:C_4 was found to be > 1. A bimolecular reaction process is said to be more adequate in explaining the excess formation of C_5 and C_4 products over C_2 and C_3 products.

1.2 OBJECTIVE

n-hexane cracking reaction is very useful in characterizing the nature of the acid site present as well as the structural constraints born out by the framework structure of the molecular sieve. It is the objective of this work to evaluate these parameters by studying the n-hexane cracking patterns of three molecular sieves of different structures, namely ZSM-5, Theta-1, and MCM-41. To our knowledge there is no published data comparing ZSM-5 with Theta-1 at similar catalyst composition. Furthermore, although there is some literature showing that MCM-41 is not active for n-hexane cracking, none of these stated this as a function of composition.

More specifically the outline of the research is as follows:

- Undertaking the synthesis of three molecular sieves, namely ZSM-5, Theta-1, and MCM 41. Both ZSM-5 and Theta-1 should be synthesized at constant composition in terms of ratio, whereas the MCM-41 should be synthesized with varying SiO_2/Al_2O_3.

- Characterize the molecular sieves by XRD to ascertain their crystallinity.

- Evaluate by n-hexane cracking catalytic activities at various suitable space velocities and temperatures to enable the calculation of various indicative parameters of the catalyst properties as discussed above.

CHAPTER 2

REVIEW WORK ON n-HEXANE CRACKING

2.1 Mechanism of Paraffin Cracking

Several authors have suggested that the catalytic cracking of hydrocarbons takes place by a mono-molecular and a bimolecular mechanism.[5,11,18,19] The two cracking routes is believed to be integrated in the course of a cracking reaction, and thus referred to as a chain mechanism.[4,52] The bimolecular mechanism is the classical chain process involving hydride transfer between an alkane and an adsorbed carbenium ion (which is strongly coordinated to the surface oxide ions resembling a surface alkoxy) followed by isomerization and β–scission. The hydride transfer step does not involve direct interaction of a Bronsted proton with a hydrocarbon molecule, only hydride – transfer between two hydrocarbon species.[52] Figure 2.1 showed a general chemical equation of the reaction mechanism.

The monomolecular mechanism involves the direct protonation of an alkane to form a high energy transition state of non classical penta-coordinated carbonium ion, which subsequently cracks or dehydrogenates to yield an alkane (or dihydrogen) and an alkene. [80] The activation energy of this reaction is high because of the high – energy transition state.[81,82] And in the formation of this

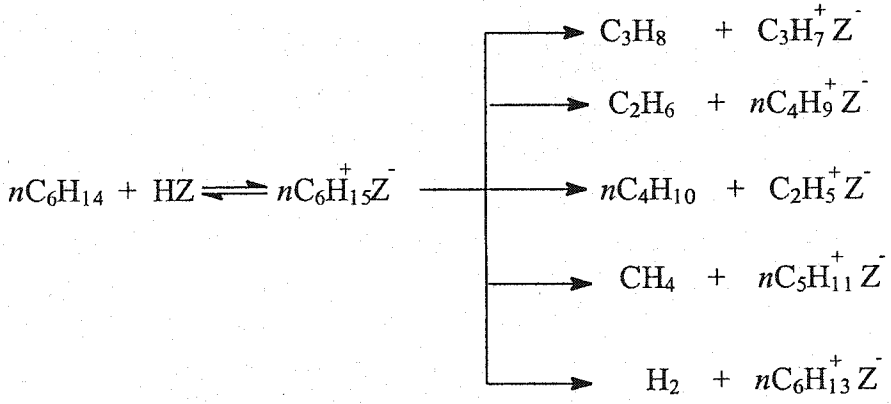

The above is the Monoprotolytic cracking mechanism scheme, where H^+Z^- indicate the acid site.

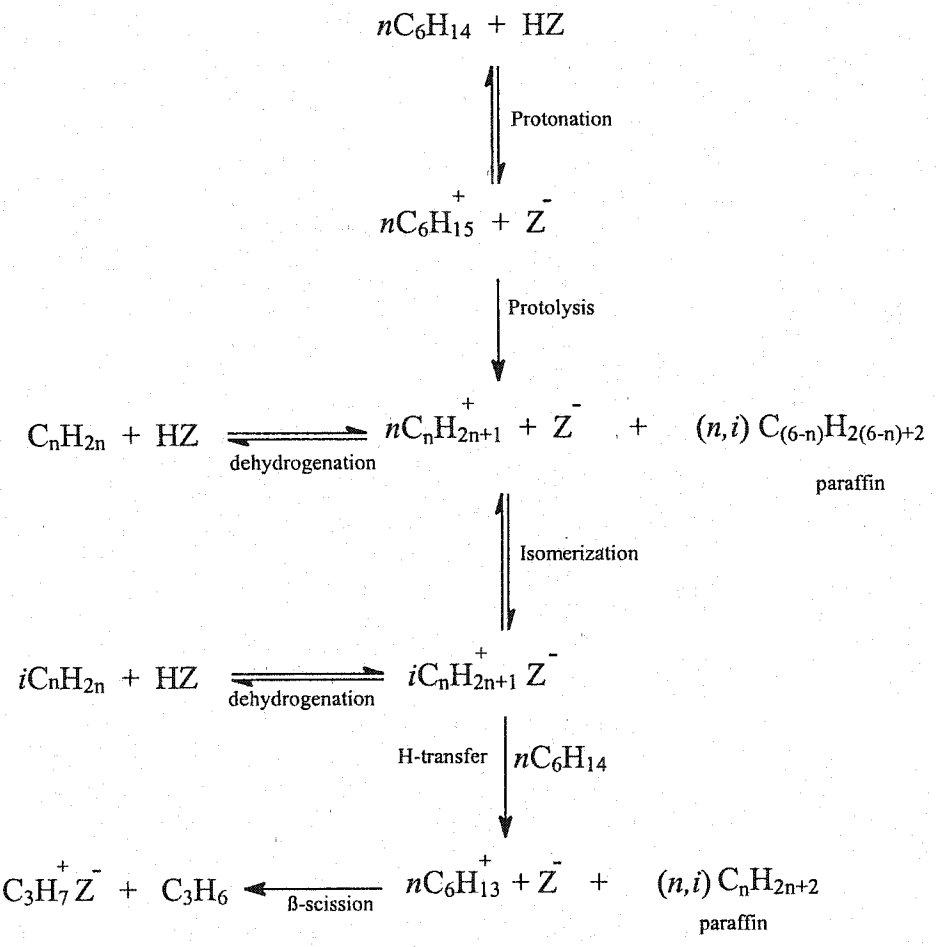

Figure 2.1 Scheme showing the general chemical equations for both the two cracking routes.

transition state, the zeolite acidic O-H bridge bond is significantly lengthen. [82] It is reasonably assumed that the rate of this step is very sensitive to the acid strength of a Bronsted proton. [83] Therefore the rate of the monomolecular cracking pathway is expected to be more sensitive to the acid strength of the Bronsted proton than the rate of the bimolecular pathway. The expected high sensitivity of monomolecular cracking activity on the strength of Bronsted protons should make the reaction a sensitive probe to compare the acid strengths of different aluminosilicate materials.[84]

2. 2 Kinetics of *n*-Hexane Cracking

The two main cracking routes, protolytic and classical bimolecular mechanisms are expressed quantitatively using kinetic criteria's, which also account for both the major and minor products obtained in paraffin cracking. Several literatures consider 300 – 400 °C as low reaction temperatures, while high temperatures are > 400 – 540 °C. The kinetic criteria's are:

- Cracking Mechanism ratio (CMR) evolved as a tool to evaluate the relative contribution of each of the two cracking routes in acid catalyzed *n*-hexane cracking. According to Wieler et al [16], the bimolecular cracking route primarily yield butanes, especially iso-butane since the precursor carbenium ion is the most stable one at the condition of reaction that enhances its formation with little formation of methane, ethane and ethene. Alternatively, if the protolytic mechanism is operative, n-hexane cracking result in the formation of hydrogen and linear C_1 - C_4 hydrocarbons with C_2 and $C_{2=}$ being

the typical products of the protolytic cracking route, with the precursor ions being readily generated from the penta-coordinated carbonium ion. Thus CMR is defined as a ratio of $[(C_1 + \Sigma C_2)/iC_4]$, where C_1, ΣC_2 and i-C_4 denote the molar selectivities to methane, ethane, ethene and iso-butane. A high value of this index points to a relatively high contribution of the protolytic-cracking route, while a low value indicates that the classical β–scission route is the main cracking path. Wielers et al shows that with increasing temperature, decreasing aluminum content and decreasing pore dimensions of *n*-hexane cracking over Faujisite, Mordenite, MFI and Ferrite zeolites, the relative contribution of the protolytic cracking increases compared to the bimolecular cracking route. [11]

- β - Test is a method used to quantitatively characterize the hydrogen transfer activity of zeolite based on the rate of iso-butane formation to the concentration of iso-butene, or the ratio of propane formation rate in the hydrogen transfer steps to the propene concentration of n-hexane cracking.[14,15] The hydrogen transfer activity of H-mordenite was found to be higher than H-ZSM-5. [11,85-87] These was found to be in agreement with steric explanation that hydride transfer proceed through a sterically bulky bimolecular transition state [88] and will be inhibited if pore size is reduced. Hydrogen transfer has been found to be a function of the acid strength, number of zeolite active sites, and the density of these sites.
- Paraffin to Olefin (P/O) is often used to ascertain changes in the kinetic chains. A P/O >1 correspond to shorter chain length, while a P/O value <

1 correspond to a longer chain length.[52] A mathematical model has been proposed by wojciechowski [52] to evaluate the relative contribution of the two cracking routes. P/O is also dependent on the pore sizes of the catalyst,[11,18,89] the density of the acid sites, strength of the acid site and temperature of reaction if chain mechanism is consider as the mechanism of reaction.[52]

- Chain Length: Hall et al called the ratio of bimolecular to monomolecular processes as chain length. [89] This was measured by using the ratio of reactant molecules consumed by hydride transfer to those consumed by protonation. However, kinetic chain length (KCL) is defined as the ratio of the overall rate of feed conversion to the rate of initiation by protolysis, when considering chain mechanism reaction as the reaction path. [16] The reactivity of the acid sites for protolysis and the KCL due to propagation reaction varies substantially with temperature, catalyst formulation, feed diluents and molecular species. This in turn leads to a significant difference in the P/O ratio, coking and various selectivity phenomenon.[59-62]

- Constrain Index (CI): is also used to evaluate the relative contribution of the protolytic cracking route as compare to the bimolecular route, by measuring the ratio of the first order rate constant for the conversion of n-hexane to 3-methylpentane. It was found that with increasing temperature, decreasing aluminum content and decreasing pore dimension, the monomolecular route is favored with a CI > 1.[16,18, 76,78]

Wielers et al [16] explained the change in activation energy of *n*-hexane cracking over ZSM-5 (MFI) with variable aluminum content. They tentatively concluded that the bimolecular route is favored by the presence of two neighboring acid sites and lower reaction temperatures. As a result the relation between the reaction rate constant and the lattice aluminum content changes with the reaction temperature. A first order kinetic was observed at 532 °C, when the cracking rate constant varies linearly with the aluminum content, while a second order was observed with the aluminum content at 350 °C. [16] However, Jolly et al [25] reported a second order/high temperature (>450 °C) mechanism which involved one *n*-hexane molecule and one zeolite acid site in the rate determining step. And a third order /low temperature mechanism was proposed, to involve one *n*-hexane molecule and two zeolite acid sites in the rate determining step during the protolysis process, using MFI with varied aluminum content (Si/Al = 10 – 75).[25] Protolytic mechanism was found to be favored at 400 °C reaction, with hydride transfer at high conversions, long contact times and high aluminum content. [25]

The activity and activation energy for cracking of *n*-hexane where measured over three zeolites: HZSM-5, H-MOR, H-USY and CDHY (chemically dealuminated Y-zeolite), under conditions where the product selectivities were nearly identical without observing deactivation of the catalyst. The identical selectivities implied that the same reaction mechanism for cracking was occurring over all three catalysts. The apparent activation energies were different and attributed to the differences in heats of *n*-hexane adsorption, such that the intrinsic activation energies were identical. The results reported suggested that the kinetics of

cracking is insensitive to any possible differences in acid strength among the catalysts. A large enhancement in activity was observed at lower temperatures upon dealumination of zeolite Y by steaming, and the effects were due to other than changes in the acid strength. [84] It has also been found that calcined MCM-41 catalyst with Si/Al ratio (< 100) are active and more selective for cracking vacuum gas oil better than amorphous silica – alumina catalyst. The larger pore sizes have a beneficial effect on cracking the large size molecules present in gas oil. The acid strength of the sites in MCM-41 and its catalytic activity for cracking a small molecule such as *n*-heptane is lower than that of USY (ultra stable Y zeolite). [91]

CHAPTER 3

EXPERIMENTAL METHODS

3.1 Catalyst Synthesis

Eleven catalysts were used in this research work. Six mesoporous catalyst labelled Ak1, Ak3, Ak4, Ak5, Ak7 and Ak8 were synthesized by an in house method. The Ak1-7 samples are made up of aluminosilicate framework materials, while Ak8 contain only all silica. In addition three catalysts were prepared by supporting sulfuric acid and phosphoric acid on Ak8. Finally two microporous catalysts were synthesized, namely ZSM-5 and Theta-1. Both of these catalysts had Si/Al ratio of 50. A 1 : 1 ratio of Ak8 to ZSM-5, Ak8 to Theta-1 and ZSM-5 to carborandum were also evaulated using n-hexane cracking.

The reagents used in the above mentioned catalyst synthesis were Ludox AS40 (Dupont) a colloidal silica (SiO_2), which served as the silica source, while sodium aluminate ($NaAlO_2$) was the source of sodium (Na^+) ions and aluminate. Cetyltrimethylammonium bromide ($CH_3(CH_2)_{15}N(CH_3)_3Br$) a surfactant (aldrich), serves as a template, while tetramethylmmonium hydroxide ($(CH_3)_4NOH$) solution (Aldrich) serves as an auxillary template and as a major contributor to the basicity of the reaction medium (hydrogel). Sulfuric acid (H_2SO_4) and phosphoric

(H_3PO_4) acid (baker) were used for the modification of the Ak8 catalyst. Ammonium nitrate (Baker) was used for the preparation of the cation exchange solution.

3. 1. 1 As-Synthesized MCM 41 (Ak1) Catalyst

Hydrogel molar composition:

$1.32Na_2O : 1.07Al_2O_3 : 5.61CTAMBr : 5.56TMAOH : 25.17SiO_2 : 1000.8H_2O$

2.10g sodium aluminate was dissolved in 180g of distill water by swirling. This was followed by adding 20.80g of tetramethylammonium hydroxide solution, and 20.75g cetyltrimethylammonium bromide (CTABr). The mixture was stirred and heated to warm by dissolving the CTABr, to obtain a clear solution. 37.56g ludox AS40 was added and the hydrogel obtained was well mixed, with a PH of 12 - 14. The hydrogel was charged into a 300ml stainless steel autoclave, and heated to 130 °C under its autogeneous pressure for 72 hours by stirring. At the end of the reaction time, the crystallized sample was filtered, and washed with distill water several times to ensure that most of the bromide have been removed with some of the unreacted CTABr. The filterate was checked with 0.1N $AgNO_3$ solution regularly as a test for the bromide, while the pH of the filterate dropped to 8-9 at the end of washing. The as-synthesized sample was dried at 90 °C for 8 hours.

Tables 3.1 and 3.2 showed detailed hydrogel compositions of Ak1 - Ak8 and the quantities of reagents used for each synthesis respectively. Ak7 and Ak8 were both synthesized using the same experimental condition and procedure as stated in 3.1.2.

Table 3.1 Show's the hydrogel composition by weight of the Ak catalysts.

Sample code	$NaAlO_2$.	CTABr	TMAOH	Ludox AS40	Distill water	Reaction Temp.	Reaction Time
Ak1	2.10g	20.78g	20.60g	37.56g	180.0g	130 °C	72 hrs
Ak3	2.90g	18.80g	18.80g	34.22g	130.6g	130 °C	72 hrs
Ak4	3.82g	18.82g	18.89g	34.86	180.0g	130 °C	72 hrs
Ak5	0.96g	18.82g	18.89g	34.20g	180.0g	130 °C	72 hrs
Ak7	1.03g	10.09g	10.09g	18.05g	45.73g	100 °C	168 hrs
Ak8	-	20.84g	20.70g	37.86g	100.0g	100 °C	168 hrs

Table 3.2 showing hydrogel molar compositions of the as-synthesized MCM-41 Mesoporous catalysts

Sample code	Na_2O	Al_2O_3	CTABr	TMAOH	SiO_4	H_2O
Ak1	1.32	1.07	5.61	5.56	25.17	1000.8
Ak3	1.83	1.48	5.08	5.08	22.93	726
Ak4	2.41	1.95	5.08	5.10	23.36	1000.8
Ak5	0.60	0.49	5.08	5.10	22.91	1000.8
Ak7	0.66	0.53	2.72	2.73	12.09	254.26
Ak8	-	-	2.72	2.72	12.10	260

3. 1.2 As-synthesized all Silica MCM 41 (Ak8)

20.84g of cetyltrimethylammonium bromide was dissolved in 100g distill water, followed by 20.70g tetramethylammonium hydroxide solution. The solution was swirled properly, while 37.86g of Ludox AS40 was added and mixed thoroughly. The hydrogel formed was charged into autoclave having a teflon lining, and heated to 100 °C for 7 days under its autogeneous pressure without stirring. The crystallized sample was washed several times with distill water, and then dried for 8 hours at 90 °C.

3.2 Modified Forms of as-synthesized Ak Catalysts

3. 2 .1 Treatment of the As-synthesized Ak8

All the as-synthesized molecular sieves were calcined at 833 K for 24 hours to remove the organic template occluded in the channels. The oven temperature was raised at the rate of 1 °C from room temperature in dry air. Calcined Ak8 material was used as support for the impregnation of sulfuric and phosphoric acid as mentioned in the next section. The powdered like calcined materials were ion exchanged and converted to the protonated form by refluxing with 20.0ml aqueous ammonium nitrate (1M NH_4NO_3) solution per gram of catalyst for 1 hour, cooled and decanted. The ion exchange was done twice, and the ammonium

form of the AK materials were dried at 120 °C, and calcined again at 823 K for 16 hours to remove ammonia and obtain the protonated form of AK samples.

3 .2 .2 Preparation of Sulfuric acid Supported on Ak8 (S-Ak8)

1.50g Ak8 was transferred into a 100ml round bottom flask, and 15.3g of distill water was added to the content of the flask, followed by 0.43g of concentrated sulfuric acid (96.3% purity). The solution was evaporated to dryness using a rotatory evaporator by heating over steam bath under vacuum for 6 hours.

3 .2 .3 Preparation of Phosphoric acid supported on Ak8 (P-Ak8)

0.22g of concentrated H_3PO_4 acid was transferred into a 50 ml round bottom flask and 1.12g of Ak8was added into the content in the flask, followed by 11.25g of distill water as diluent. The content in the flask was evaporated to dryness using a rotatory evaporator by heating over steam bath, under vacuum for 4 hours.

3.2.4 Preparation of Phosphoric acid supported on Ak4 (P-Ak4)

1.05 g concentrated H_3PO_4 acid was transferred into a 50 ml round bottom flask, and diluted with 10g distill water. 1.01g protonated Ak4 was added to the content in the flask, and evaporated to dryness using a rotatory evaporator by heating over steam bath, under vacuum for 4 hours. The catalyst was activated by calcination

through 1 °C rise in the oven temperature from room temperature to 400 °C for 12 hours.

3.2.5 ZSM-5 (MFI) catalyst admixed with Ak8 (Ak8-ZSM-5)

A 1: 1 ratio of protonated form ZSM-5 catalyst was carefully, but properly mixed with Ak8 catalyst using a pestle and mortar.

3.2.6 Theta-1 catalyst admixed with Ak8 (T-Ak8)

A 1:1 ratio of protonated form Theta-1 zeolite catalyst was mixed in the same way as above with Ak8 catalyst.

3.2.7 ZSM-5 catalyst supported on Carborandum (CR-ZSM-5)

A 1:1 ratio of protonated form of ZSM-5 catalyst was mixed in the same way as above with carborandum.

3.2.8 ZSM-5 catalyst admixed with Amorphous Silica (A-ZSM-5)

A 1:1 ratio of protonated form of ZSM-5 catalyst was fixed in the same way as above with amorphous silica.

3.3 ZSM-5

2.61g of sodium aluminate and 3.30g of sodium hydroxide were dissolved in 200g of distilled water. 24.30g of butanol was added followed by 200g of ludox AS40 while stirring vigorously to keep the hydrogel homogeneous. The hydrogel was crystallized at 180 °C for 7 days.

The crystalline product was filtered, washed well with distilled water and dried at 100 °C. The dried product was calcined at 550 °C for 18 hours. It was then ammonium ion exchanged at reflux temperature three times. The ion-exchanged zeolite was then calcined again at 450 °C for 24 hours.

3.3.1 Theta-1 catalyst

The same method of synthesizing ZSM-5 was followed except that 4.60g of potassium hydroxide were used in place of sodium hydroxide.

3. 4 Characterization of the Catalyst

In addition to the catalytic characterization using n-hexane conversion, physical methods were also used to understand the structural characteristics of the catalyst synthesized.

3.4.1 Powder X-Ray Diffraction

The powder XRD involves the use of a collimated beam of X-rays, with wavelengths Cu K_α ~ 0.5-2 Å, incident on a specimen, which is diffracted by the crystalline phases in the specimen according to Bragg's law. The intensity of the diffracted X-rays is measured as a function of the diffraction angle 2θ, and the specimen orientation as stated by the Bragg's equation ($n\lambda = 2d\sin\theta$). A Siemen D5005 X-Ray diffractormeter was used for the characterization of the synthesized mesoporous materials. The operating conditions of the XRD analysis were:

- Copper K X-ray radiation (λ =1.541Å) from a broad focus tube at 40 KV and 30mA.
- Autodivergence slit with no scatter slit and a receiving slit of 0.1mm
- Scanning speed and interval of data collection was 0.01 degree 2θ/sec.
- Angle scanned are from 0.5 – 50 degree 2θ
- A graphite monochromator was used.

3. 4 .2 Inductively Couple Plasma Atomic Emission Spectroscopy (ICP – AES)

ICP-AES requires gaseous or liquid (as aerosol) sample aspirated to the center of a plasma. The sample is vaporized, atomized and partially ionized in the

plasma. Atoms and ions are excited which emit light at characteristic wavelengths in the ultraviolet or visible region of the spectrum. The emission line intensities are proportional to the concentration of each element in the sample. A grating spectrometer is used for either simultaneous or sequential multi-element analysis. The concentration of each element is determined from measured intensities via calibration with standards.

Sample preparation for the Ak samples was done by fusion. A 250 mg sample of dried as-synthesized Ak samples was weighed in a 10 ml platinum crucible and mixed with 1.25 g of lithium metaborate. The crucible was kept in a muffle furnace at 950 ^{o}C for 1 hour. When a clear melt was obtained, it was cooled and the melt agitated in 5 % nitric acid with gentle warming. When completely dissolved, it was transferred to a 100 ml volumetric flask and diluted with deionized water to the final volume. This solution was used for the determination of major elements like silicon, sodium and aluminum in the Ak samples.

The instrument used for chemical analysis of the synthesized samples was Admiralty Research laboratory (ARL) atomic emission spectroscopy (AES) model ARL-3580.

3.4.3 Nuclear Magnetic Resonance (NMR)

Solid states magic angle spinning (MAS) ^{27}Al NMR and ^{29}Si NMR spectra were recorded at ambient temperature using JEOL 500 MHz, NMR system. A zirconia rotor was used for the powder Ak samples at scan rates of 2000 - 5000. Other parameters such as delay time, filter, dead time, pulse decay etc were optimized.

3.4.4 Loss On Ignition (LOI)

0.50g as-synthesized Ak catalyst was weighed into a crucible, and calcined in an oven at 600 °C for 20 hours, cooled and weighed. The difference in weight of sample before and after calcinations is LOI.

3.5. Reaction Apparatus and Parameters

The apparatus consisted of a temperature controlled water bath, bubbler containing n-hexane (99.67% purity), and high purity nitrogen gas, which serve as carrier gas and diluent for the feed. Others are preheating loop, small fixed bed reactor, and two end tap glass type gas traps for reaction product effluent sampling. The reactor is 21cm long, with a stainless tube having an internal diameter of 1.05 cm. Figure 3.1 shows the experiment setup diagram. The feed consisted of 6.0 kPa partial pressure *n*-hexane at 0 °C, and 95.3 kPa nitrogen -

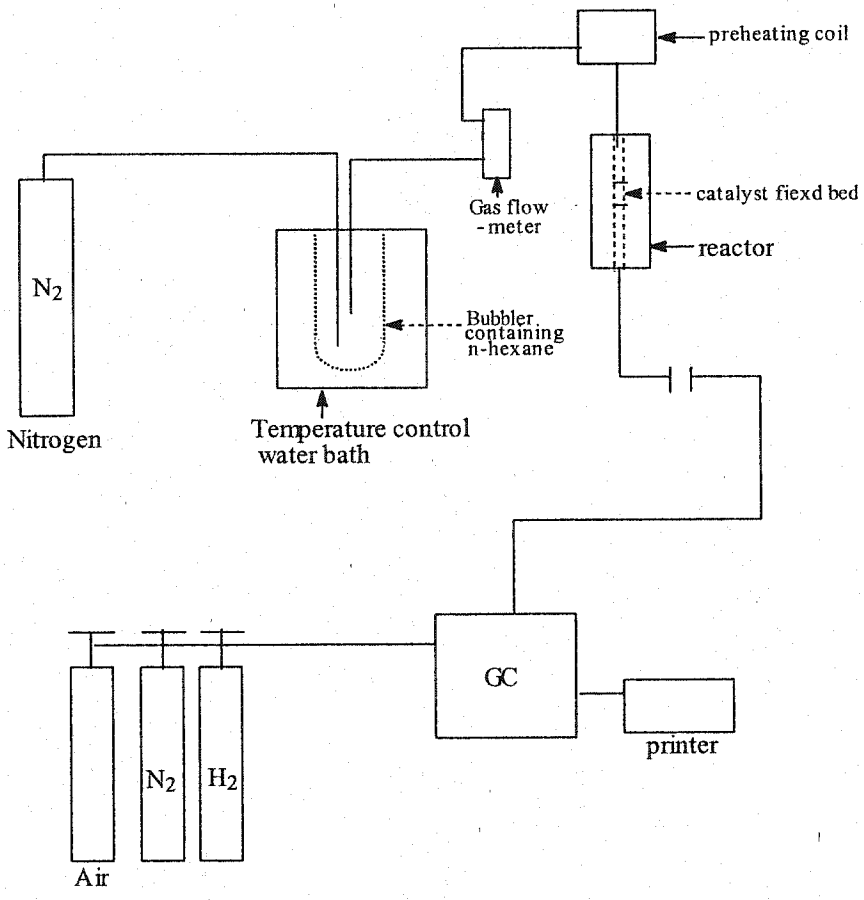

Figure 3.1 illustrating the experimental setup for the n-hexane cracking reaction.

(99.99 % purity). The reactions were carried out over 1.0g catalyst with varied temperature range of 180 °C – 450 °C, at 50 °C increment from 200 °C. The flow rate was randomly varied from 15.0 ml/min – 62.0 ml/min for the medium pores zeolites, while a smaller flow rate range of 1.0 ml/min – 8.0 ml/min for the mesoporous Ak samples. The operation was carried under atmospheric pressure.

3.6 Catalytic Evaluation and Activation

3.6.1 Catalyst Evaluation

The activity of the catalysts was evaluated by n-hexane cracking reactions, in a continuous flow reactor. This involves the preparation of the catalysts into granules, by subjecting the powder form of each catalyst into tablets under a 15 bar pressure. The tablets is crushed and sieved through a 1.17mm top and 500 micron as a bottom (BSS) mesh to obtain granules of 0.5 – 1.0 mm diameter range. 1.01g of the granules was placed between glass wool at the isothermal region of the fixed bed reactor. The rest part of the reactor was filled with carborandom inert silicon carbide granules. The feed containing a mixture of nitrogen and n-hexane was charged into the reactor from the bubbler containing n-hexane at 0 °C, through a flow meter into a preheating zone with a temperature of 100 °C and subsequently into the reactor. The gaseous cracked products was sampled and analyzed using a gas chromatography with an flame ionization detector (FID).

3.6.2 Catalyst Activation

The catalyst granules placed in the reactor was activated by passing nitrogen gas at 80.0ml/min over the catalyst, and raising the temperature of the reactor from room temperature to 773 K at 1.5 K/min for at least 6 hours. At the end of every cracking reaction run, the catalyst was reactivated at 500 °C for at least 3 hours before the next run. However, the activation & reactivation of the Ak catalysts and the modified forms of it was carried out at the operation temperatures (maximum 300 °C) using nitrogen flow of 5.0ml/min.

CHAPTER 4

RESULTS AND DISCUSSION

4.1 XRD Analysis of Ak samples

The Ak aluminosilicate mesoporous materials synthesized were characterized by a broadband at low angles in the XRD spectrum $2\theta < 6.0$, which agreed with the literature.[36-40] From the XRD spectra (figure 4.1) calcined Ak3, Ak4 & Ak7 showed a well defined hexagonal pattern, whereas Ak5 and Ak1 showed less ordered pore packing. This may be attributed to the slight difference in the synthesis condition. The intensities of reflections and resolutions of diffraction pattern is substantially decreased. With increasing Al content (see table 4.1)

4. 2 Elemental Composition Analysis of As-synthesized Alumino-silicate Ak samples

The weight % of the oxides of silicon, aluminum, and sodium is shown in table 4.1, determined by ICP - AES and AAS. The silica to alumina corresponded well with the composition of the initial hydrogel precursor. As seen the total weights of the inorganic framework plus the weight loss on ignition added up to

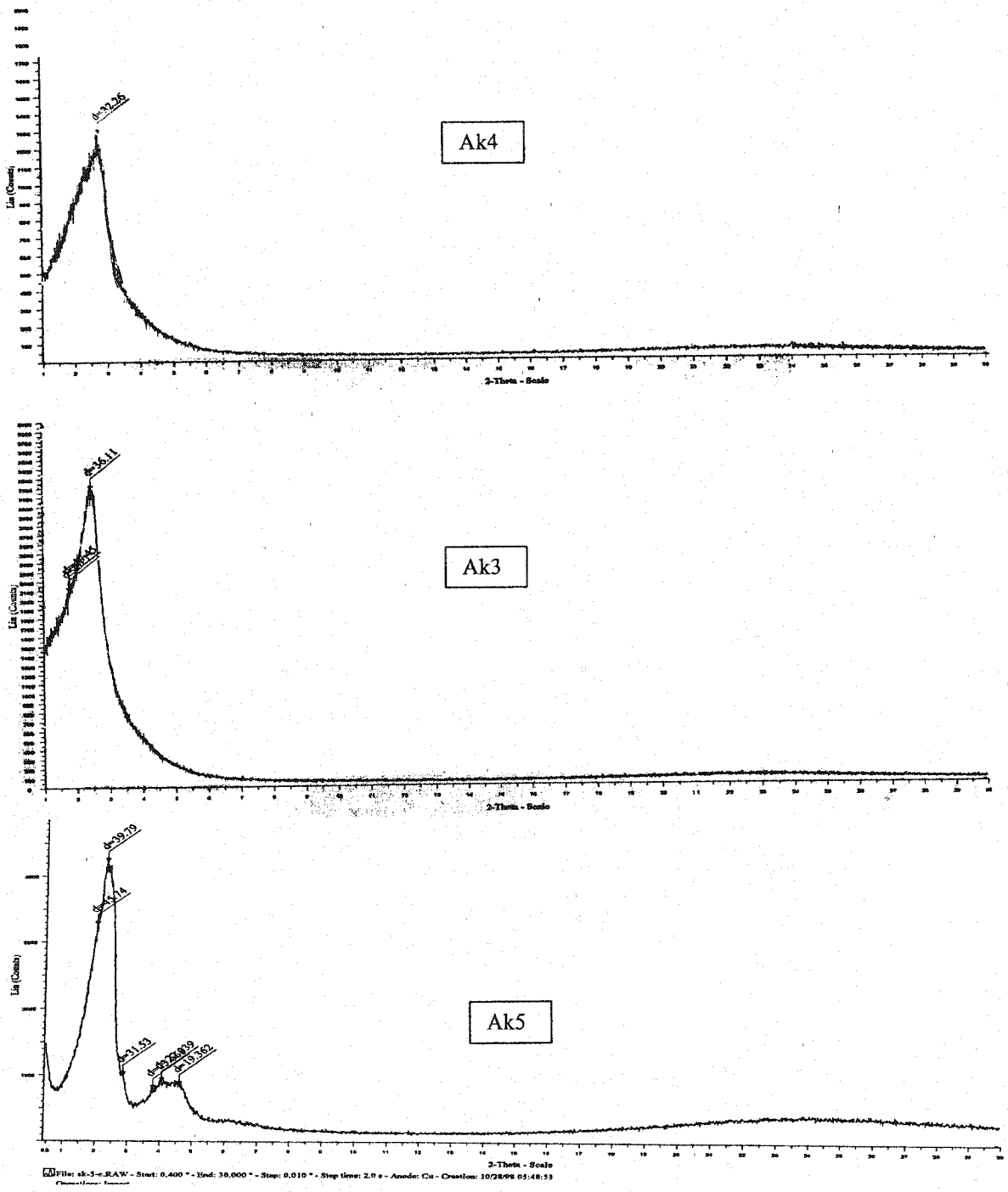

Figure **4.1a** XRD pattern of calcined Ak3, Ak4 and Ak5 MCM-41 catalysts.

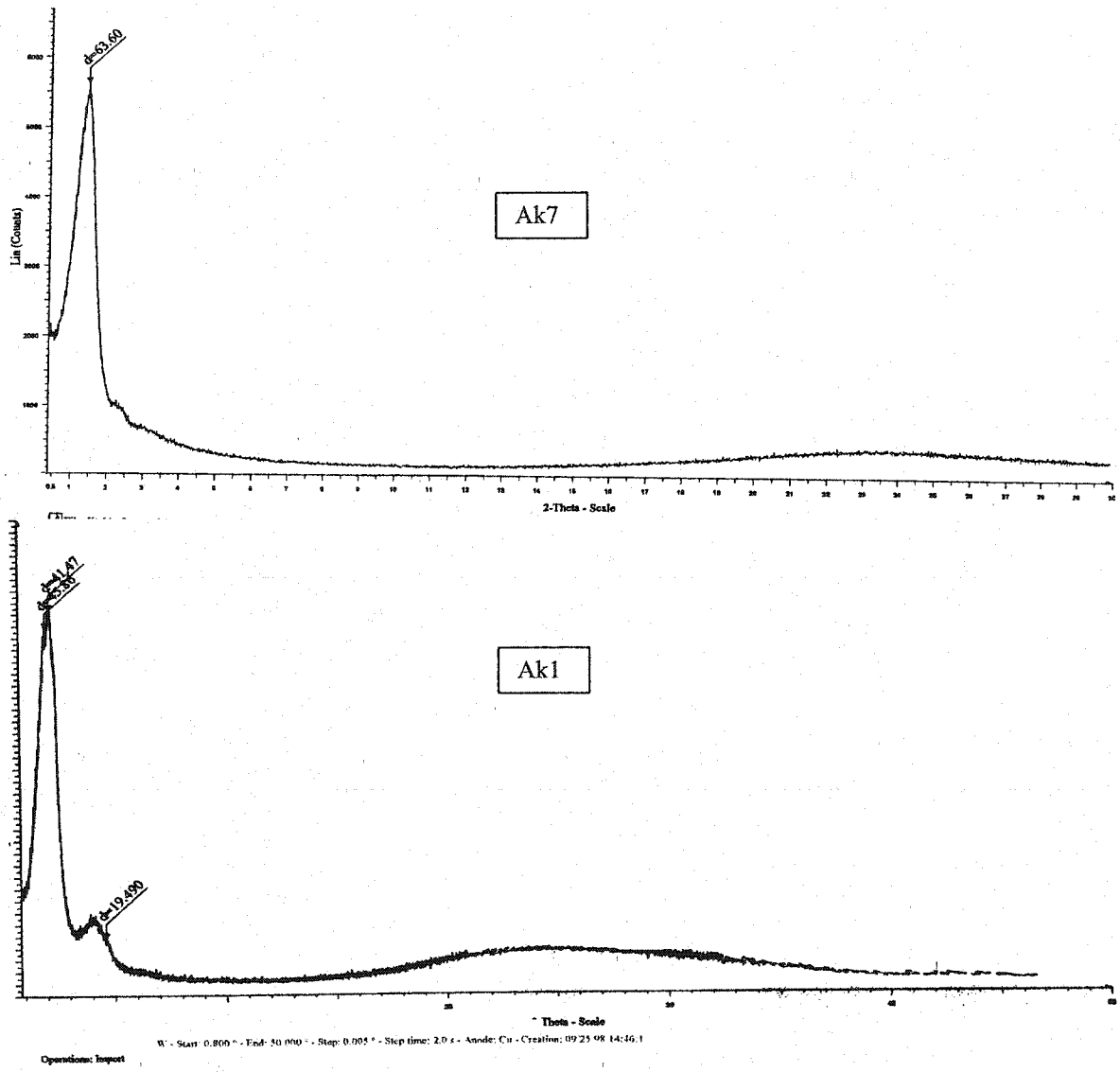

Figure **4.1b** XRD pattern of calcined Ak1 and Ak7 MCM-41 catalysts.

Table 4.1

ICP-AES chemical analysis of as-synthesized aluminosilicate mesoporous catalysts.

Sample ID	Na_2O (wt%)	Al_2O_3 (wt %)	SiO_2 (wt%)	LOI (wt%)	ICP-AS SiO_2/Al_2O_3	Hydrogel Composition
Ak3	2.28	5.82	41.59	49.69	7.15	7.75
Ak4	4.1	10.13	47.67	61.9	4.71	5.99
Ak5	0.13	1.88	38.46	40.47	20.46	23.38
Ak7	1.31	4.32	47.5	53.13	11.00	11.41

Table 4.2

The apparent activation energies of n-hexane cracking over 1.01g of each molecular sieves - used at 1 atm.

Type of catalyst	Ea (KJ/mol)
A-ZSM	72.55
Ak8-T	59.49
Theta-1	50.29
CR-ZSM-5	47.79
Ak8-ZSM-5	41.18
ZSM-5	39.04

Close to 100 % reflecting the high accuracy of the analyses. The weight loss on ignition was assumed to correspond to the organic template occluded in the crystalline materials.

4.3 NMR Spectra of Ak catalysts

^{27}Al MAS NMR spectra of the as-synthesized Ak mesoporous catalysts are clearly dominated by the signal in the range of 53 – 55 ppm as shown in figure 4.2, which is a characteristic of tetrahedrally coordinated Al sites. Thus, the incorporation of most of the aluminum into tetrahedral positions in the framework didn't reflect any significant difference between the Ak 7 synthesis methods, a literature based method and the in house modified synthesis conditions for the remaining Ak catalysts (Ak1, Ak3, Ak4 & Ak5).

Calcination and transformation of the Ak catalysts into the protonated form, results in the shift of the ^{27}Al NMR signal of the Ak catalysts to a lower value by ~1.5 ppm from the as-synthesized value for each catalyst as show in figure 4.3. Broad shoulder of the peaks observed for H-Ak3 and H-Ak7 spectra, may mean the presence of various types of aluminum coordinated group, such as penta-coordinated Al, octahedral coordinated Al etc which are extra-framework aluminum. H-Ak7 showed a peak at –3.29 ppm attributed to the presence of octahedral incorporated aluminum $(Al^{VI})^{(100)}$ in addition to the tetrahedral incorporated aluminum at 53.5 ppm. Other Ak catalysts showed only a single peak at a range of 51.67 – 52.85 ppm indicating a tetrahedral incorporated

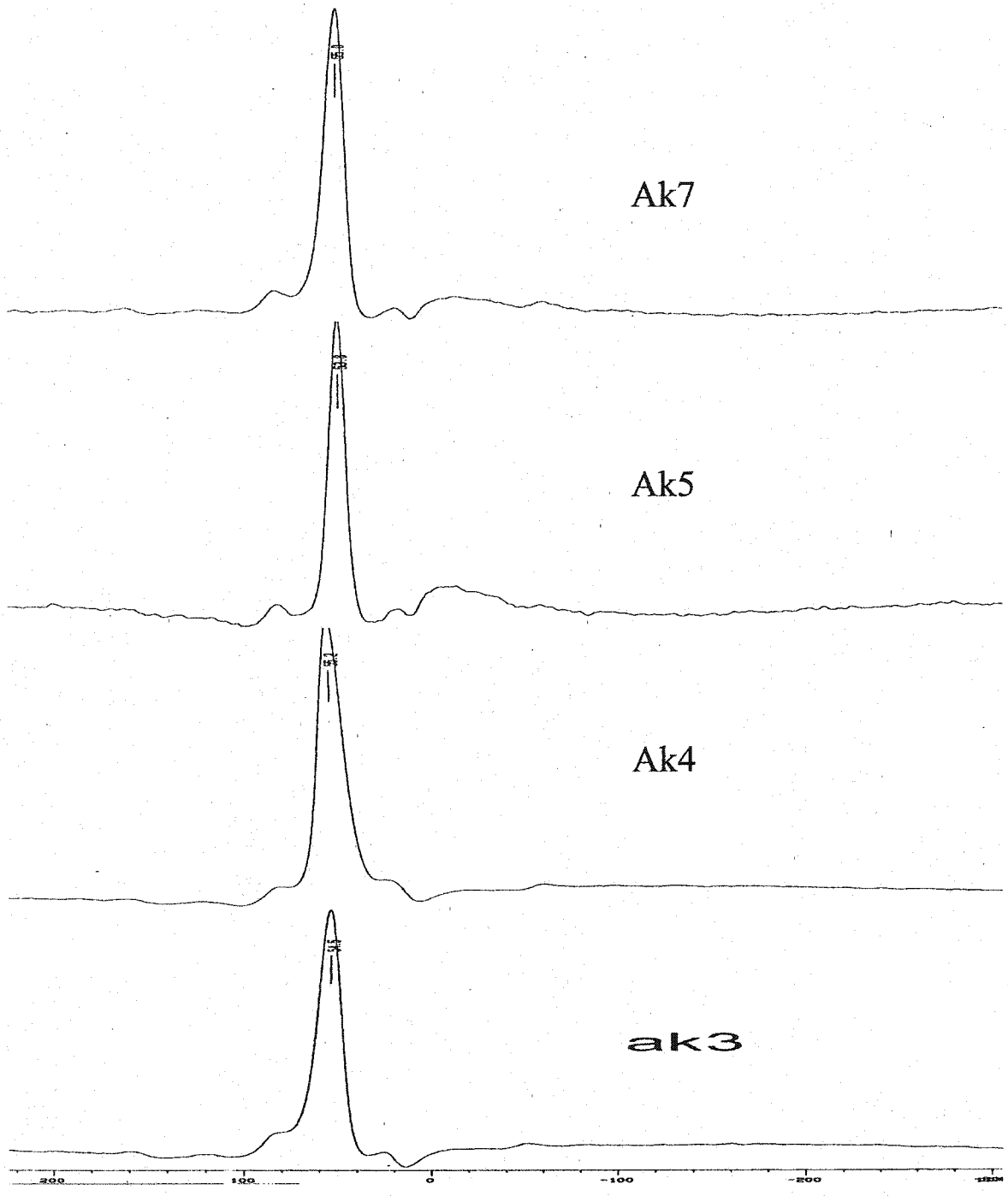

Figure **4.2a,** ^{27}Al NMR spectra of as-synthesized Ak mesoporous catalysts.

aluminum. The presence of two peaks in the H-Ak7 spectra, compared with the rest Ak catalyst analyzed, may be attributed to the difference in the synthesis Procedure, compared to the modified synthesis method, which showed no change in the framework composition of the as-synthesized and calcined Ak catalysts.

The ^{29}Si NMR spectra of the Ak catalysts did not show any significant difference between the as-synthesized and calcined form. However, a characteristic broad spectra indicating less ordered pore packing (that is more defect in the wall of the catalyst) was observed at –90 ppm to –115 ppm.

The ^{29}Si NMR spectra of calcined ZSM-5 and Theta-1 catalysts were also observed in the same region as Ak catalyst, with less broad spectra compared to Ak catalysts. This may be due to the more ordered pore packing and well formed wall of the microporous zeolites. The presence of signal at about 116.0 ppm, 112.4 ppm and 106.0 ppm may be assigned to the Si(0Al), Si(1Al), and Si(2Al) sites respectively.

Similar spectra values and range like the Ak catalysts was also observed for Theta-1 and ZSM-5 using the ^{27}Al NMR, with both catalyst having sharp peak values of 55.3 ppm and 51.66 ppm respectively. This is assigned to Al $^{(IV)}$ species indicating that it is incorporated into the framework of the catalyst. However, a pronounced peak is observed for both catalysts at around 0 ppm, which again indicates the presence of extra framework Al $^{(VI)}$ in the catalysts.

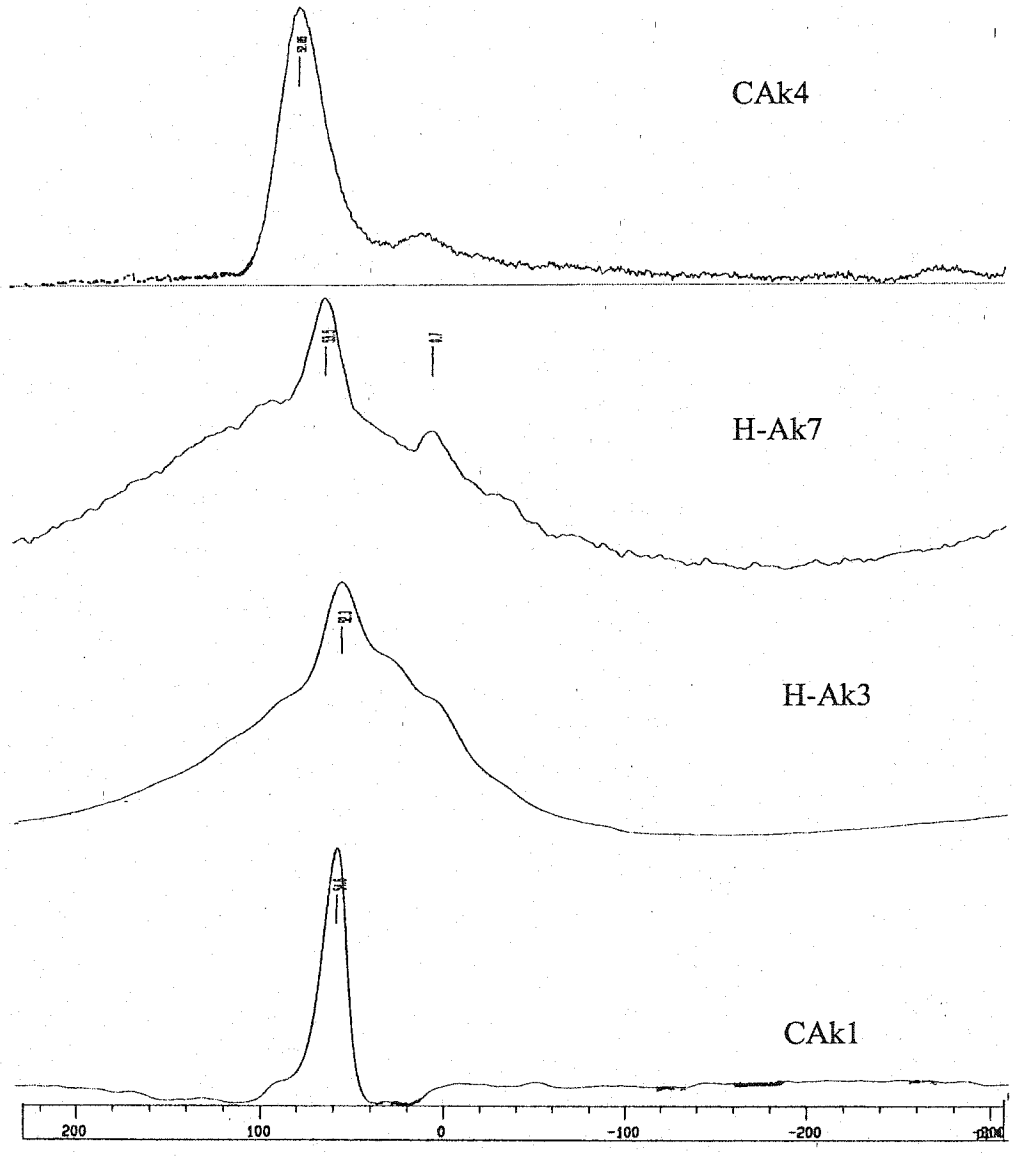

Figure **4.2b** ^{27}Al NMR spectra of calcined Ak mesoporous catalysts.

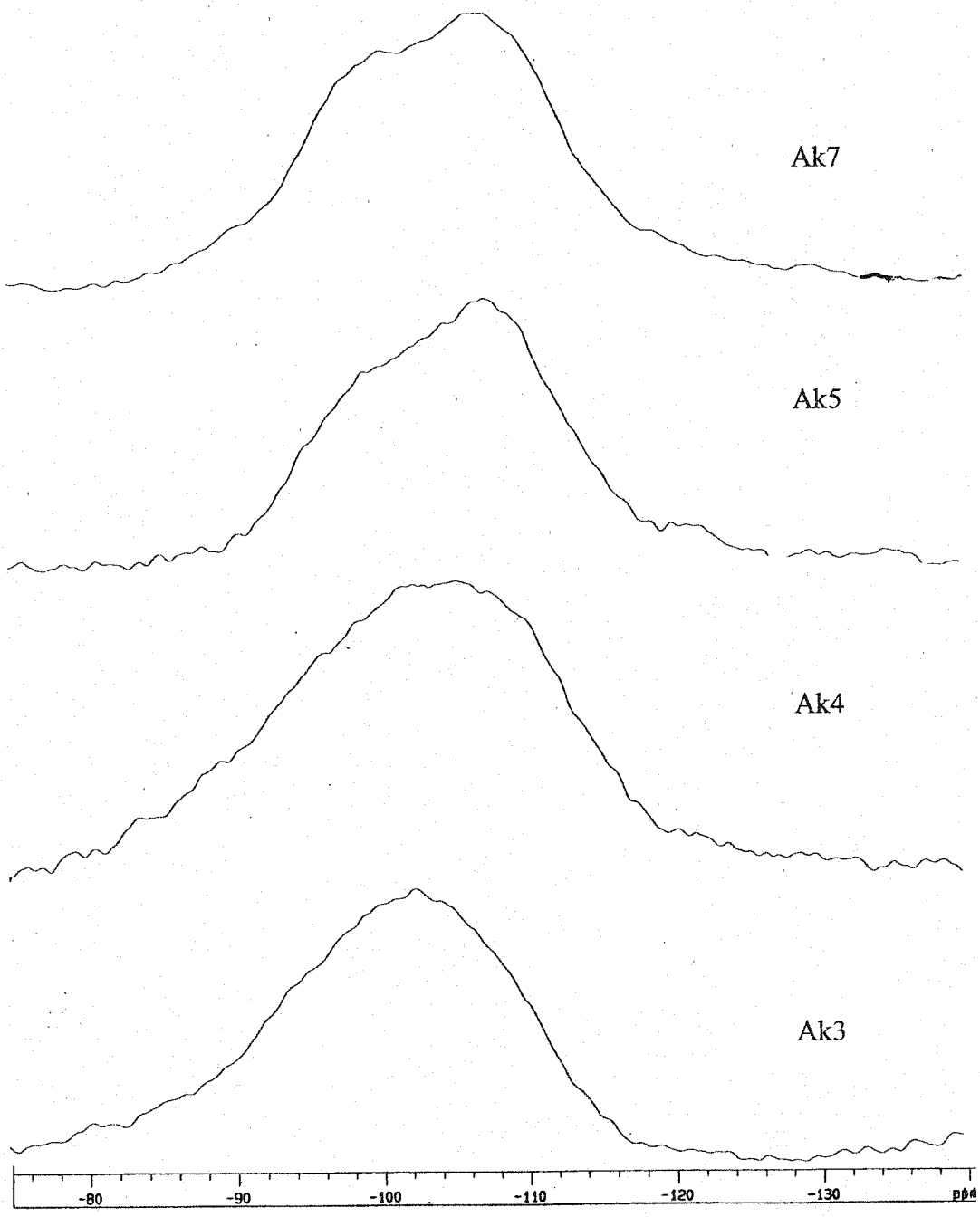

Figure **4.2c** ^{29}Si NMR spectra of as-synthesized Ak mesoporous catalysts.

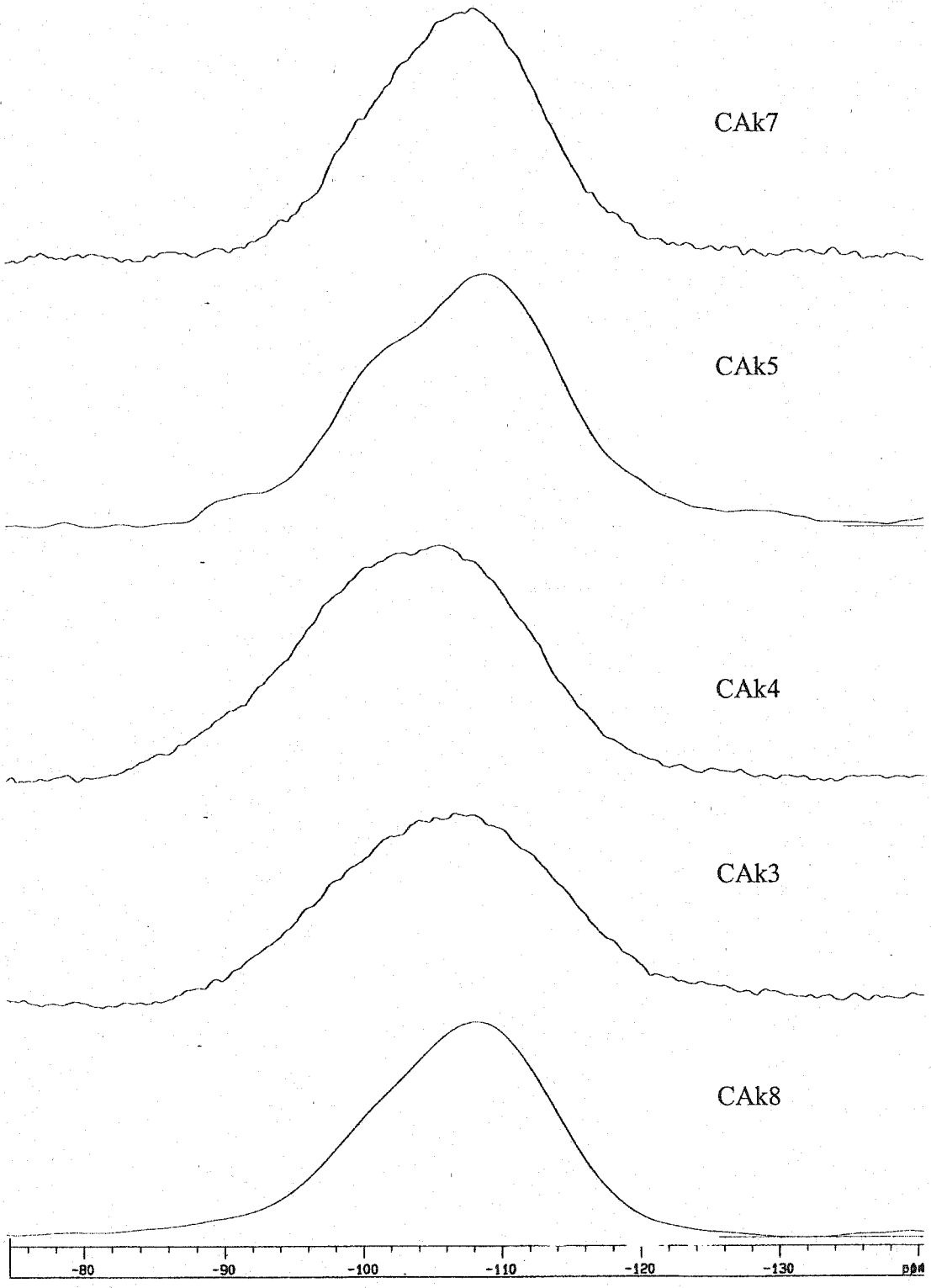

Figure **4.2d** ^{29}SiNMR spectra of calcined Ak mesoporous catalysts.

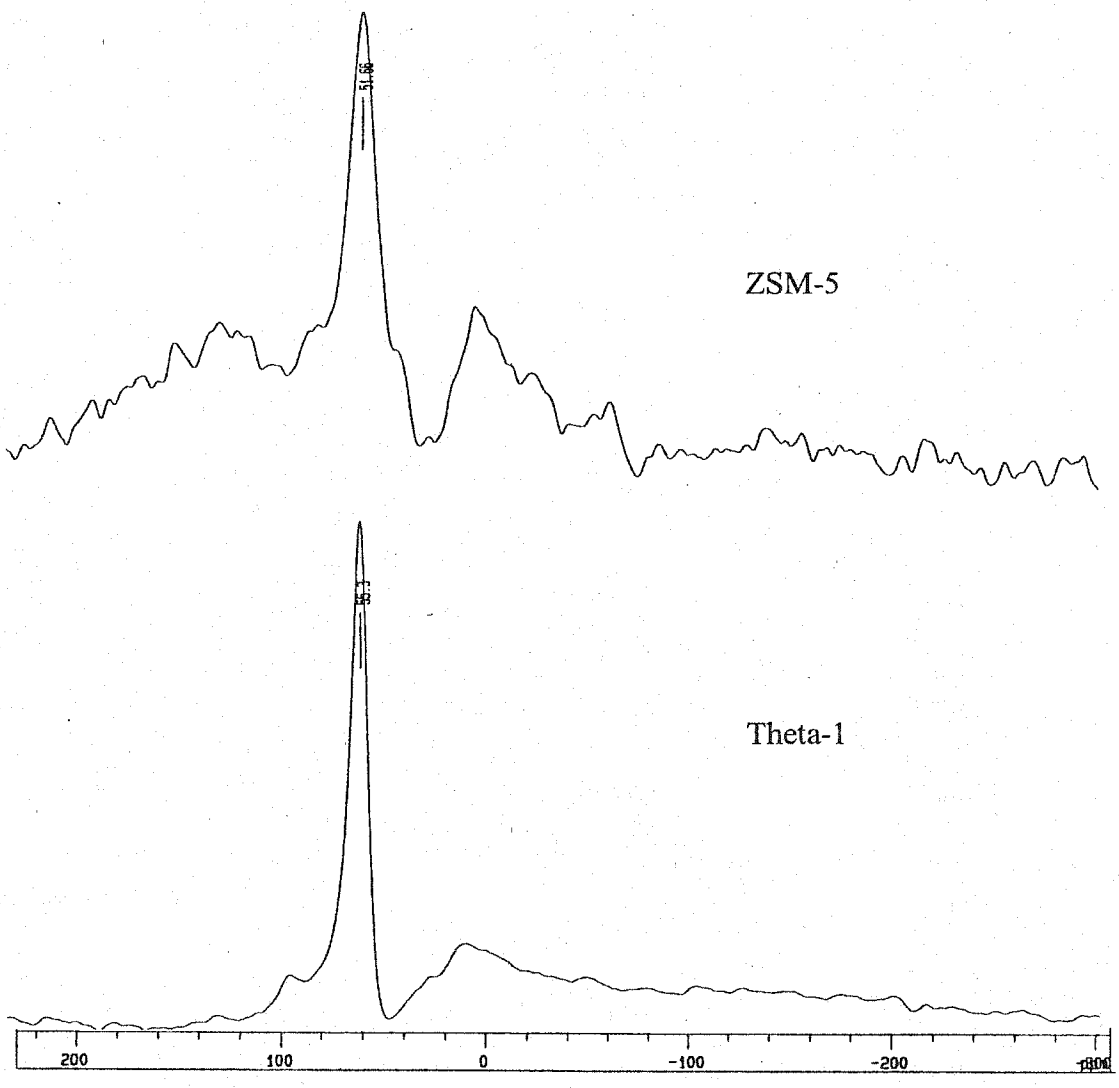

Figure **4.2e** ^{27}Al NMR Spectra of calcined medium pore zeolites (Si/Al = 50)

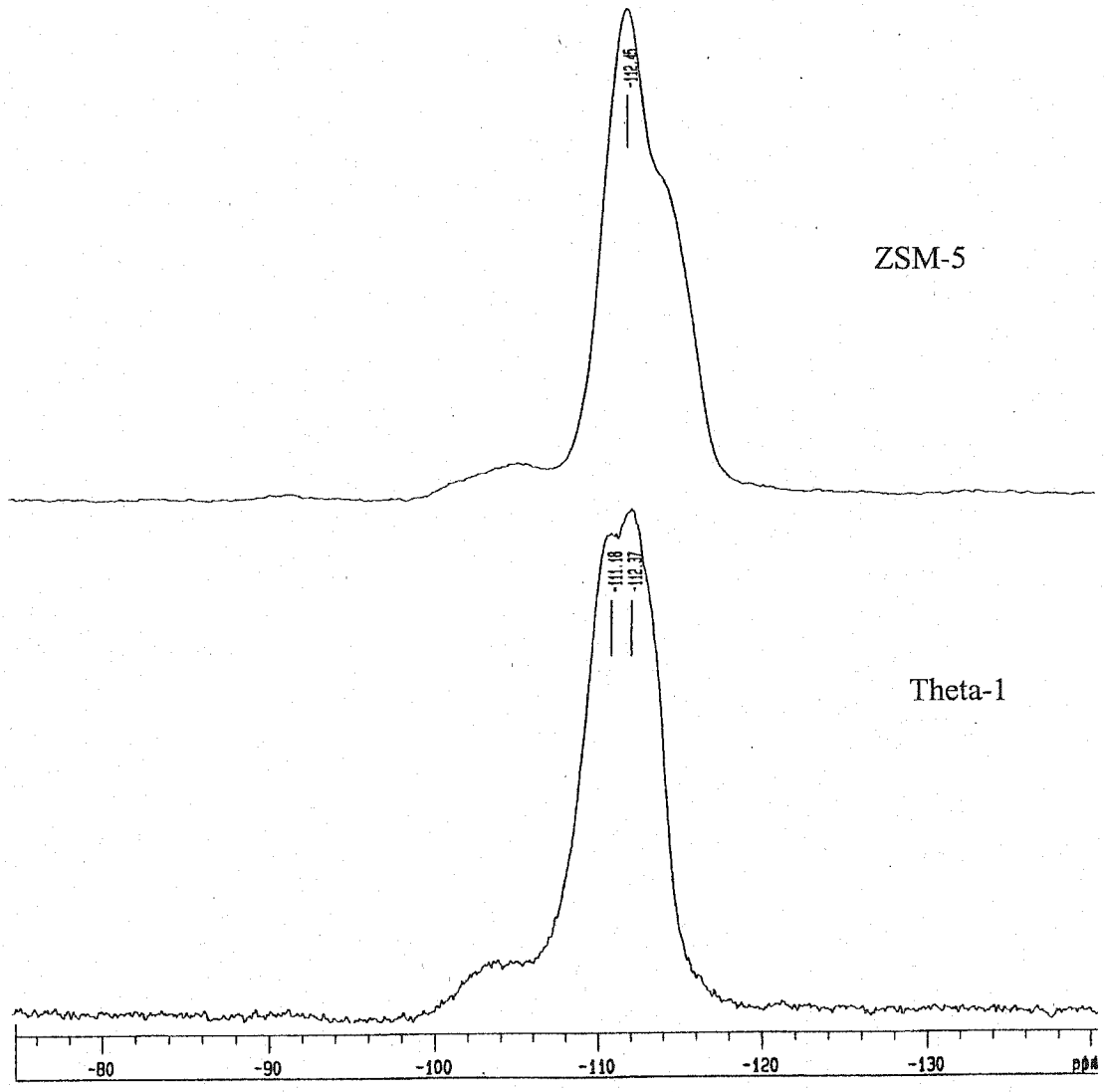

Figure **4.2f,** ^{29}Si NMR spectra of calcined medium pore zeolites (Si/Al = 50)

4. 4 *n*-Hexane Cracking Activity

The activity plot of n-hexane cracking reaction over ZSM-5 catalyst with (Si/Al = 50) using the well known equation (K= -ln(1-x) * WHSV), where x is the % fractional conversion of hexane, showed a linear plot which passed through the origin when -ln(1-x) was plotted against 1/WHSV. This indicated that the cracking rate is first order in n-hexane cracking, even at temperatures lower than 300 °C (180 °C, 200 °C, and 250 °C). Thus secondary reaction do not affect the hexane cracking rate under the experimental condition, since the secondary reaction involves primarily alkene products which are known to be many magnitude faster than alkane cracking. From figure 4.3, it is clear that as the temperature of reaction increases, the activity of the catalyst also increases due to increase in the acid strength, and decreases with increase in space velocity. The result obtained agreed with the literature [11,13,25,46,84] and in the same view, the cracking activity of Ak8-ZSM-5, Theta-1, Ak8-T, A-ZSM-5, and CR-ZSM-5 catalysts can be considered to be first order in n-hexane as shown in figures 4.3-4.8. The same trend of catalyst cracking activity was observed at the operational condition used 180 - 450 °C, 15 - 65 ml/min range flow rates, randomly chosen with high conversion (>30 %). The cracking reaction was attributed to mainly the catalysts used, with no thermal contribution observed at the condition of reaction used.

There was no significant deactivation observed at the experimental conditions used, which involves the increase of flow rates at a fixed temperature with a check on the deactivation by randomly returning to a flow rate earlier used

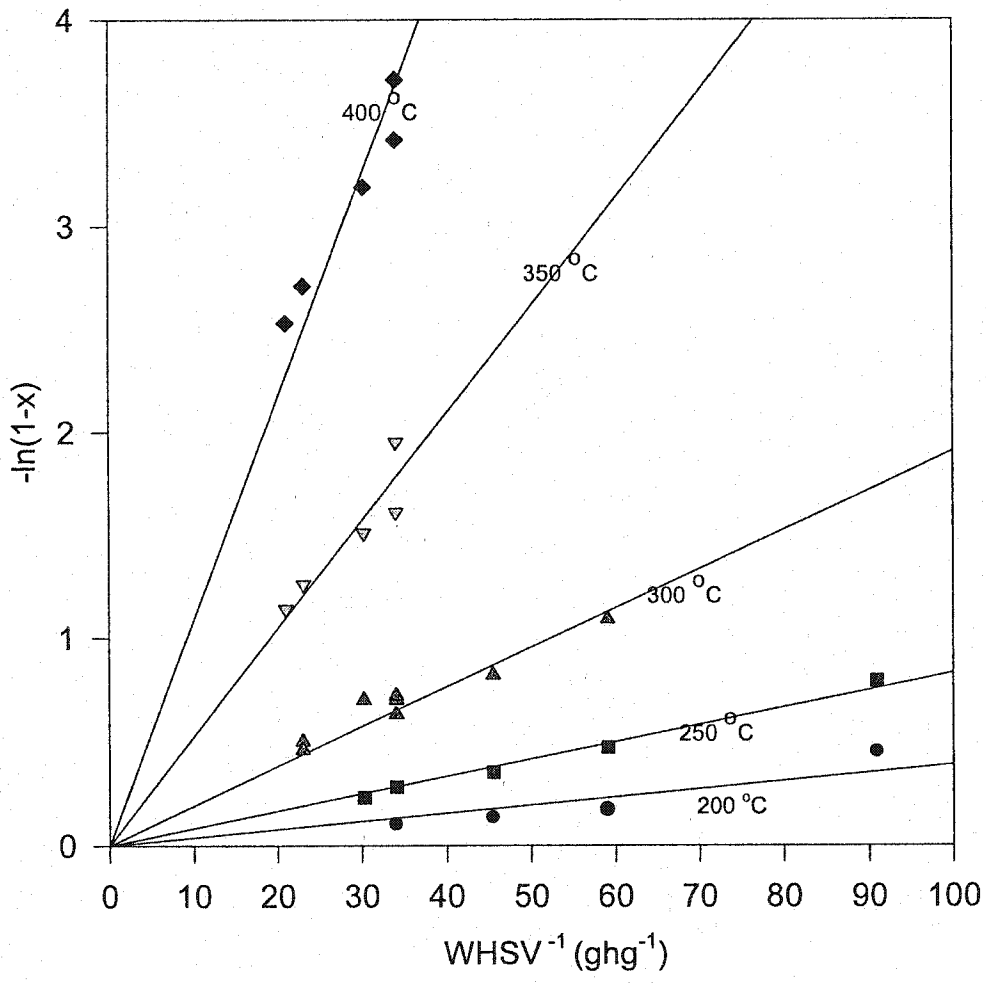

Figure 4.3 A plot of -ln(1-x) vs 1/WHSV of hexane cracking over 1.01g ZSM-5 catalyst.

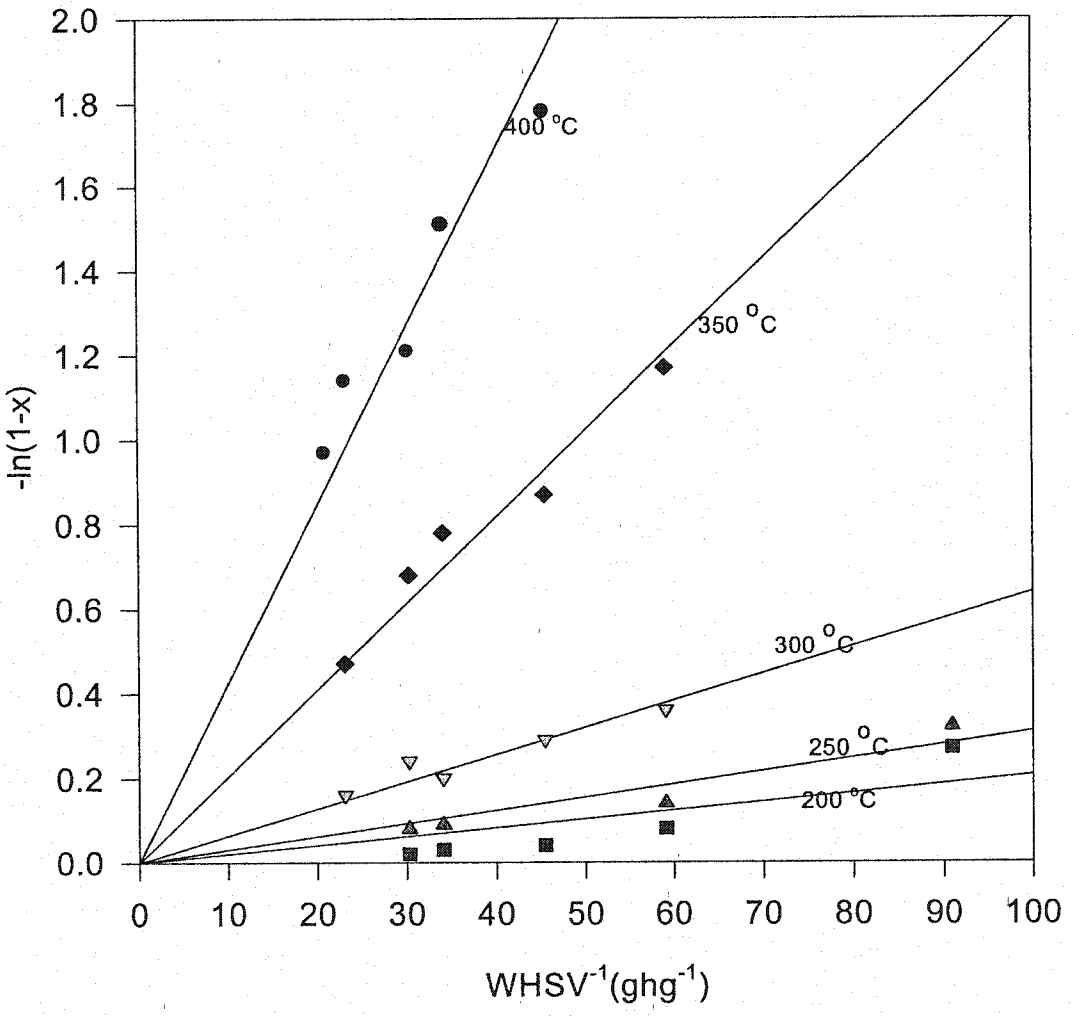

Figure 4.4 A plot of -ln(1-x) against 1/WHSV of n-hexane cracking over 1.01g Theta-1 catalyst.

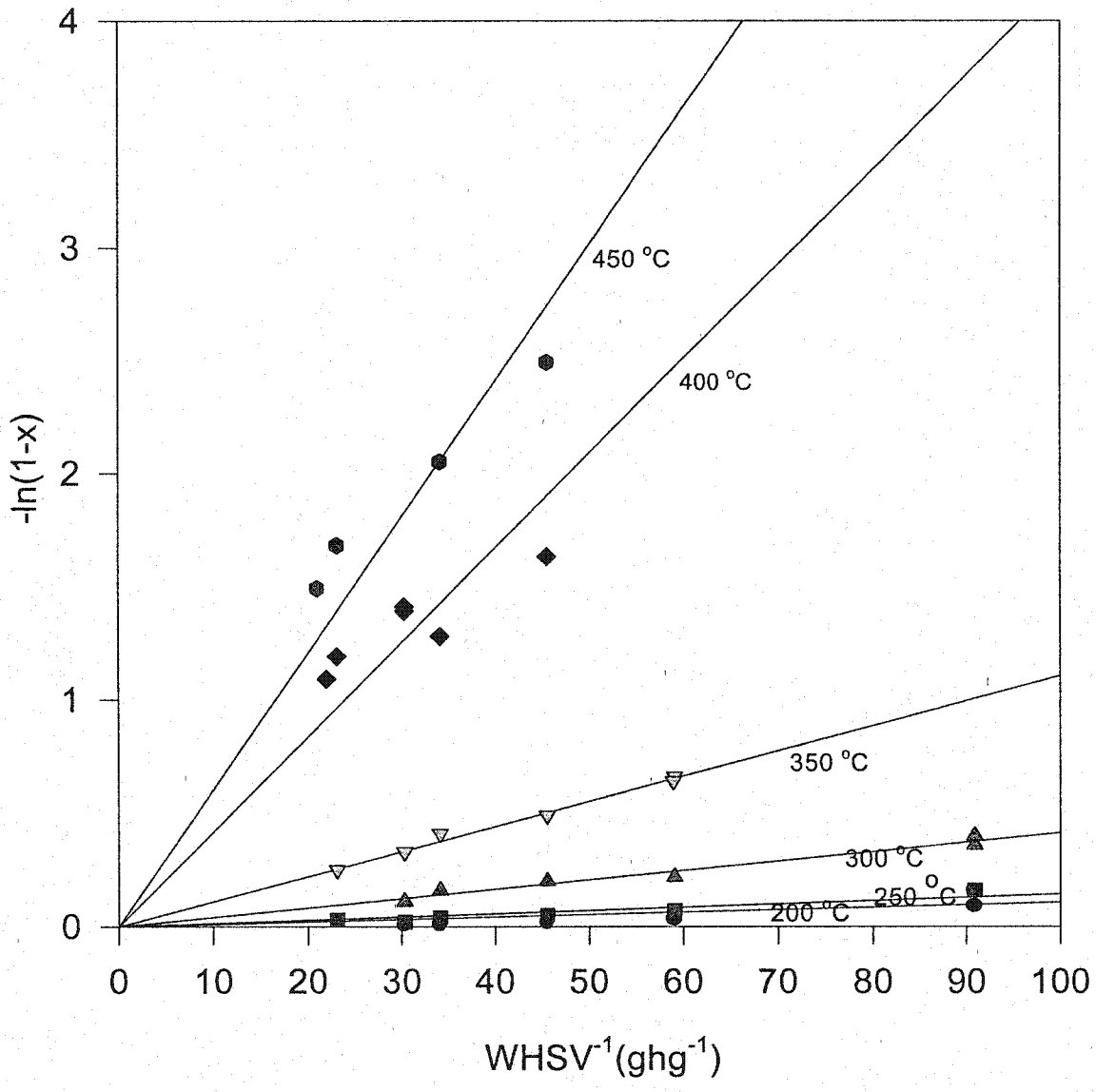

Figure 4.5 A plot of -ln(1-x) against 1/WHSV of n-hexane cracking over 1.01g AK8-ZSM-5 catalyst.

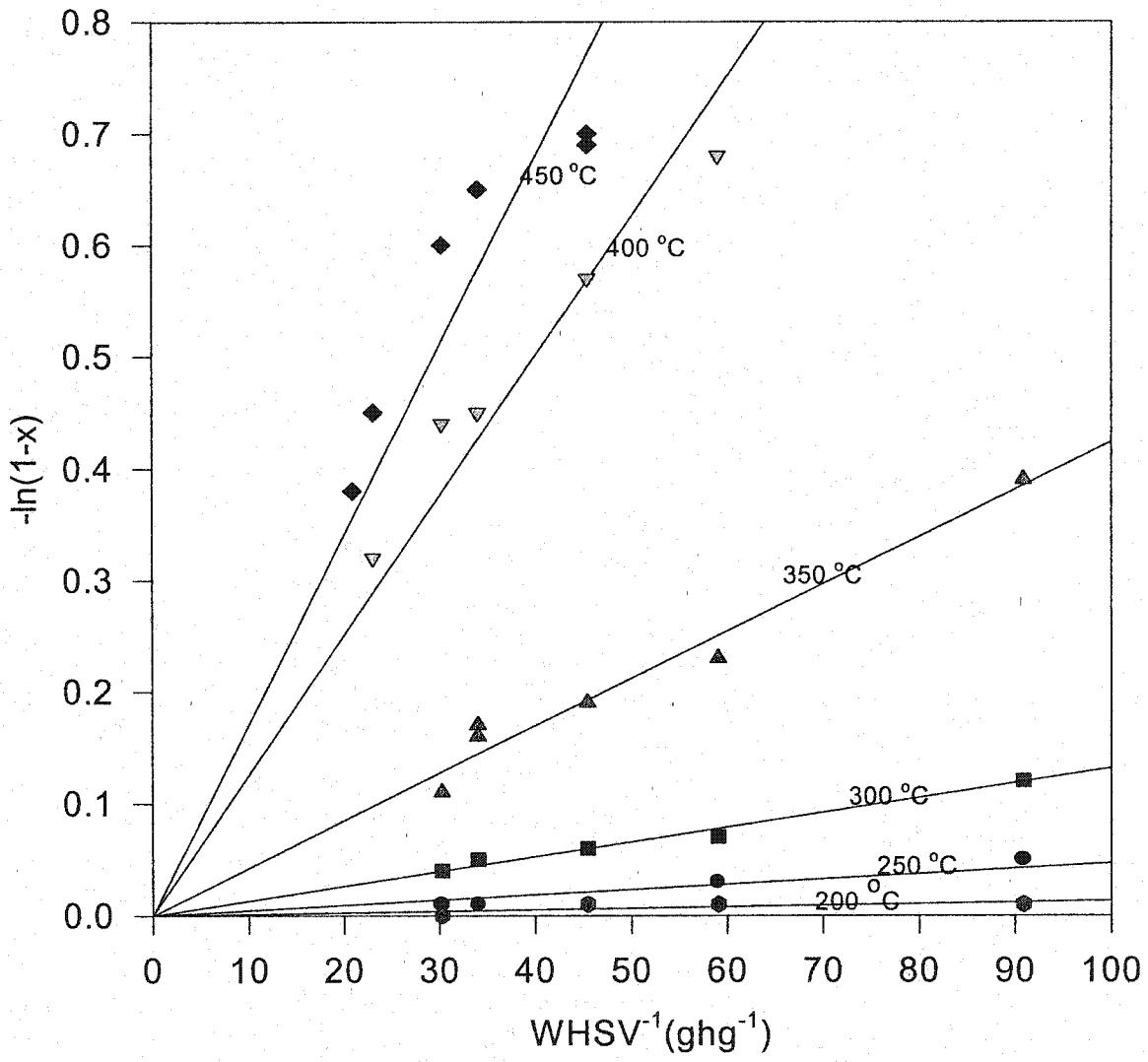

Figure 4.6 A plot of -ln(1-x) against 1/WHSV of n-hexane cracking over 1.01g Ak8-Theta-1 catalyst.

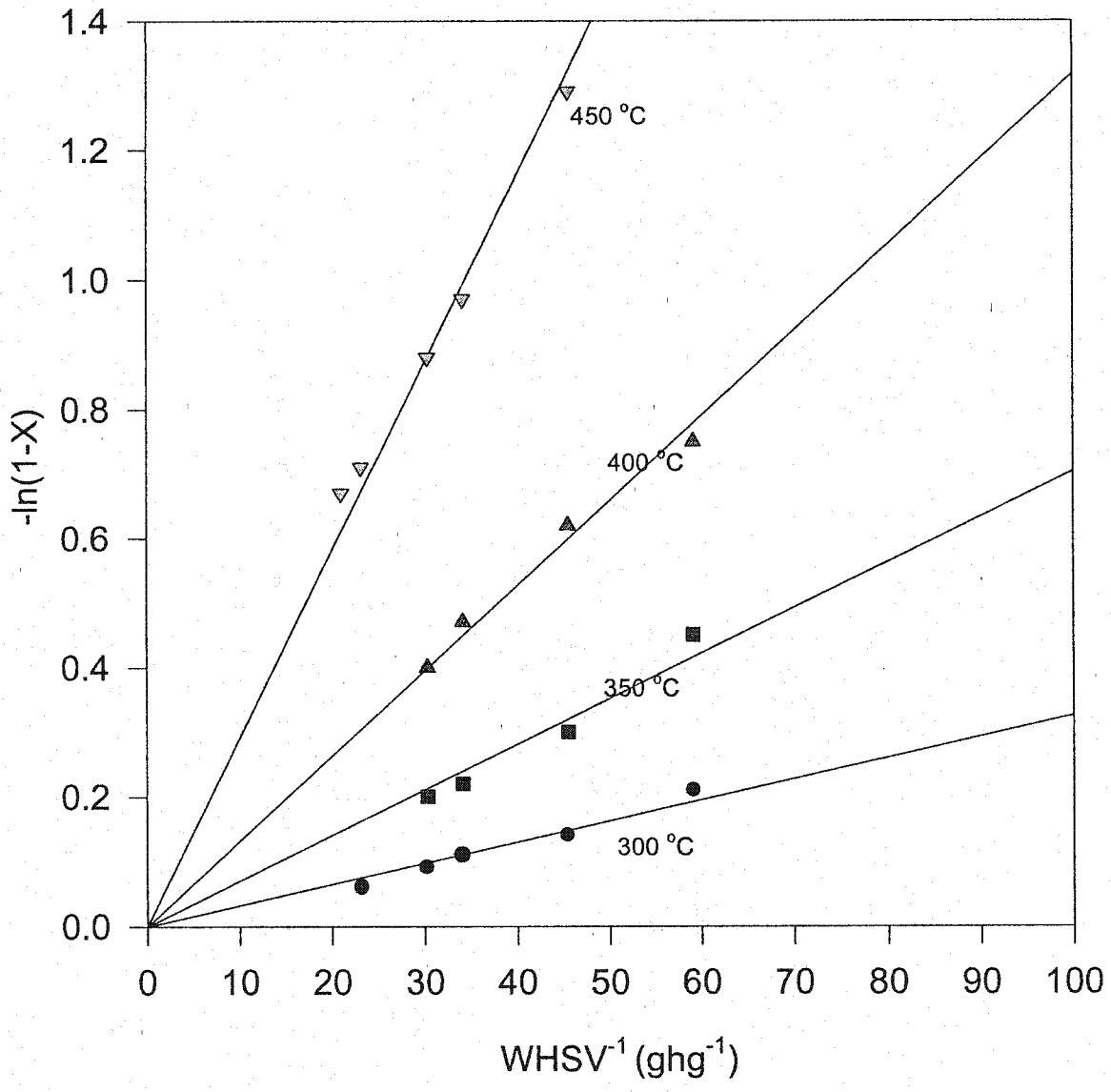

Figure 4.7 A plot of -ln(1-x) against 1/WHSV of n-hexane cracking over 1.01g CR-ZSM-5 catalyst.

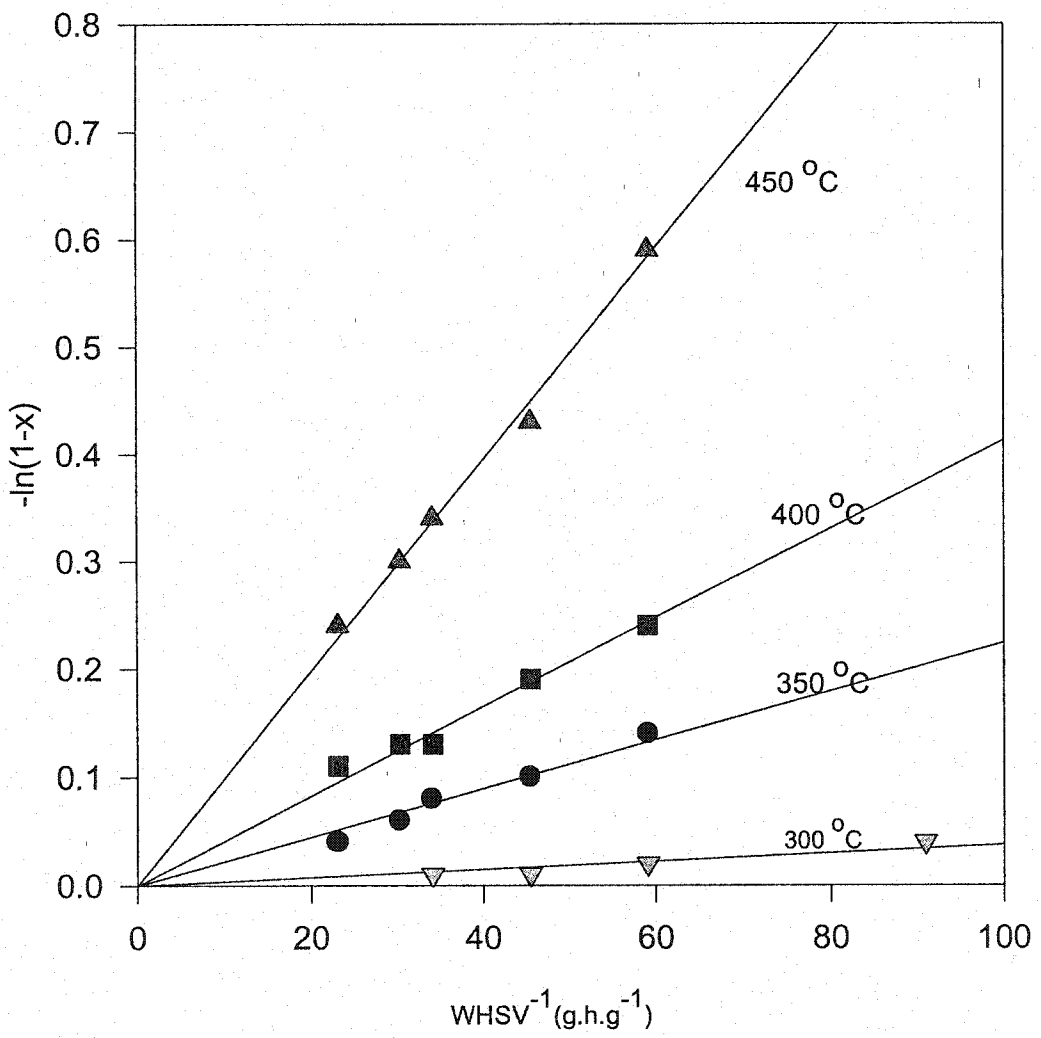

Figure 4.8 A plot of -ln(1-x) against 1/WHSV of n-hexane cracking over 1.01g A-ZSM-5 catalyst.

in the run. The results obtained are reproducible indicating that a steady state activity was achieved during the catalytic cracking reaction at fixed temperature.

The effect of the catalyst structure (pore dimension and channel structure) of the aluminosilicate materials in the cracking of hexane was further investigated under the same experimental condition as ZSM-5. The cracking activity of Theta-1 was found to be lower than ZSM-5 as shown in figure 4.9a - 4.9c, even though both are medium pore zeolites having the same Si/Al ratio of 50. An explanation for this trend can be ascribed to the structural effect of the catalyst that determined the proportion of the reaction route that will prevail at a fixed reaction temperature. The 1-D channel structure of theta-1 catalyst favors the protolytic cracking route known to require high activation energy and temperature to occur, resulting in lower turn over frequency of cracking, compared to the ZSM-5 catalyst having an interconnecting 2-D channel structure that favors more secondary reaction which required lower activation energy and temperature to occur.

Ak8 is an all silica mesoporous material with no cracking activity due to the absence of strong Bronsted acid sites as a result of the zero aluminum in the catalyst. However Ak8 serves as a diluent in the admixture catalyst Ak8-ZSM and Ak8-T as reflected in the activity of the catalysts (shown in figure 4.9a - 4.9c), and found to be lower as compared to pure ZSM-5 and Theta-1 catalyst respectively. The activation energy of ZSM-5 & Ak8-ZSM, Ak8-T and Theta-1 are about the same respectively as shown in table 4.8, indicating that Ak8 has no significant effect on the intrinsic activity of the catalyst.

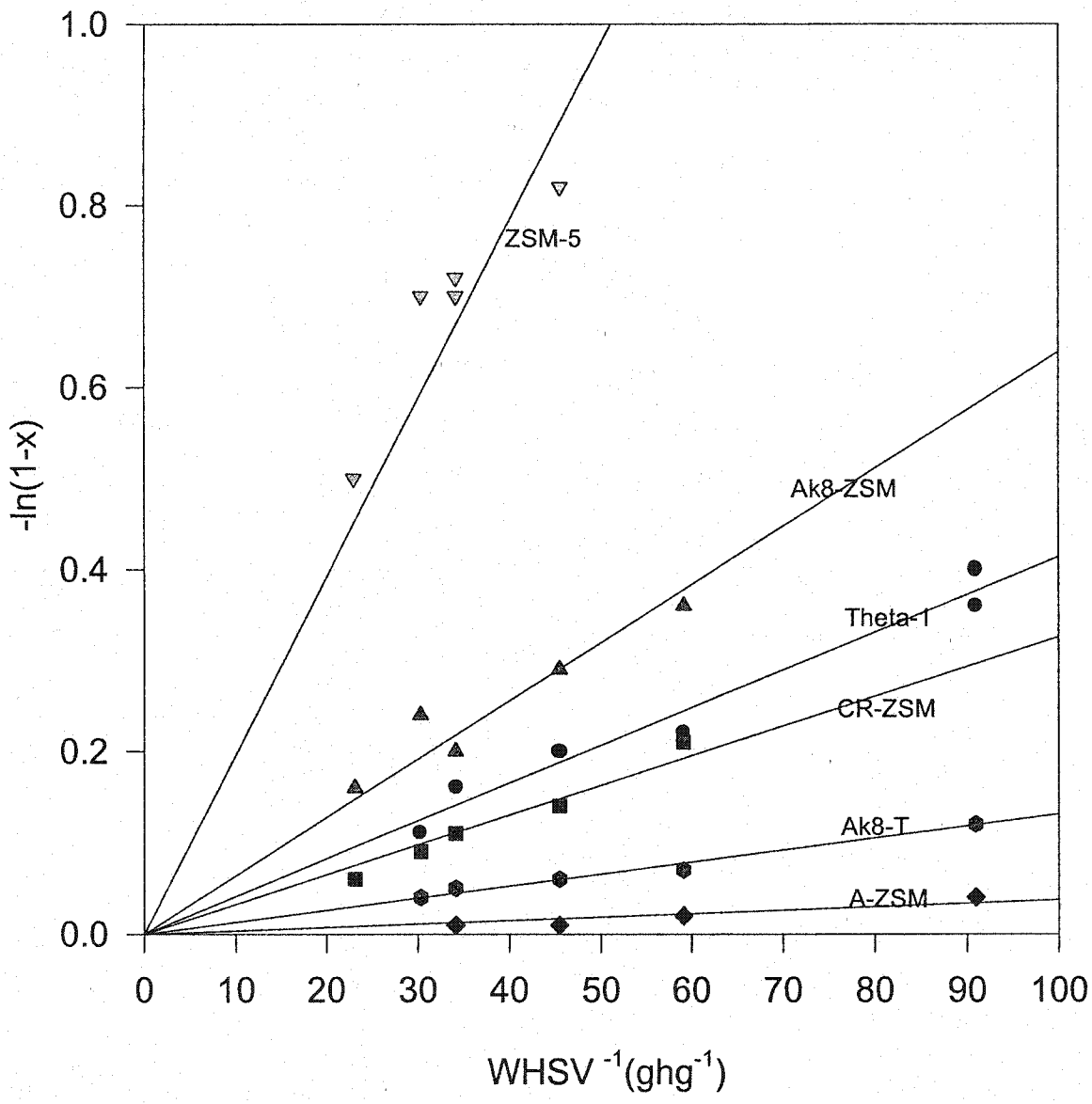

Figure 4.9a, A plot of -ln(1-x) against 1/WHSV of n-hexane cracking at 300 °C of catalysts with varied composition.

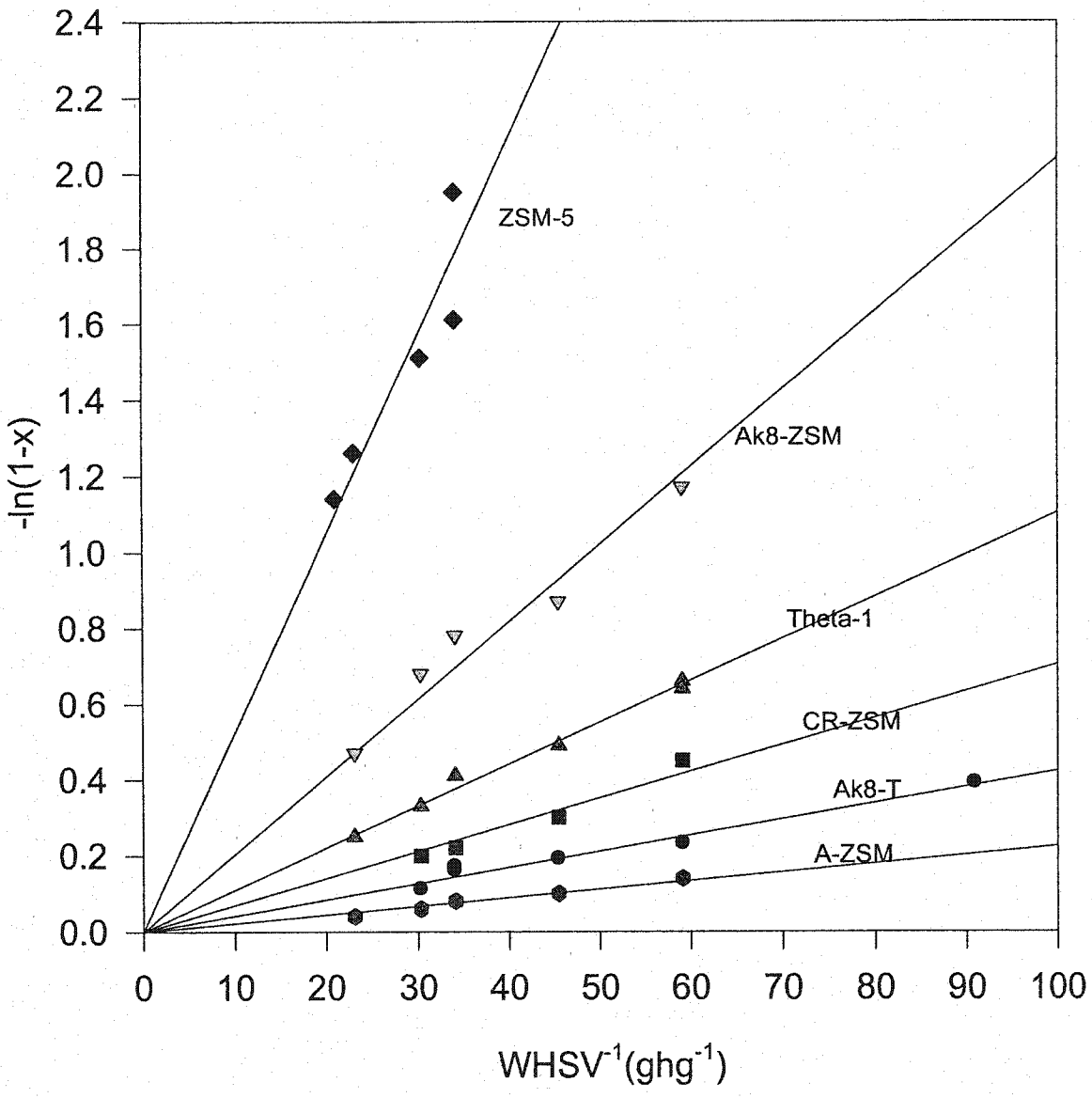

Figure 4.9b, A plot of -ln(1-x) against 1/WHSV of n-hexane cracking at 350 °C with catalysts of varied composition.

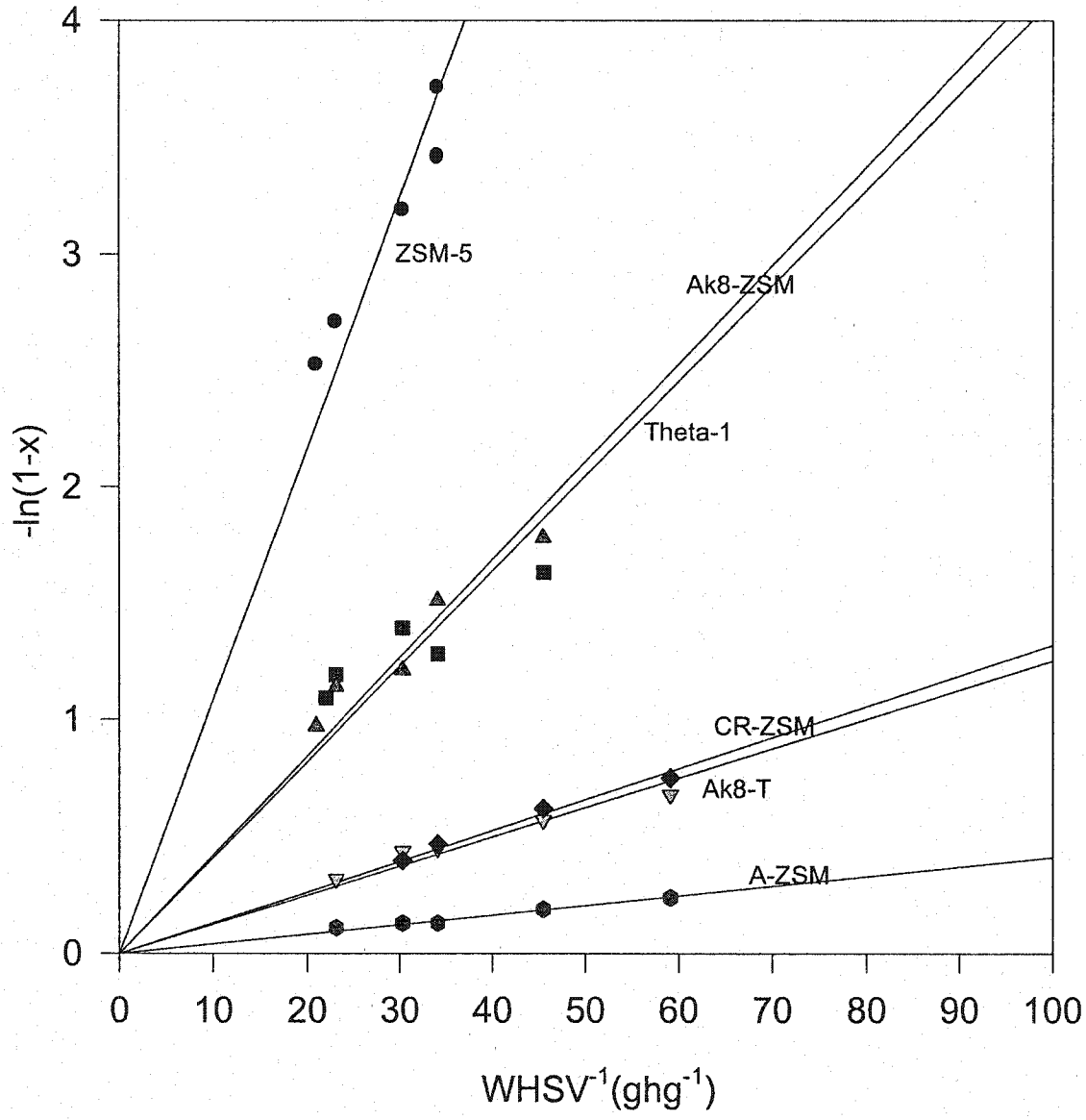

Figure 4.9c, A plot of -ln(1-x) against 1/WHSV at 400 °C of hexane cracking over catalysts with varied composition.

The effect of the carborandum and amorphous silica in the admixture CR-ZSM and A-ZSM signified the importance of having crystalline porous molecular sieve to enhance the cracking activity of a catalyst. Thus the low cracking activity of A-ZSM and CR-ZSM as indicated in figures 4.9a - 4.9c can be explained on the basis of poor hexane accessibility to the active site during cracking due to the non-porous nature of the amorphous and carborandum materials.

The apparent rate constant was determined from the slope of the curve - ln(1-x) vs 1/WHSV for each of the six catalysts, with ZSM-5 having the highest value while A-ZSM showed the lowest value with respect to the ZSM-5 type catalyst. In addition to the earlier stated factors that might have been responsible for the differences in the cracking activity of the catalysts is the "nest effect". The "nest effect" [96,97] states that molecules and the internal structure of a zeolite pore will interact in a manner that maximize their van der waal attraction energy. That is, the pore diameter with sizes close to the critical diameter or van der waal diameters of an adsorbing molecule will interact more strongly than with larger pore sizes with same molecules. The pore diameter of ZSM-5 is 5.3 x 5.6Å, closer to the critical diameter of linear alkane chains (4.6 Å).

Unlike the medium pore zeolites that have been characterized and known to exhibit a first order reaction kinetic, Ak4 materials (mesoporous catalyst) were tested for *n*-hexane cracking at high temperatures (400 °C & 500 °C) and flow rates range of 20 ml/min to 120 ml/min. A plot of –ln(1-x) against $WHSV^{-1}$ as shown in figure 4.10a, gave a none linear curve that did not pass through the

origin. However, below 400 °C, there was no cracking reaction observed for all the Ak catalyst at high flow rates (20 - 100 ml/min). The thermal contribution of the catalyst activity at such high temperature can be considered minimal, since iso-hexane of the feed didn't undergo any significant conversion at the operational conditions for the Ak4 catalyst. At temperatures less than 350 °C and low flow rate (<10ml/min), a plot of -ln(1-x) against $WHSV^{-1}$ showed linearity for all the Ak catalyst tested as shown in figure 4.10b, with non of the plot that passed through the origin. Furthermore, Ak7 was observed to have more activity than the rest Ak catalysts used. This could be due to the presence of $Al^{(VI)}$ species located within the mesostructure channels yielding strong lewis sites, which might have interacted inductively with Bronsted acid sites to increase the acid strength of the Bronsted acidity, thus enhancing the activity of the catalyst. The Ak catalysts showed a severe deactivation at the end of each run with the catalyst color changing from white to dark grey after testing.

Due to the very large pore sizes of the mesoporous materials, "nest effect" might explain the low conversions (< 5 %) obtained with very slow rate of protolysis at temperatures ≤ 300 °C, for all the Ak catalysts. The same explanation could be applied to the modified mesoporous KT catalysts (P-KT, S-KT and P-Ak4) tested which equally showed very low conversion and catalytic activity at temperatures less than 350 °C.

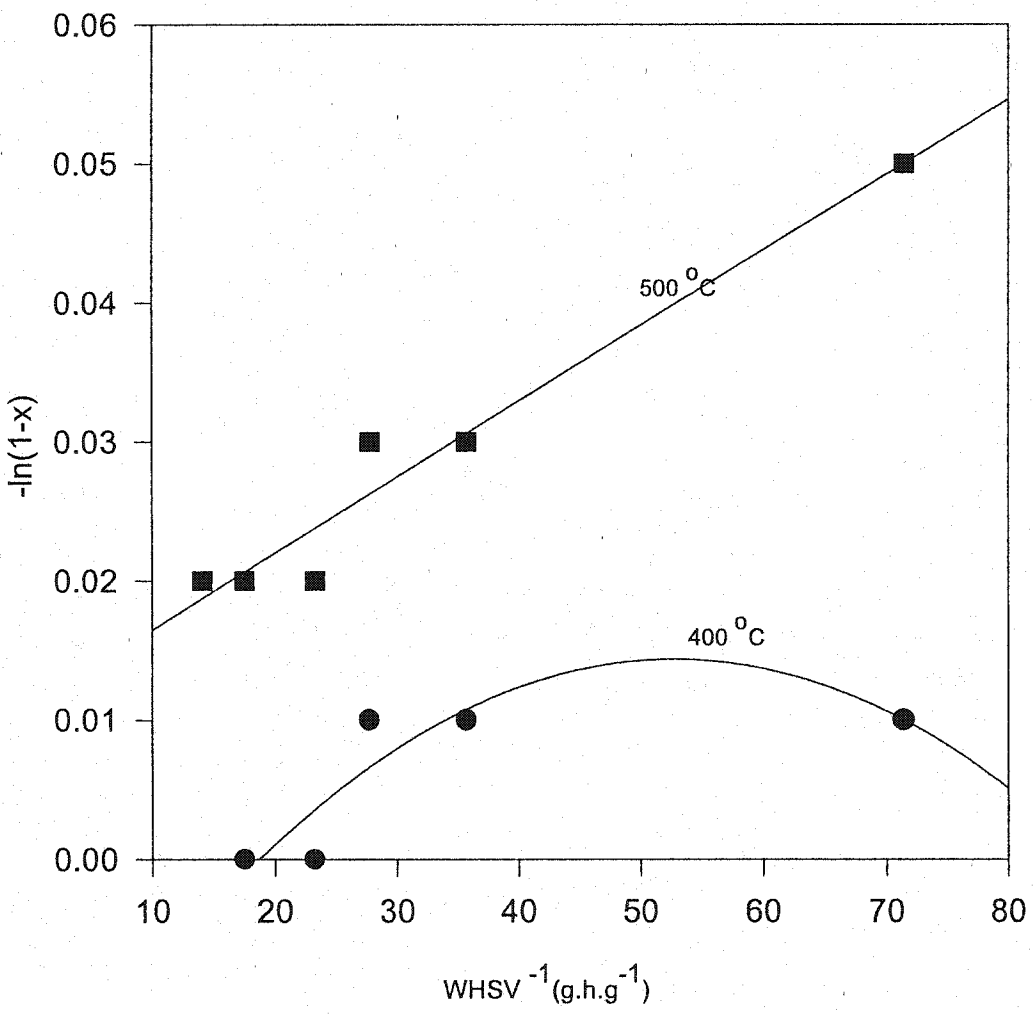

Figure 4.10a, A plot of -ln(1-x) against 1/WHSV of n-hexane cracking over 1.04g Ak4 catalyst.

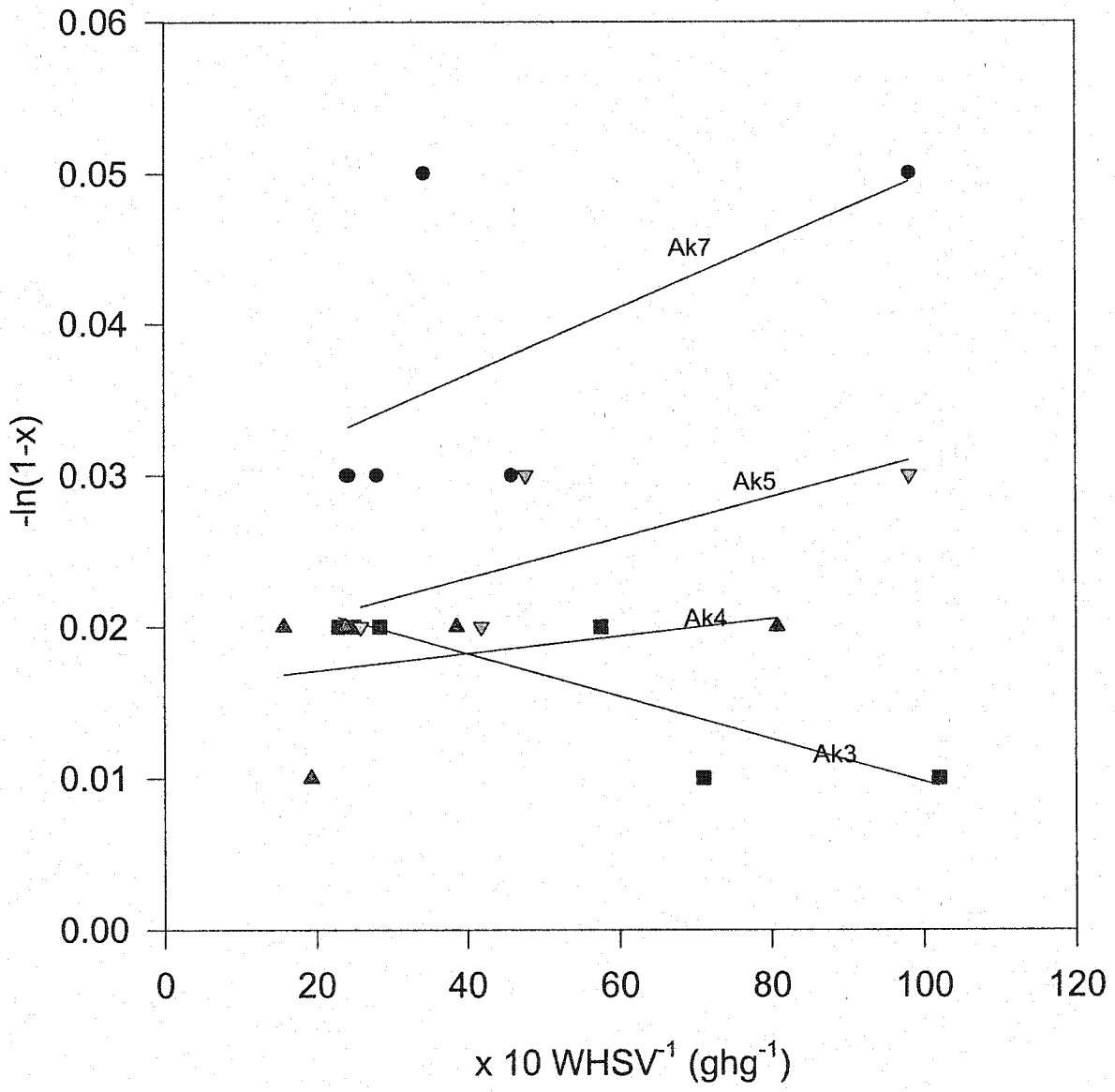

Figure 4.10b, A plot of -ln(1-x) against 1/WHSV of n-hexane cracking over 1.03g Ak catalyst at 300 °C.

4.4.1 Activation Energy

The apparent activation energy and trend values as shown in figure 4.11 and table 4.2, agreed with the activity of the catalyst considering the experimental condition. ZSM-5 catalyst showed the lowest value of 39.04 KJ/mole at 180 - 400 °C, in agreement with literature value of 42.0 KJ/mole for HZSM-5 at 300 - 400 °C.[98] Furthermore, it explains the high cracking activity of ZSM-5 in hexane conversion via the bimolecular reaction mechanism (a secondary reaction process) as the predominate route. A-ZSM showed the highest activation energy of 72.55 KJ/mole and lowest cracking activity indicating the favoring of monomolecular cracking mechanism in the cracking reaction as the temperature of reaction increases with the higher CMR value compare to ZSM-5, CR-ZSM and Ak8-ZSM-5 as shown in figure 4.12. This means that more energy was required to attain the transition state complex for the formation of the penta-coordinated carbonium ion and primary carbenium ion intermediate during the hexane cracking in A-ZSM catalyst. The activation energy of Theta-1 and Ak8-T was also found to be higher than ZSM-5 and Ak8-ZSM catalysts as shown in table 4.2, which explain why cracking activity of Theta-1 is lower than ZSM-5. It further reflected the very high CMR values of Theta-1 and Ak8-T compared to ZSM-5, indicating the difference in the predominate mechanism of reaction involved in both types of catalyst. The non - porous carborandum and amorphous silica in the composition of CR-ZSM and A-ZSM might have reduced the number of active sites of the ZSM-5 component by blocking some of the pores which eventually led to low cracking activity of the two catalysts. Furthermore the

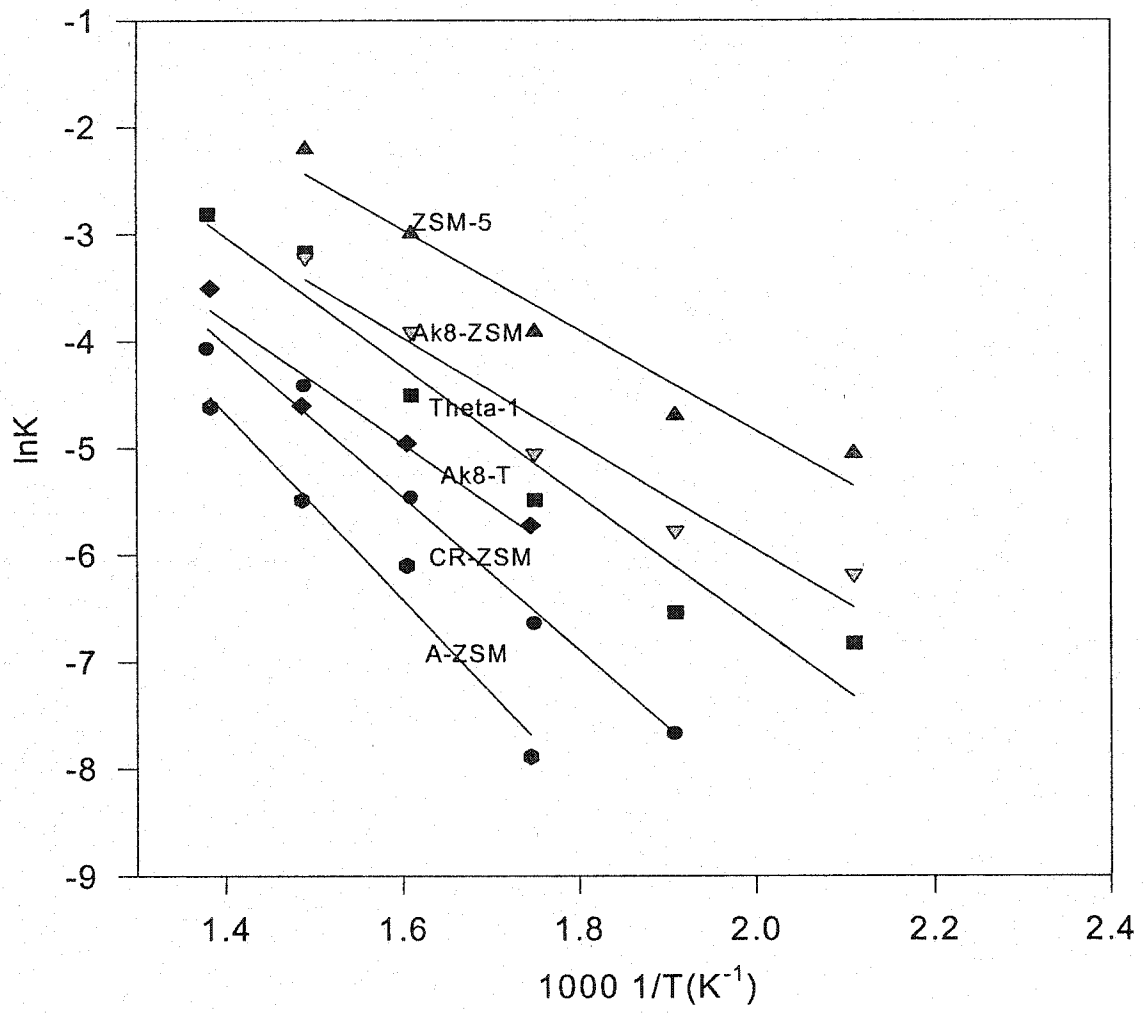

Figure 4.11, A plot of lnK (apparent rate constant) against 1/T (K^{-1}) for each catalyst used.

apparent activation energy is identical for each catalyst at the range of reaction temperatures of operation. The differences in the apparent activation energy between the unmixed and admixture ZSM-5 and Theta-1 catalyst could be attributed to their differences in the heat of adsorption of *n*-hexane. However, it has been published that the intrinsic activation energies are identical for monomolecular cracking reaction of $nC_4 - nC_{10}$ alkanes using HZSM-5.[99]

4.5 Cracking Mechanism Ratio

From figure 4.12 the CMR value increases with increase in temperature and increase in space velocity for all the catalyst. In reference to the cracking reaction mechanism scheme in figure 2.1, the very high CMR value of Theta-1 and Ak8-T catalyst compared to the ZSM-5 type catalysts indicated that the protolytic cracking reaction route prevails leading to the formation of mostly C_1 - C_4 hydrocarbons and H_2 (although not analysized). In addition the structural effect of Theta-1 zeolite with respect to the possible presence of smaller intracrystalline space in the catalyst might have suppress (high steric constrain) the formation of bulky carbenium ion, which is a characteristic of bimolecular reaction process.

At temperatures less than 300 °C, bimolecular reaction process prevails in all the catalyst, with the reaction favoring the formation of butanes, especially iC_4 with the ZSM-5 type catalyst showing higher values compare to Theta-1 type catalyst, due to the channel structure of ZSM-5 favoring the formation of the stable tertiary carbenium ions (in particular iC_4) as reaction intermediate. Based on the experimental condition used, the very high CMR value >>> 1 reflect a

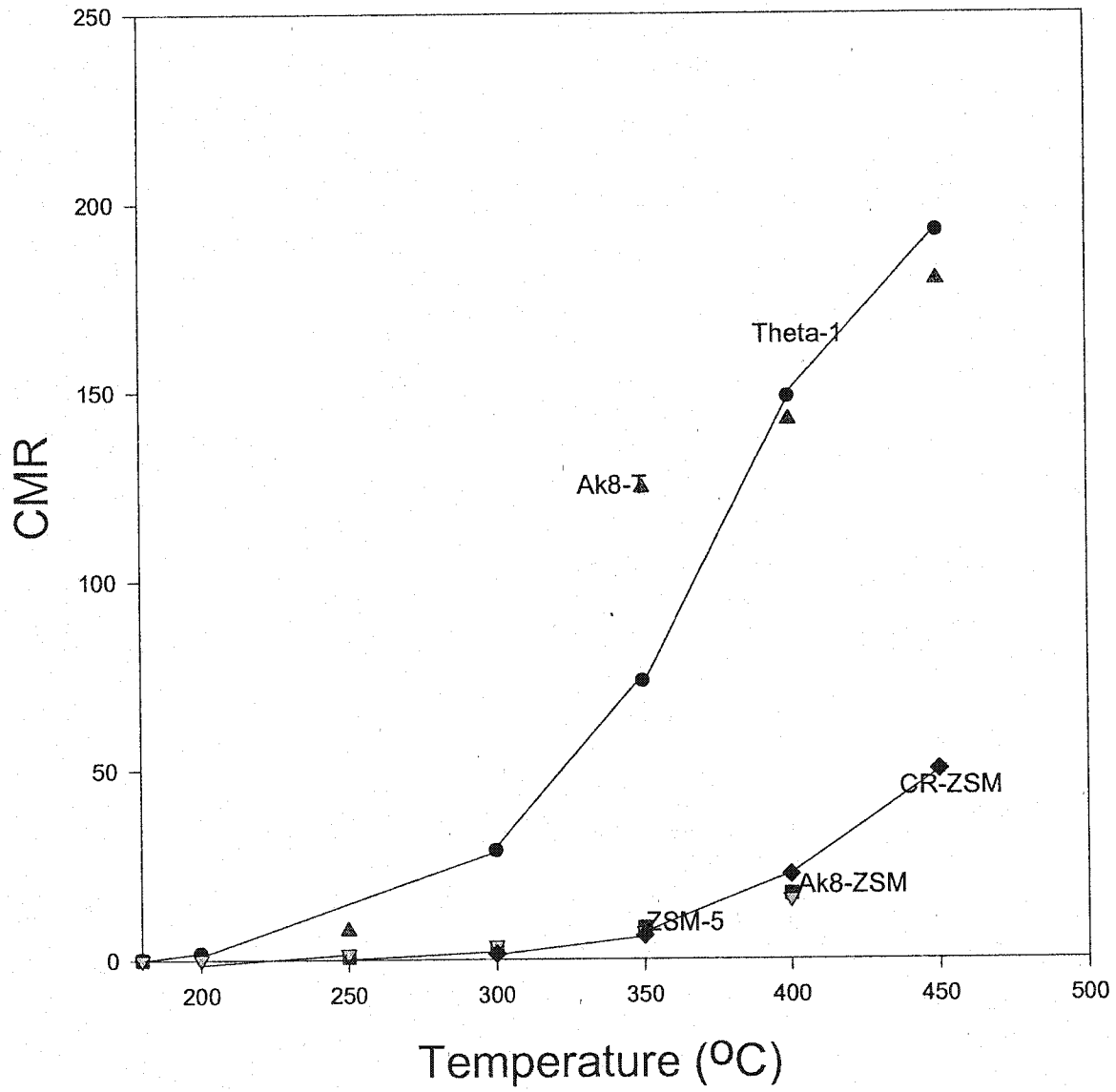

Figure 4.12, Relationship between CMR against temperature at 45.5 g.h.g^{-1} using 1.01g catalyst.

significant contribution of the protolytic cracking route, while a low value (0<CMR<1) show a predominant contribution from the classical bimolecular reaction route. Evidence from the activation energy supported the low acid site density of the Theta-1 & Ak8-T catalyst with relatively higher activation energies value, indicating that the steps for the formation of both carbonium and carbenium ions requires a high energy of activation. The formation of bulky bimolecular reaction transition state complex of iC_4 carbenium ion is suppressed as the temperature of the reaction increases as reflected in figure 4.13. The iC_4/nC_4 ratio was observed to be relatively low for the medium pore zeolites at the experimental condition of reaction used as shown in tables A-4.8 - 4.13. However, an increase in the iC_4/nC_4 ratio was observed as the catalyst favor formation of large carbenium ion (or bulky transition state) intermediate via the bimolecular reaction mechanism. The paraffin to olefin (P/O) ratio was observed to increase with increase in intersection between the channel pore dimension & decreases with increase in temperature and contact time. The CMR was found to decreases as the conversion increases and also have an inverse relationship with the P/O ratio, thus as the CMR increases the P/O decreases, indicating that the bimolecular reaction process favor the formation of more paraffin than olefin and the reverse is favor by monomolecular cracking process. The reactions involved in the formation of more paraffin over olefin, can be explain in terms of hydride transfer reaction between carbenium ion and n-hexane, β-scission of carbenium ion, or isomerization of carbenium ion follow by hydride transfer from n-hexane as outline in figure 2.1. The result obtained quite agreed with the literature. [11]

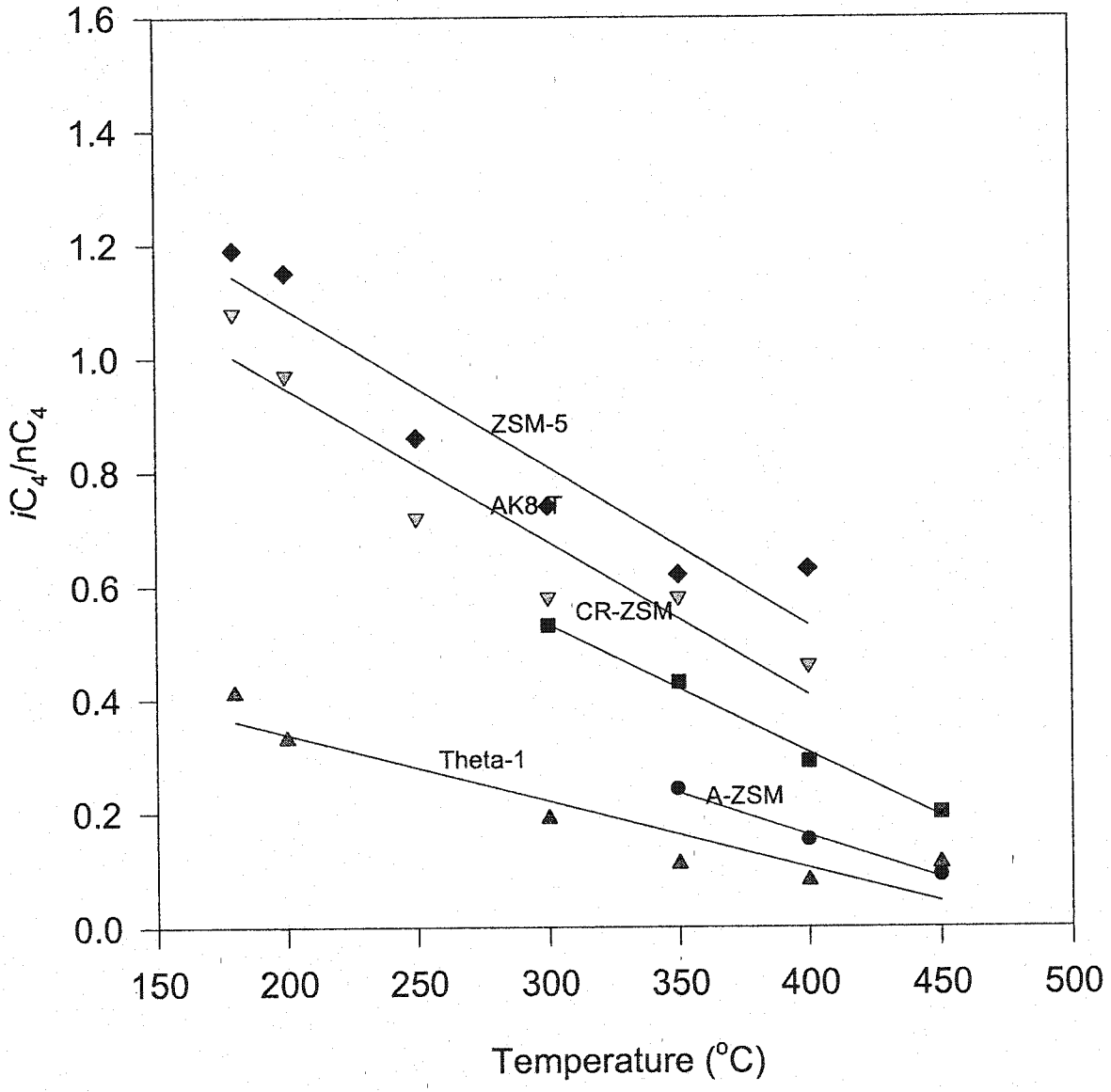

Figure 4.13 A plot of iC_4/nC_4 against temperature of n-hexane cracking over catalyst with varied composition.

For the Ak catalysts, the CMR values were observed to be >1 but < 10. No conclusive remark can be made on the Ak catalysts, which requires more studies at higher temperatures (> 300 °C). However, from the product distribution as shown in table A- 4.14, bimolecular reaction mechanism might have prevailed due to the large values of C_7, $C_{6=}$ and C_3 yield. Further more the CMR values for P-Ak8, S-Ak8 and P-Ak4 catalysts could not be determined due to the absence of iso-butane at the same condition of reactions as the Ak catalysts.

4.6 Selectivity of n-hexane cracking

In reference to figure 2.1, the effect of the catalyst composition viz a viz structure of the catalysts will be used to explain the product distribution obtained. C_3 hydrocarbons were selectively formed as one of the major products in all the catalyst tested at conditions of reaction used. This can be attributed to the ease in the formation of propane & propenium ion intermediate as a result of the cleavage of the central C – C in n-hexane through the protolytic mechanism. Secondary reaction is another process that may result in the formation of propane via hydride transfer and β-scission, since the ration of $C_3/C_{3=}$ is not equal to unity. In spite of the smaller intracrystalline channel present in Theta-1 catalyst, bimolecular reaction mechanism prevailed at temperature <300 °C, via a less bulky and less stable secondary carbenium ions resulting in the formation of significant amount of linear C_4 and C_3 hydrocarbons. Other major products formed by Theta-1 catalyst due to the secondary reaction process, in addition to iC_4 are linear C_5, iC_6 and $iC_{4=}$. Hexenes and iso-butene were minor products in the bimolecular reaction

mechanism process of ZSM-5 catalyst in contrast to Theta-1 at the same reaction temperature (less than 300 °C). The difference in the structure of the two catalysts might account for this phenomenon, with Theta-1 relatively having lower rate of hydride transfer and β-scission.

Butenes increases with increase in space velocity and decrease in contact time. In Theta-1 & ZSM-5 zeolites, the selectivity for methane and ethane increases with increase in temperature, while butanes, pentanes and iso-hexane decreases as the temperature of reaction increases, signifying the change in reaction mechanism from the classical reaction process to a protolytic mechanism. At the condition of reaction used, propane formation increases from 180 °C to 300 °C and decreases as the temperature of reaction increases beyond 300 °C.

It has been established that as the temperature of reaction increases, the Bronsted acid strength increases which connotes a decrease in the conjugate base strength, consequently increasing the protolytic reaction of the feed. These result in the formation of paraffin and carbenium ions, with the carbenium ion residing on the conjugate base site of the catalyst surface. The adsorbed carbenium ions may desorbed and rejuvinate the Bronsted acid sites to form olefin. More olefins may be formed through this process by the desorption of more carbeniunm ions, a feature characteristic of protolytic reaction, indicating less hydride transfer reaction. The decrease in $iC_4/iC_{4=}$ have been used to evalute the hydride transfer reaction.

The Ak catalysts selectively formed iso-hexane, hexenes, n-heptane and propene as the major reaction products. The large hydrocarbon molecules formed

(iC_6, $C_{6=}$, & C_7) show the favoring of bulky transition-state allowed by the mesoporous catalyst due to its large pore size. Considering the reaction condition used, C_1 formation decreases with increase in temperature (200 °C – 350 °C) and decrease in contact time. Although hydrogen molecules were not analyzed, but large amount of it must have been formed, considering the amount of hexenes selectively formed when evaluating the Ak catalysts. Furthermore, at 200 °C – 350 °C the effect of temperature showed the selective formation of propene, which increases as the temperature of reaction increases while hexenes decreases with increase in temperature for all the Ak catalysts. Similarly, results obtained as shown in table A- 4.14 for P-KT, S-KT and P-Ak4 catalyst, indicated that the cracking reaction predominantly favored the formation of $C_{2=}$, $C_{3=}$, iC_6, $C_{6=}$ and C_7, while ethane, propane, iso-butane and pentene were observed to be absent at the condition of reaction used.

CHAPTER 5

CONCLUSION AND RECOMMENDATION

5.1 CONCLUSION

The result of the investigation indicate the following:

- Synthesis of MCM-41 materials can be achieved by stirring the hydrogel at 130 °C with the tetrahedral coordinated aluminum stable in the framework after thermal treatment of the as-synthesized materials.
- Most of the cracking activity of Theta-1 catalyst was via monomolecular cracking mechanism because of the 1-D channel system provided by the structure of the catalyst.
- ZSM-5 was the most active cracking catalyst by n-hexane cracking due to the extensive bimolecular cracking activity in the channel intersection.
- The catalyst structure and cracking temperature are the two main parameters that affect the activity and mechanism involved.
- Catalytic cracking activity of MCM-41 material are extremely low compared with microporous molecular sieves, possibly due to low acid strength of the active sites present in the amorphous wall.
- CMR can be used to characterize the acid strength of acid sites and the structural properties of molecular sieves.

5.2 RECOMMENDATION

a. Investigate further the structural properties of amorphous binder and mesoporous binder.

b. Optimize the composition of the admixture catalyst ratio in particular ZSM-5 to achieve more suitable turn over frequency of the catalyst.

APPENDIX -A

Table A-4.2a

Summary of n-hexane cracking reaction at 180 °C , over 1.01g ZSM-5 catalyst at 1 atm, different flow rate of $16N_2$:$1nC_6$ feed.

Time on stream (min)	6.05	9.98	13.01	15.28	18.31
Flow rate (ml/min)	15.00	23.08	30.00	40.00	30.00
$WHSV^{-1}(g/gh^{-1})$	90.90	59.10	45.50	34.10	45.50
CMR	0.02	0.02	0.03	0.04	0.03
P/O	102.43	18.63	9.14	6.72	9.57
iC_4/nC_4	1.12	1.17	1.19	1.21	1.27
$iC_4/iC_{4=}$	320.00	26.60	12.59	7.52	11.68
Conversion(%wt)	64.39	30.22	18.89	13.59	17.91
Selectivity(%wt)					
C_1	0.04	0.00	0.00	0.00	0.00
C_2	0.14	0.15	0.19	0.18	0.18
$C_{2=}$	0.28	0.41	0.58	0.75	0.63
C_3	24.33	18.73	17.63	17.34	17.90
$C_{3=}$	0.33	1.16	2.03	3.24	2.23
i-C_4	28.72	24.35	22.92	22.25	24.24
n-C_4	25.54	20.85	19.23	18.42	19.06
T-$C_{4=}$	0.08	0.43	0.86	1.24	0.89
1-$C_{4=}$	0.00	0.12	0.23	0.36	0.25
i-$C_{4=}$	0.09	0.92	1.82	2.96	2.08
c-$C_{4=}$	0.05	0.26	0.48	0.74	0.53
i-C_5	9.09	10.41	9.88	9.33	10.25
n-C_5	8.96	12.37	11.70	11.13	10.98
$C_{5=+}$	0.00	0.41	1.30	2.08	1.52
i-C_6	2.21	7.77	7.96	7.65	7.45
n,i$C_{6=}$	0.14	1.39	2.55	1.59	1.32
C_7	0.00	0.26	0.63	0.75	0.50

Table A - 4.2b

Summary of n-hexane cracking reaction at 200 °C , over 1.01g zsm-5 catalyst at 1 atm, varied flow rate of $16N_2$:$1nC_6$ feed.

Time on stream (min)	6.05	9.98	13.01	15.28	18.31
Flow rate (ml/min)	15.00	23.08	30.00	40.00	30.00
$WHSV^{-1}(g/gh^{-1})$	90.90	59.10	45.50	34.10	45.50
CMR	0.22	0.28	0.30	0.33	0.21
P/O	21.47	8.55	6.11	4.65	7.67
iC_4/nC_4	1.01	1.11	1.15	1.14	1.28
$iC_4/iC_{4=}$	116.15	14.00	8.77	5.71	11.48
Conversion(%wt)	35.96	15.89	12.49	9.58	11.77
Selectivity(%wt)					
C_1	0.96	0.72	0.63	0.60	0.63
C_2	1.84	1.29	1.12	0.93	1.14
$C_{2=}$	2.08	3.48	4.05	4.24	2.75
C_3	26.57	20.90	20.79	18.94	25.55
$C_{3=}$	1.16	2.69	3.76	4.80	2.96
i-C_4	22.30	19.72	19.69	17.64	21.25
n-C_4	22.13	17.83	17.16	15.51	16.56
T-$C_{4=}$	0.32	0.86	1.21	1.64	1.01
1-$C_{4=}$	0.28	0.23	0.35	0.56	0.32
i-$C_{4=}$	0.19	1.41	2.24	3.09	1.85
c-$C_{4=}$	0.15	0.52	0.74	0.97	0.69
i-C_5	8.05	8.74	8.35	7.52	7.71
n-C_5	7.70	8.20	7.80	7.22	7.19
$C_{5=+}$	0.00	0.69	1.36	1.56	1.39
i-C_6	5.59	9.54	8.57	12.32	7.36
n,i$C_{6=}$	0.27	0.59	0.34	0.86	0.56
C_7	0.38	2.60	1.84	1.64	1.04

Table A - 4.2c

Summary of n-hexane cracking reaction at 250 °C , over 1.01g ZSM 5 catalyst at 1 atm, different flow rate of $16N_2$:$1nC_6$ feed

Time on stream (min)	6.05	9.98	13.01	15.28	17.30
Flow rate (ml/min)	15.00	23.08	30.00	40.00	45.00
$WHSV^{-1}(g/gh^{-1})$	90.90	59.10	45.50	34.10	30.30
CMR	2.57	2.56	2.62	2.67	2.81
P/O	9.36	5.09	3.75	3.03	2.45
iC_4/nC_4	1.04	0.93	0.86	0.82	0.78
$iC_4/iC_{4=}$	14.42	6.12	3.96	2.94	2.21
Conversion(%wt)	54.83	37.62	29.82	24.40	20.93
Selectivity(%wt)					
C_1	0.45	0.42	0.41	0.35	0.34
C_2	1.93	1.80	1.73	1.71	1.77
$C_{2=}$	3.20	4.66	5.24	5.62	6.01
C_3	38.46	34.25	32.19	31.31	30.18
$C_{3=}$	4.11	6.73	8.59	10.35	12.31
i-C_4	17.63	14.74	12.92	11.81	10.53
n-C_4	16.97	15.89	14.95	14.47	13.51
T-$C_{4=}$	0.75	1.30	1.70	2.07	2.41
1-$C_{4=}$	0.29	0.52	0.70	0.86	1.01
i-$C_{4=}$	1.22	2.41	3.27	4.01	4.76
c-$C_{4=}$	0.86	1.29	1.55	1.79	1.95
i-C_5	4.72	4.16	3.62	3.30	2.83
n-C_5	3.68	4.03	3.95	3.90	3.56
$C_{5=+}$	0.54	1.36	1.93	2.42	2.79
i-C_6	2.48	3.16	3.08	2.75	2.57
n,$iC_{6=}$	0.13	0.37	0.60	0.78	0.90
C_7	2.58	2.92	3.59	2.51	2.57

Table A - 4.2d

Summary of n-hexane cracking reaction at 300 °C , over 1.01g ZSM-5 catalyst at 1 atm, different flow rate of $16N_2$:$1nC_6$ feed

Time on stream (min)	3.93	6.96	9.23	11.25	12.79	15.06
Flow rate (ml/min)	23.08	30.00	40.00	45.00	59.00	40.00
$WHSV^{-1}(g/gh^{-1})$	59.10	45.50	34.10	30.30	23.00	34.10
CMR	1.33	1.66	2.39	2.80	3.45	2.53
P/O	2.70	2.23	1.61	1.41	1.21	1.51
iC_4/nC_4	1.03	0.93	0.79	0.74	0.65	0.76
$iC_4/iC_{4=}$	4.37	3.09	1.90	1.57	1.13	1.71
Conversion(%wt)	66.51	56.01	50.48	50.42	39.40	51.40
Selectivity(%wt)						
C_1	0.84	0.86	0.87	0.88	0.83	0.85
C_2	5.24	5.34	5.49	5.67	5.56	5.52
$C_{2=}$	7.85	8.63	10.11	10.71	10.65	10.26
C_3	38.18	36.28	33.81	33.16	30.51	33.45
$C_{3=}$	11.75	13.54	17.13	19.18	21.54	18.19
$i\text{-}C_4$	10.48	8.91	6.89	6.16	4.94	6.58
$n\text{-}C_4$	10.16	9.63	8.76	8.31	7.61	8.62
$T\text{-}C_{4=}$	1.48	1.72	2.16	2.28	2.62	2.23
$1\text{-}C_{4=}$	0.73	0.87	1.12	1.21	1.38	1.18
$i\text{-}C_{4=}$	2.40	2.88	3.63	3.91	4.37	3.86
$c\text{-}C_{4=}$	1.53	1.75	2.05	2.05	2.25	2.08
$i\text{-}C_5$	2.21	1.80	1.33	1.09	0.90	1.19
$n\text{-}C_5$	1.26	1.20	1.09	0.95	0.91	1.02
$C_{5=+}$	1.08	1.42	1.81	1.78	1.97	1.85
$i\text{-}C_6$	0.98	0.95	0.88	0.61	0.63	0.70
$n,iC_{6=}$	0.19	0.13	0.34	0.36	0.52	0.24
C_7	3.63	4.09	2.51	1.67	2.85	2.17

Table A - 4.2e

Summary of n-hexane cracking reaction at 350 °C , over 1.01g ZSM-5 catalyst at 1 atm, varied flow rate of $16N_2$:$1nC_6$ feed

Time on stream (min)	2.27	4.29	5.83	7.23	9.50
Flow rate (ml/min)	40.00	45.00	59.00	65.00	40.00
$WHSV^{-1}(g/gh^{-1})$	34.10	30.30	23.10	21.00	34.10
CMR	7.51	8.13	9.81	10.44	6.24
P/O	1.37	1.28	1.05	1.01	1.36
iC_4/nC_4	0.65	0.62	0.54	0.50	0.76
$iC_4/iC_{4=}$	1.34	1.13	0.87	0.76	1.49
Conversion(%wt)	80.00	77.86	71.59	68.00	85.78
Selectivity(%wt)					
C_1	2.17	2.00	1.94	1.82	2.12
C_2	10.62	10.17	10.28	9.88	10.50
$C_{2=}$	14.73	14.84	15.83	15.37	14.69
C_3	28.77	27.27	26.29	24.94	29.81
$C_{3=}$	18.81	19.92	22.94	24.00	18.79
i-C_4	3.66	3.32	2.86	2.59	4.37
n-C_4	5.61	5.40	5.27	5.18	5.74
T-$C_{4=}$	1.77	1.87	2.07	2.18	1.83
1-$C_{4=}$	1.05	1.13	1.29	1.37	1.08
i-$C_{4=}$	2.74	2.93	3.27	3.43	2.93
c-$C_{4=}$	1.63	1.69	1.81	1.89	1.68
i-C_5	0.49	0.43	0.35	0.31	0.57
n-C_5	0.29	0.26	0.26	0.25	0.31
$C_{5=+}$	1.15	1.23	1.18	1.28	1.30
i-C_6	0.47	0.48	0.53	0.55	0.40
n,$iC_{6=}$	0.29	0.26	0.30	0.33	0.16
C_7	5.76	6.80	3.53	4.63	3.74

Table A-4.2f

Summary of n-hexane cracking reaction at 400 °C , over 1.01g ZSM-5 catalyst at 1 atm, varied flow rate $16N_2 : 1nC_6$ feed

Flow rate (ml/min)	40.00	45.00	59.00	65.00	40.00
$WHSV^{-1}(g/gh^{-1})$	34.1	30.3	23.1	21	34.1
Conversion(%wt)	97.56	95.89	93.37	92.03	96.74
CMR	14.94	16.99	19.54	21.35	17.84
P/O	0.96	0.86	0.76	0.71	0.92
iC_4/nC_4	0.78	0.63	0.50	0.45	0.67
$iC_4/iC_{4=}$	1.13	0.79	0.59	0.51	0.82
Selectivity(%wt)					
C_1	3.85	3.44	3.06	2.95	3.79
C_2	13.45	12.69	12.28	12.24	13.08
$C_{2=}$	21.73	21.19	20.61	20.47	21.80
C_3	21.53	20.39	19.50	19.17	20.90
$C_{3=}$	22.44	23.76	25.65	27.03	22.80
$i\text{-}C_4$	2.61	2.20	1.84	1.67	2.17
$n\text{-}C_4$	3.34	3.49	3.66	3.72	3.25
$T\text{-}C_{4=}$	1.56	1.75	1.95	2.05	1.66
$1\text{-}C_{4=}$	1.06	1.20	1.37	1.47	1.13
$i\text{-}C_{4=}$	2.31	2.78	3.10	3.29	2.64
$c\text{-}C_{4=}$	1.29	1.46	1.62	1.67	1.38
$i\text{-}C_5$	0.26	0.23	0.20	0.18	0.33
$n\text{-}C_5$	0.26	0.25	0.20	0.18	0.28
$C_{5=+}$	0.72	0.89	0.93	0.91	1.20
$i\text{-}C_6$	0.18	0.14	0.16	0.16	0.32
$n,iC_{6=}$	0.14	0.13	0.08	0.16	0.15
C_7	3.27	4.03	3.87	2.67	3.12

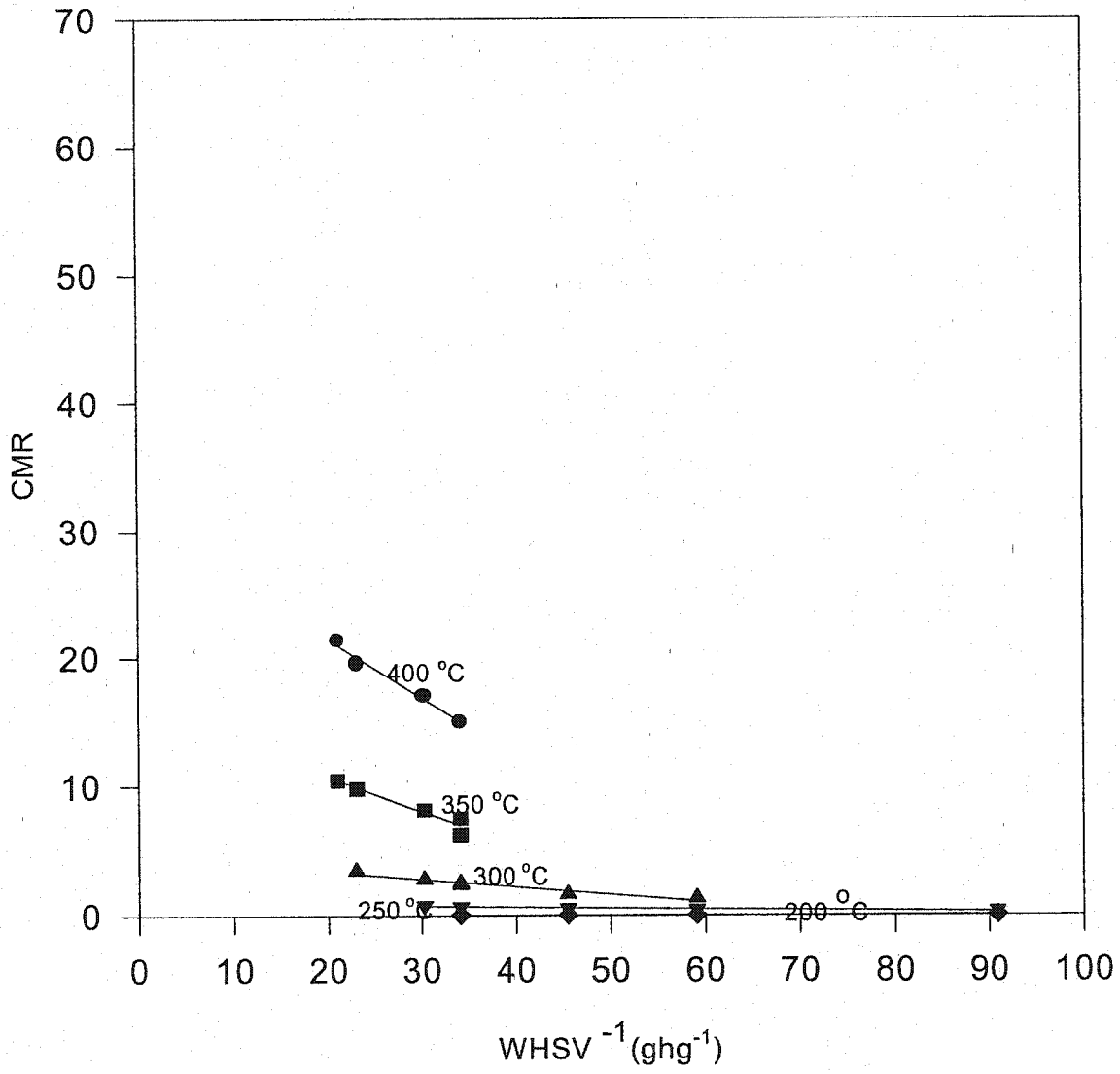

Figure A-1. A plot of CMR against 1/WHSV of n-hexane cracking over 1.01g ZSM-5

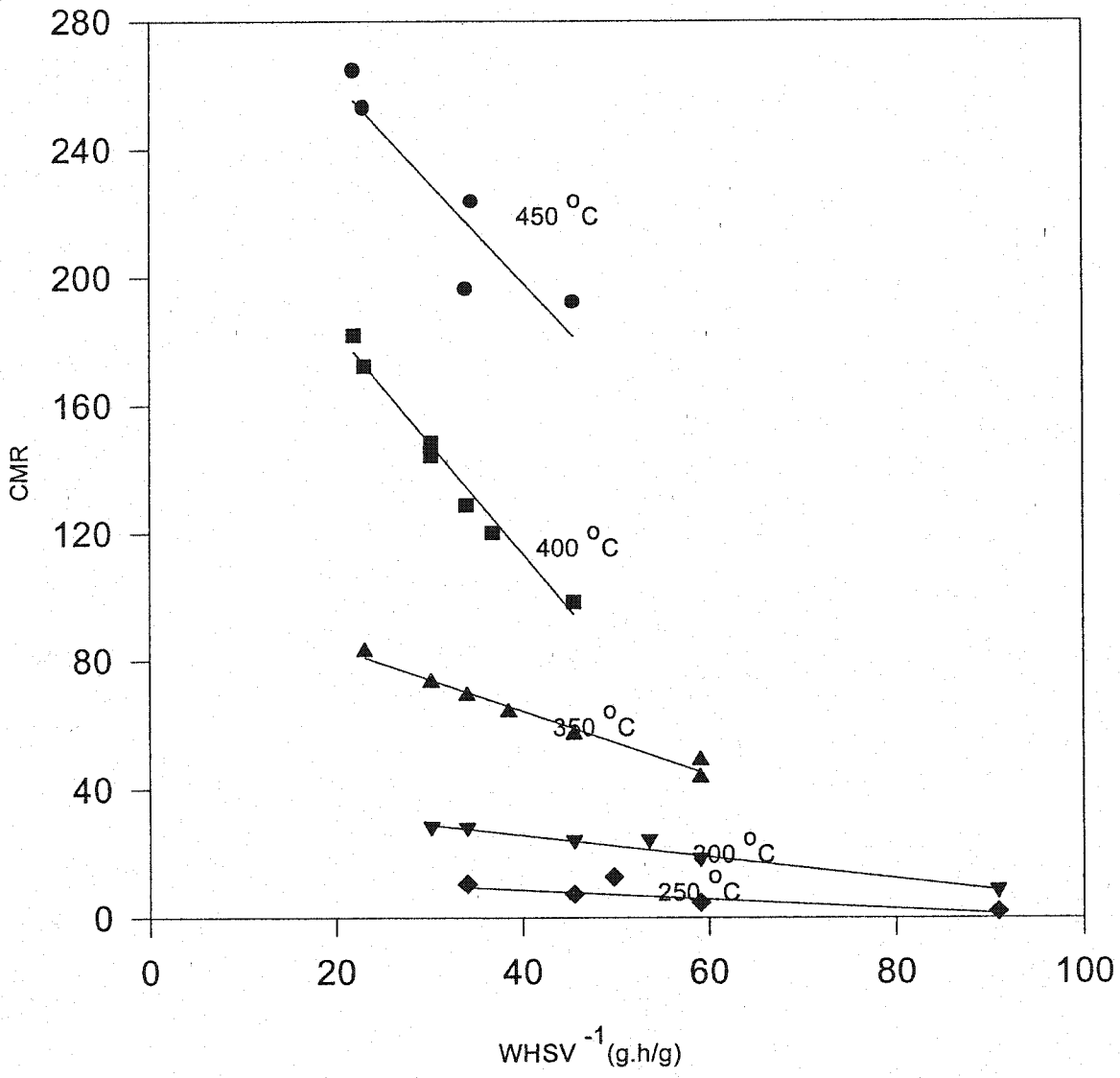

Figure A-2. A plot of CMR against 1/WHSV of n-hexane cracking over 1.01g Theta-1 catalyst

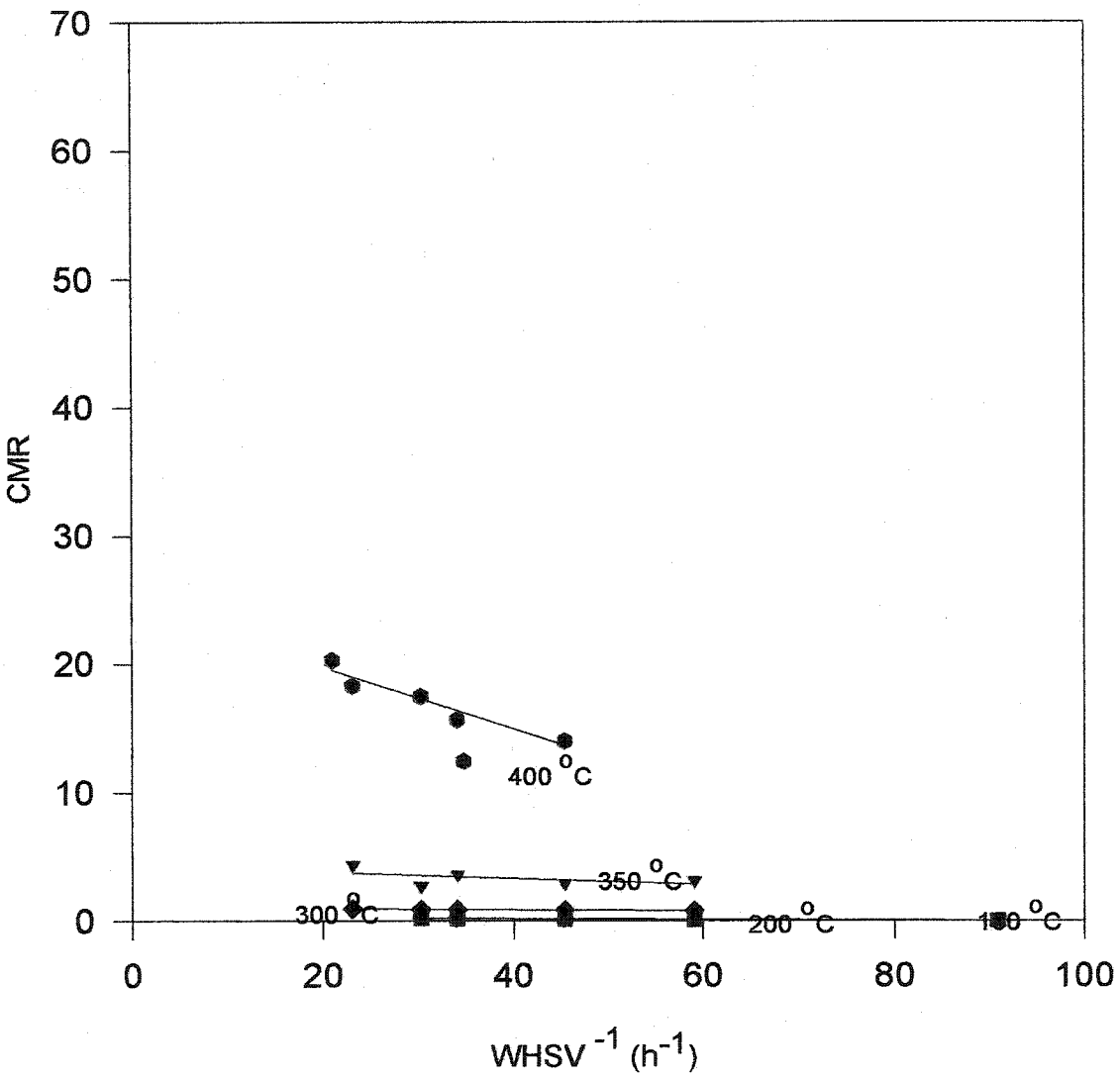

Figure A-3 A plot of CMR vs 1/WHSV of n-hexane cracking over 1.01g AK8-ZSM-5

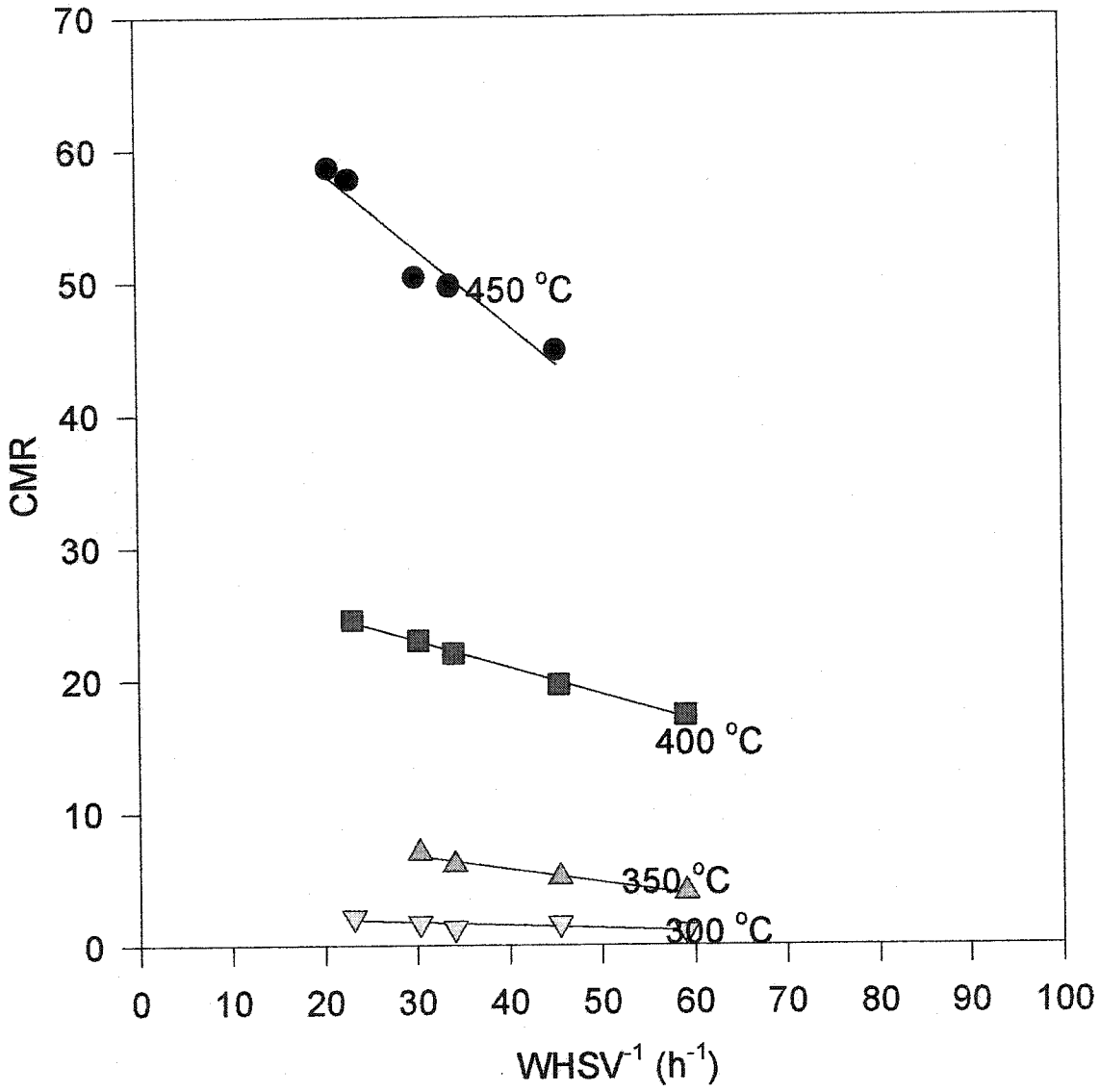

Figure A-4. A plot of CMR vs 1/WHSV of n-hexane cracking over 1.01g CR-ZSM-5

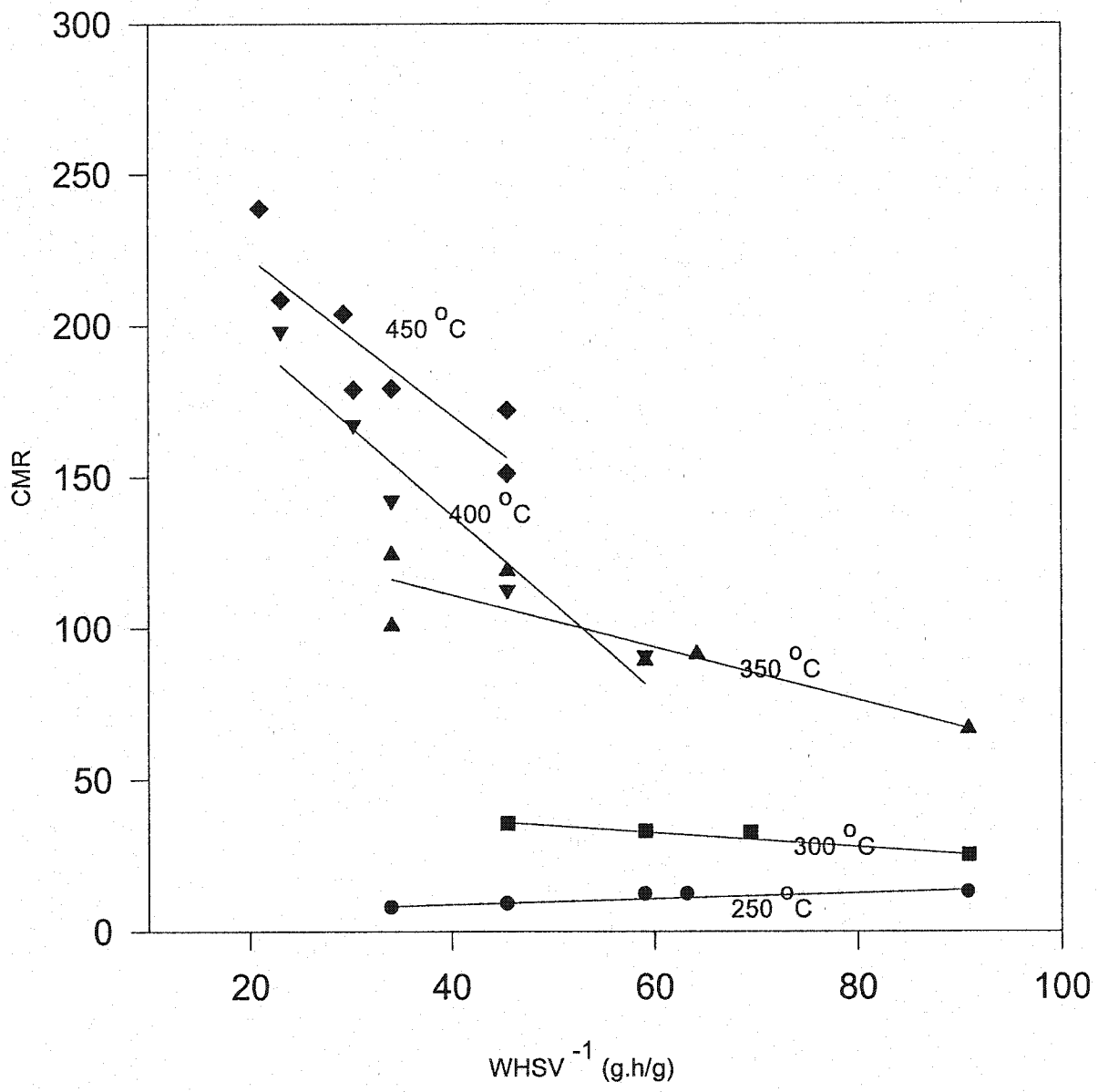

Figure A-5. A plot of CMR vs $WHSV^{-1}$ of n-hexane cracking over 1.01g Ak8-T

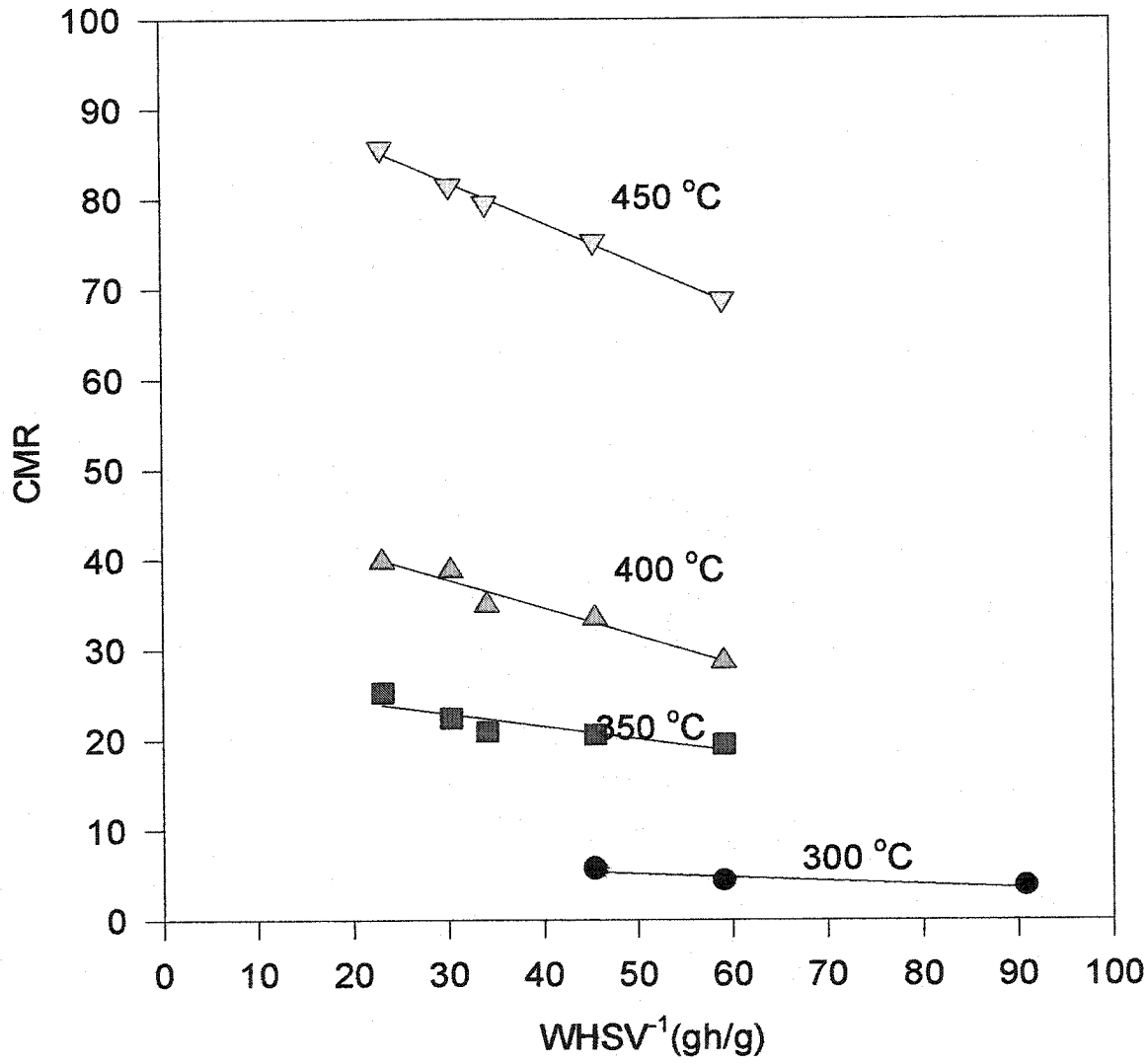

Figure A-6. A plot of CMR vs 1/WHSV of n-hexane cracking over 1.01g A-ZSM-5

Table A - 4.3a

Summary of n-hexane cracking reaction at 180 °C , over 1.01g Theta-1 catalyst at 1 atm varied flow rate of $16N_2$:$1nC_6$ feed

Time on stream (min)	6.05	9.98	13.01	15.28	17.29
Flow rate (ml/min)	15.00	23.08	30.00	40.00	45.00
$WHSV^{-1}(g/gh^{-1})$	90.90	59.10	45.5	34.10	30.30
CMR	0.08	0.35	0.42	0.00	#DIV/0!
P/O	10.97	3.10	2.25	1.80	1.41
iC_4/nC_4	0.51	0.41	0.41	0.37	0.00
$iC_4/iC_{4=}$	7.11	0.95	0.67	0.52	0.00
Conversion(%wt)	3.27	1.67	0.99	0.59	0.44
Selectivity(%wt)					
C_1	0.00	0.00	0.00	0.00	0.00
C_2	0.00	0.00	0.00	0.00	0.00
$C_{2=}$	0.97	2.00	2.15	0.00	0.00
C_3	25.71	19.10	19.31	19.67	15.23
$C_{3=}$	2.34	6.15	8.58	10.93	10.77
i-C_4	11.91	5.75	5.12	4.37	0.00
n-C_4	23.14	13.99	12.38	11.87	8.92
T-$C_{4=}$	0.82	2.56	4.79	4.37	4.46
1-$C_{4=}$	0.00	1.52	0.00	0.00	0.00
i-$C_{4=}$	1.67	6.07	7.59	8.43	7.06
c-$C_{4=}$	0.00	4.80	2.81	0.00	0.00
i-C_5	4.95	4.80	3.63	3.75	0.00
n-C_5	14.51	10.71	9.57	9.68	9.29
$C_{5=+}$	0.00	3.12	4.13	6.87	5.20
i-C_6	12.98	13.99	14.19	13.74	31.20
n,$iC_{6=}$	1.12	5.44	6.27	6.25	8.54

Table A - 4.3b

Summary of n-hexane cracking reaction at 200 °C , using 1.01g Theta-1 catalyst at 1 atm, varied flow rate of $16N_2$:$1nC_6$ feed.

Time on stream (min)	6.05	9.98	13.01	15.28	17.29	23.35
Flow rate (ml/min)	15.00	23.08	30.00	40.00	45.00	15.00
$WHSV^{-1}(g/gh^{-1})$	90.93	59.10	45.46	34.10	30.31	90.93
CMR	0.15	0.52	0.96	1.43	1.57	0.23
P/O	3.32	1.83	1.64	1.35	1.31	2.37
iC_4/nC_4	0.44	0.35	0.33	0.31	0.33	0.42
$iC_4/iC_{4=}$	1.76	0.69	0.52	0.37	0.37	1.22
Conversion(%wt)	14.73	2.98	1.72	1.14	0.84	9.00
Selectivity(%wt)						
C_1	0.00	0.00	0.00	0.00	0.00	0.00
C_2	0.36	0.88	1.50	1.74	2.13	0.54
$C_{2=}$	0.94	1.53	1.86	1.74	1.77	1.26
C_3	26.09	22.25	22.35	19.96	20.37	26.18
$C_{3=}$	5.39	9.06	10.82	11.84	13.29	8.12
$i\text{-}C_4$	8.41	4.66	3.51	2.44	2.48	7.77
$n\text{-}C_4$	19.11	13.34	10.75	7.89	7.44	18.36
$T\text{-}C_{4=}$	2.08	2.83	3.58	4.99	2.83	2.69
$1\text{-}C_{4=}$	0.70	0.99	1.15	1.16	1.24	0.91
$i\text{-}C_{4=}$	4.79	6.73	6.81	6.62	6.73	6.39
$c\text{-}C_{4=}$	1.31	1.84	2.15	2.44	2.48	1.69
$i\text{-}C_5$	4.11	2.14	1.93	2.09	1.95	3.14
$n\text{-}C_5$	12.27	10.21	7.38	5.80	5.14	10.09
$C_{5=+}$	4.29	5.77	5.87	3.60	3.54	5.17
$i\text{-}C_6$	6.46	11.09	14.54	17.41	17.18	4.18
$n,iC_{6=}$	3.66	6.58	5.52	10.10	11.34	3.46

Table A - 4.3c

Summary of n-hexane cracking reaction at 250 °C , over 1.01g Theta-1 catalyst at, 1 atm same flow rate of $16N_2$:$1nC_6$ feed

Time on stream (min)	6.05	9.98	13.01	15.28	17.29	18.83
Flow rate (ml/min)	15.00	23.08	30.00	40.00	45.00	59.00
$WHSV^{-1}(g/gh^{-1})$	90.90	59.10	45.50	34.10	30.30	23.10
CMR	1.95	4.67	7.29	10.48	#DIV/0!	#DIV/0!
P/O	1.64	0.98	0.76	0.67	0.52	0.68
iC_4/nC_4	0.38	0.31	0.29	0.26	0.00	0.00
$iC_4/iC_{4=}$	0.79	0.32	0.23	0.17	0.00	0.00
Conversion(%wt)	15.30	6.65	5.19	3.95	2.14	3.11
Selectivity(%wt)						
C_1	0.45	0.50	0.64	0.75	0.00	0.00
C_2	3.05	3.93	5.07	5.94	6.23	5.95
$C_{2=}$	4.62	5.07	4.98	4.92	3.99	4.45
C_3	34.81	28.48	26.08	24.76	19.44	22.03
$C_{3=}$	17.14	25.03	32.40	36.59	37.05	36.25
i-C_4	4.16	2.04	1.47	1.11	0.00	0.00
n-C_4	10.92	6.55	5.01	4.34	3.49	3.88
T-$C_{4=}$	2.98	3.43	3.51	3.54	3.49	1.71
1-$C_{4=}$	1.33	1.52	1.59	1.59	1.66	6.88
i-$C_{4=}$	5.25	6.37	6.50	6.64	6.48	1.24
c-$C_{4=}$	1.98	2.35	2.38	2.44	2.41	2.95
i-C_5	1.31	0.60	0.46	0.00	0.00	0.83
n-C_5	2.82	1.69	1.16	1.02	1.16	2.53
$C_{5=+}$	2.33	3.10	2.26	1.73	0.00	2.64
i-C_6	3.45	4.57	2.26	1.33	1.83	3.93
n,i$C_{6=}$	2.26	3.67	3.08	2.52	10.55	3.41
C_7	1.15	1.10	1.22	0.80	1.99	1.24

Table A - 43d

Summary of n-hexane cracking reaction at 300 °C , using 1.01g Theta-1 catalyst at 1 atm varied flow rate of $16N_2$:$1nC_6$ feed.

Time on stream (min)	6.05	9.98	13.01	15.28	17.29	23.34
Flow rate (ml/min)	15.00	23.08	30.00	40.00	45.00	15.00
$WHSV^{-1}(g/gh^{-1})$	90.90	59.10	45.50	34.10	30.30	90.90
CMR	8.63	18.58	24.18	28.15	28.47	8.87
P/O	1.00	0.72	0.68	0.63	0.60	1.25
iC_4/nC_4	0.38	0.25	0.22	0.20	0.19	0.47
$iC_4/iC_{4=}$	0.46	0.22	0.18	0.15	0.13	0.80
Conversion(%wt)	30.14	19.97	17.92	14.68	9.97	33.28
Selectivity(%wt)						
C_1	1.01	1.14	1.19	1.27	1.24	1.47
C_2	8.09	9.40	10.28	10.59	10.57	10.44
$C_{2=}$	8.64	7.59	7.11	6.36	5.61	9.45
C_3	29.34	23.46	22.13	20.47	19.30	33.61
$C_{3=}$	26.47	34.61	37.54	38.94	39.28	24.61
i-C_4	2.06	0.98	0.77	0.65	0.61	2.41
n-C_4	5.44	3.88	3.53	3.23	3.14	5.11
T-$C_{4=}$	2.93	3.15	3.17	3.45	3.73	2.21
1-$C_{4=}$	1.60	1.73	1.74	1.79	1.90	1.11
i-$C_{4=}$	4.46	4.54	4.34	4.40	4.57	3.00
c-$C_{4=}$	2.50	2.48	2.38	2.28	2.47	1.86
i-C_5	0.76	0.81	1.12	1.48	1.47	1.11
n-C_5	0.63	0.29	0.24	0.26	0.37	0.36
$C_{5=+}$	1.47	0.79	0.44	0.40	0.45	0.68
i-C_6	1.27	0.85	0.12	0.05	0.51	0.17
n,i$C_{6=}$	1.92	3.20	2.95	3.60	4.57	1.57
C_7	1.38	1.12	0.93	0.80	0.22	0.82

Table A - 4.3e

Summary of n-hexane cracking reaction at 400 °C , over 1.01g Theta-1 catalyst at 1 atm, different flow rate of $16N_2$:$1nC_6$ feed.

Flow rate (ml/min)	30.00	40.00	45.00	59.00	62.00	45.00
$WHSV^{-1}(g/gh^{-1})$	45.5	34.1	30.3	23.1	22	30.3
CMR	98.38	128.75	148.37	172.30	181.89	144.16
P/O	0.44	0.40	0.38	0.37	0.36	0.37
iC_4/nC_4	0.13	0.09	0.08	0.06	0.06	0.08
$iC_4/iC_{4=}$	0.08	0.04	0.04	0.03	0.02	0.03
Conversion(%wt)	80.36	72.12	75.03	69.57	66.30	75.64
Selectivity(%wt)						
C_1	2.77	2.54	2.58	2.39	2.38	2.54
C_2	13.10	12.51	12.61	12.42	12.35	12.32
$C_{2=}$	15.55	13.55	13.19	11.89	11.32	12.87
C_3	15.56	14.76	14.44	14.22	14.05	14.09
$C_{3=}$	35.02	36.88	38.01	38.77	38.97	37.93
i-C_4	0.32	0.22	0.19	0.15	0.14	0.19
n-C_4	2.46	2.56	2.48	2.55	2.59	2.51
T-$C_{4=}$	2.49	3.05	3.19	3.47	3.69	3.51
1-$C_{4=}$	1.75	2.24	2.43	2.73	2.93	2.75
i-$C_{4=}$	4.25	5.02	5.24	5.63	5.92	5.71
c-$C_{4=}$	1.91	2.36	2.44	2.66	2.75	2.72
i-C_5	0.00	0.00	0.00	0.00	0.00	0.00
n-C_5	1.29	0.92	0.77	0.69	0.62	0.59
$C_{5=+}$	0.54	0.72	0.61	0.60	0.59	0.63
i-C_6	0.32	0.38	0.31	0.35	0.37	0.30
n,i$C_{6=}$	0.53	0.52	0.41	0.44	0.37	0.36
C_7	2.11	1.74	1.08	1.04	0.96	0.96

Table A - 4.3f

Summary of n-hexane cracking reaction at 450 °C , over 1.01g Theta-1 catalyst at 1 atm, different flow rate of $16N_2$:$1nC_6$ feed

Time on stream (min)	3.03	5.30	6.84	8.30
Flow rate (ml/min)	30.00	40.00	59.00	62.00
$WHSV^{-1}(g/gh^{-1})$	45.50	34.10	23.10	22.00
CMR	192.29	196.18	252.86	264.52
P/O	0.55	0.51	0.50	0.49
iC_4/nC_4	0.11	0.08	0.05	0.05
$iC_4/iC_{4=}$	0.06	0.04	0.02	0.02
Conversion(%wt)	91.72	87.12	81.33	77.52
Selectivity(%wt)				
C_1	3.95	3.25	2.97	2.88
C_2	13.18	12.64	12.49	12.40
$C_{2=}$	20.50	17.51	14.43	13.55
C_3	12.60	12.70	13.01	12.97
$C_{3=}$	35.17	37.03	38.56	38.86
i-C_4	0.20	0.17	0.12	0.11
n-C_4	1.70	2.03	2.32	2.37
T-$C_{4=}$	1.98	2.63	3.15	3.30
1-$C_{4=}$	1.45	2.06	2.58	2.73
i-$C_{4=}$	3.37	4.36	5.13	5.34
c-$C_{4=}$	1.44	2.00	2.39	2.52
i-C_5	0.00	0.00	0.00	0.00
n-C_5	1.54	1.10	0.94	0.90
$C_{5=+}$	0.34	0.41	0.44	0.45
i-C_6	0.19	0.22	0.23	0.26
n,$iC_{6=}$	0.36	0.18	0.17	0.38
C_7	2.04	1.70	1.06	0.98

Table A - 4. 4a

Summary of n-hexane cracking reaction at 180 °C , over 1.01g Ak8- ZSM-5 catalyst at , 1 atm different flow rate of $16N_2$:$1nC_6$ feed

TOS (min)	6.05	9.98	13.01	15.28	17.3
Flow rate (ml/min)	15.00	23.08	30.00	40.00	45.00
$WHSV^{-1}(g/gh^{-1})$	90.93	59.10	45.46	34.10	30.31
CMR	0.01	0.03	0.06	0.08	0.09
P/O	29.79	7.42	4.29	2.70	2.75
iC_4/nC_4	1.06	1.11	1.11	1.08	1.07
$iC_4/iC_{4=}$	37.20	8.79	4.94	2.98	2.73
Conversion(%wt)	27.30	9.28	4.99	3.38	2.32
Selectivity(%wt)					
C_1	0.00	0.00	0.00	0.00	0.00
C_2	0.00	0.00	0.00	0.00	0.00
$C_{2=}$	0.25	0.64	1.03	1.17	1.40
C_3	21.31	16.32	14.85	12.53	13.45
$C_{3=}$	0.86	2.44	3.88	4.99	6.21
i-C_4	25.71	21.08	18.43	15.48	15.97
n-C_4	24.18	19.01	16.57	14.35	14.93
T-$C_{4=}$	0.32	0.97	1.51	2.99	2.73
1-$C_{4=}$	0.09	0.29	0.45	0.87	0.00
i-$C_{4=}$	0.69	2.40	3.73	5.20	5.84
c-$C_{4=}$	0.19	0.59	0.91	1.30	1.63
i-C_5	9.02	9.21	8.42	7.54	7.54
n-C_5	11.45	12.20	11.20	10.10	9.98
$C_{5=+}$	0.20	1.30	3.05	5.59	3.47
i-C_6	5.07	10.35	11.60	12.88	11.53
n,i$C_{6=}$	0.64	3.25	4.31	4.90	5.40
C_7	0.00	0.00	0.00	0.00	0.00

Table A - 4. 4b

Summary of n-hexane cracking reaction at 200 °C , over 1.01g Ak8-ZSM-5 catalyst at, 1 atm different flow rate of $16N_2$:$1nC_6$ feed

TOS (min)	6.05	9.98	13.01	15.28	17.3
Flow rate (ml/min)	15.00	23.08	30.00	40.00	45.00
$WHSV^{-1}(g/gh^{-1})$	90.93	59.10	45.46	34.10	30.31
CMR	0.04	0.09	0.15	0.21	0.24
P/O	16.99	4.62	2.78	2.14	1.94
iC_4/nC_4	0.98	1.01	0.99	0.97	0.97
$iC_4/iC_{4=}$	19.42	5.21	3.14	2.32	1.94
Conversion(%wt)	23.83	8.03	4.31	3.11	2.38
Selectivity(%wt)					
C_1	0.15	0.00	0.00	0.00	0.00
C_2	0.13	0.00	0.00	0.00	0.00
$C_{2=}$	0.64	1.62	2.24	2.74	3.02
C_3	20.44	17.40	15.34	14.42	14.17
$C_{3=}$	1.42	4.08	5.88	7.09	8.06
i-C_4	21.70	17.54	14.76	13.22	12.49
n-C_4	22.24	17.45	14.90	13.62	12.89
T-$C_{4=}$	0.49	1.42	2.01	2.49	4.36
1-$C_{4=}$	0.14	0.48	0.68	0.85	1.21
i-$C_{4=}$	1.12	3.37	4.69	5.69	6.45
c-$C_{4=}$	0.39	0.90	1.26	1.50	1.81
i-C_5	9.51	8.09	7.04	6.39	6.18
n-C_5	12.32	10.27	9.22	8.13	8.13
$C_{5=+}$	0.64	3.09	4.12	6.84	3.89
i-C_6	7.69	10.79	11.53	11.63	12.09
n,$iC_{6=}$	0.72	2.84	5.58	4.64	5.24
C_7	0.28	0.70	0.82	0.75	0.00

Table A - 4.4c

Summary of n-hexane cracking reaction at 250 °C , over 1.01g Ak8-ZSM-5 catalyst at 1 atm, different flow rate of $16N_2$:$1nC_6$ feed

TOS (min)	6.05	9.98	12.25	14.27
Flow rate (ml/min)	15.00	23.08	40.00	45.00
$WHSV^{-1}(g/gh^{-1})$	90.93	59.10	34.10	30.31
CMR	0.74	1.23	1.51	1.71
P/O	3.79	2.11	1.57	1.33
iC_4/nC_4	0.90	0.76	0.72	0.70
$iC_4/iC_{4=}$	5.91	2.44	1.59	1.12
Conversion(%wt)	27.28	13.44	8.97	8.14
Selectivity(%wt)				
C_1	0.72	0.51	0.44	0.43
C_2	2.02	1.74	1.65	1.68
$C_{2=}$	6.84	8.74	8.97	9.20
C_3	32.54	26.96	24.14	23.26
$C_{3=}$	6.86	11.00	14.28	16.14
i-C_4	12.86	8.95	7.34	6.61
n-C_4	14.26	11.71	10.18	9.46
T-$C_{4=}$	1.27	2.08	2.55	2.80
1-$C_{4=}$	0.54	0.90	1.13	1.24
i-$C_{4=}$	2.18	3.67	4.62	5.89
c-$C_{4=}$	1.14	1.66	1.96	2.10
i-C_5	3.80	2.77	2.24	1.99
n-C_5	3.58	3.32	3.00	2.67
$C_{5=+}$	1.15	2.35	3.01	2.92
i-C_6	3.95	4.86	5.64	4.75
n,$iC_{6=}$	0.90	1.71	2.41	2.56
C_7	5.36	7.03	6.44	6.29

Table A - 4.4d

Summary of n-hexane cracking reaction at 300 °C , over 1.01g Ak8-ZSM catalyst at, 1 atm different flow rate of $16N_2$:$1nC_6$ feed.

TOS (min)	3.93	6.96	9.23	11.25	12.79
Flow rate (ml/min)	23.08	30.00	40.00	45	59.00
$WHSV^{-1}(g/gh^{-1})$	59.10	45.46	34.10	30.31	23.12
CMR	3.11	2.93	3.62	2.72	4.35
P/O	1.75	1.29	1.08	1.28	0.93
iC_4/nC_4	0.80	0.65	0.58	0.56	0.50
$iC_4/iC_{4=}$	1.72	1.00	0.78	0.87	0.60
Conversion(%wt)	29.97	25.44	18.38	20.98	14.44
Selectivity(%wt)					
C_1	0.84	0.63	0.65	0.53	0.69
C_2	4.88	4.55	4.67	4.01	5.08
$C_{2=}$	11.82	9.50	8.96	8.05	8.50
C_3	31.48	29.45	26.72	28.54	26.28
$C_{3=}$	18.01	22.88	24.83	22.28	28.34
i-C_4	5.64	5.02	3.95	4.63	3.28
n-C_4	7.08	7.77	6.78	8.27	6.56
T-$C_{4=}$	1.97	2.79	2.91	3.02	3.03
1-$C_{4=}$	1.06	1.51	1.54	1.62	1.68
i-$C_{4=}$	3.27	5.00	5.05	5.32	5.43
c-$C_{4=}$	1.73	2.34	2.38	2.40	2.40
i-C_5	1.20	0.98	0.77	1.00	0.61
n-C_5	0.92	1.05	0.90	1.34	0.89
$C_{5=+}$	1.47	2.32	2.23	2.59	2.07
i-C_6	1.55	1.29	1.00	0.61	1.15
n,$iC_{6=}$	1.67	1.17	2.06	1.27	2.21
C_7	5.40	1.74	4.59	4.51	1.77

Table A - 4.4e

Summary of n-hexane cracking reaction at 350 °C , over 1.01g Ak8-ZSM-5 catalyst at, 1 atm different flow rate of $16N_2$:$1nC_6$ feed

TOS (min)	3.93	6.96	9.23	11.25	12.79
Flow rate (ml/min)	23.08	30.00	40.00	45	59.00
$WHSV^{-1}(g/gh^{-1})$	59.10	45.46	34.10	30.31	23.12
CMR	4.75	5.85	7.06	7.82	9.80
P/O	1.16	0.99	0.87	0.83	0.73
iC_4/nC_4	0.79	0.66	0.58	0.53	0.43
$iC_4/iC_{4=}$	1.33	0.95	0.73	0.63	0.44
Conversion(%wt)	68.88	58.01	54.36	49.19	37.77
Selectivity(%wt)					
C_1	1.51	1.38	1.38	1.32	1.31
C_2	8.71	8.47	8.40	8.39	8.38
$C_{2=}$	13.30	13.44	13.31	13.24	12.32
C_3	29.07	26.98	25.51	25.03	23.12
$C_{3=}$	21.74	23.86	26.22	27.32	30.64
i-C_4	4.95	3.98	3.27	2.93	2.25
n-C_4	6.27	5.98	5.65	5.55	5.21
T-$C_{4=}$	2.22	2.48	2.60	2.71	3.00
1-$C_{4=}$	1.35	1.54	1.66	1.73	1.95
i-$C_{4=}$	3.72	4.18	4.47	4.64	5.08
c-$C_{4=}$	1.99	2.22	2.37	2.31	2.45
i-C_5	0.75	0.61	0.58	0.41	0.31
n-C_5	0.43	0.42	0.47	0.36	0.33
$C_{5=+}$	1.73	1.97	2.34	2.07	1.90
i-C_6	0.25	0.32	0.22	0.24	0.37
n,i$C_{6=}$	0.35	0.49	0.39	0.55	0.61
C_7	1.66	1.66	1.16	1.18	0.78

Table A - 4.4f

Summary of n-hexane cracking reaction at 400 °C , over 1.01g Ak8- ZSM-5 catalyst at, 1 atm different flow rate of $16N_2$:$1nC_6$ feed

TOS (min)	3.03	5.3	7.32	8.86	10.32
Flow rate (ml/min)	30.00	40.00	45.00	59	65.00
$WHSV^{-1}(g/gh^{-1})$	45.46	34.10	30.31	23.12	20.98
CMR	14.02	15.69	17.50	18.32	20.31
P/O	0.88	0.79	0.73	0.70	0.65
iC_4/nC_4	0.55	0.46	0.39	0.36	0.32
$iC_4/iC_{4=}$	0.70	0.52	0.42	0.37	0.30
Conversion(%wt)	83.18	77.87	70.10	68.00	62.18
Selectivity(%wt)					
C_1	2.81	2.58	2.38	2.31	2.14
C_2	11.89	11.36	10.97	10.87	10.54
$C_{2=}$	18.06	17.34	16.70	16.25	15.31
C_3	21.46	20.68	19.79	19.76	18.83
$C_{3=}$	24.88	26.86	28.37	29.42	30.51
i-C_4	2.34	1.99	1.72	1.61	1.38
n-C_4	4.22	4.36	4.40	4.44	4.34
T-$C_{4=}$	2.03	2.32	2.54	2.66	2.83
1-$C_{4=}$	1.43	1.67	1.84	1.95	2.10
i-$C_{4=}$	3.33	3.80	4.13	4.33	4.67
c-$C_{4=}$	1.72	1.96	2.15	2.20	2.39
i-C_5	0.24	0.19	0.17	0.16	0.16
n-C_5	0.11	0.12	0.12	0.12	0.17
$C_{5=+}$	1.55	1.55	1.63	1.57	2.11
i-C_6	0.06	0.03	0.05	0.07	0.25
n,$iC_{6=}$	0.33	0.38	0.45	0.42	0.52
C_7	3.55	2.80	2.59	1.87	1.76

Table A - 4.5a

Summary of n-hexane cracking reaction at 200 °C , over 1.01g Ak8-T catalyst at 1 atm, different flow rate of $16N_2 : 1nC_6$ feed

TOS (min)	6.05	9.98	13.01	15.03
Flow rate (ml/min)	15.00	23.08	30.00	45.00
$WHSV^{-1}(g/gh^{-1})$	90.93	59.10	45.46	30.31
P/O	1.52	0.85	0.79	0.53
iC_4/nC_4	0.37	0.00	0.00	0.00
$iC_4/iC_{4=}$	1.31	0.00	0.00	0.00
Conversion(%wt)	0.83	0.75	0.64	0.44
Selectivity(%wt)				
C_1	2.57	0.00	0.00	0.00
C_2	0.00	0.00	0.00	0.00
$C_{2=}$	7.71	7.28	4.45	3.98
C_3	21.58	12.99	10.07	9.14
$C_{3=}$	9.76	14.76	14.76	17.10
i-C_4	2.91	0.00	0.00	0.00
n-C_4	7.88	4.92	3.98	3.58
T-$C_{4=}$	1.71	2.95	4.92	7.16
1-$C_{4=}$	0.00	0.00	0.00	0.00
i-$C_{4=}$	2.23	2.76	4.22	5.96
c-$C_{4=}$	0.00	0.00	0.00	0.00
i-C_5	1.88	0.00	0.00	0.00
n-C_5	3.94	4.33	5.86	4.77
$C_{5=+}$	0.00	0.00	0.00	0.00
i-C_6	16.79	20.86	21.55	13.92
n,$iC_{6=}$	18.50	25.98	27.64	31.81
C_7	3.08	2.76	2.81	3.58

Table A - 4.5b

Summary of n-hexane cracking reaction at 250 °C , over 1.01g Ak8-Tcatalyst at 1 atm, different flow rate of $16N_2$:$1nC_6$ feed

TOS(min)	6.05	9.98	13.01	15.28	17.3
Flow rate (ml/min)	15.00	23.08	30.00	40.00	45.00
$WHSV^{-1}(g/gh^{-1})$	90.93	59.10	45.46	34.10	30.31
CMR	12.92	12.14	8.85	7.58	#DIV/0!
iC_4/nC_4	0.35	0.40	0.34	0.41	0.00
$iC_4/iC_{4=}$	0.35	0.29	0.20	0.25	0.00
P/O	1.51	1.14	1.01	1.19	1.01
Conversion(%wt)	4.42	2.60	1.48	1.45	1.11
Selectivity(%wt)					
C_1	0.92	0.97	0.00	0.00	0.00
C_2	3.98	3.94	3.72	3.63	3.91
$C_{2=}$	10.82	8.84	5.43	5.07	4.98
C_3	20.05	14.24	13.54	10.32	9.84
$C_{3=}$	32.15	37.32	34.37	34.51	36.41
i-C_4	1.22	1.13	1.03	1.15	0.00
n-C_4	3.45	2.86	3.00	2.77	2.02
T-$C_{4=}$	2.66	3.40	4.13	3.82	3.56
1-$C_{4=}$	1.12	1.35	1.55	1.53	1.90
i-$C_{4=}$	3.45	3.94	5.27	4.59	4.74
c-$C_{4=}$	1.74	2.05	2.27	2.10	2.49
i-C_5	0.59	1.29	1.50	1.63	0.00
n-C_5	1.08	1.89	2.27	2.58	1.66
$C_{5=+}$	1.25	0.86	1.65	1.43	0.00
i-C_6	4.83	3.29	4.50	11.85	12.81
n,$iC_{6=}$	6.05	8.90	12.35	11.28	14.00
C_7	4.70	3.94	3.36	1.53	1.78

Table A - 4.5c

Summary of n-hexane cracking reaction at 300 °C , over 1.01g Ak8-T catalyst at 1 atm, different flow rate of $16N_2$:$1nC_6$ feed

TOS (min)	6.05	9.98	13.01	15.28	17.3	19.57
Flow rate (ml/min)	15.00	23.08	30.00	40.00	45.00	40.00
$WHSV^{-1}(g/gh^{-1})$	90.93	59.10	45.46	34.10	30.31	34.10
CMR	25.08	33.00	35.53	#DIV/0!	#DIV/0!	#DIV/0!
P/O	0.65	0.52	0.39	0.35	0.34	0.39
iC_4/nC_4	0.32	0.25	0.24	0.00	0.00	0.00
$iC_4/iC_{4=}$	0.23	0.13	0.11	0.00	0.00	0.00
Conversion(%wt)	11.73	6.90	5.65	5.08	3.93	4.74
Selectivity(%wt)						
C_1	1.37	1.22	1.13	1.14	1.12	1.21
C_2	7.51	6.64	6.71	6.60	6.53	6.71
$C_{2=}$	10.48	8.54	7.74	7.14	6.64	6.77
C_3	19.02	13.95	12.23	11.29	10.48	11.97
$C_{3=}$	36.36	41.46	45.68	47.68	48.24	45.10
i-C_4	0.77	0.50	0.44	0.00	0.00	0.00
n-C_4	2.43	1.99	1.81	1.59	1.52	1.76
T-$C_{4=}$	2.37	2.75	2.89	3.13	3.34	3.40
1-$C_{4=}$	1.12	1.49	1.52	1.65	1.74	1.73
i-$C_{4=}$	3.38	3.97	4.15	4.49	4.53	4.64
c-$C_{4=}$	1.68	1.90	2.01	2.16	2.18	2.20
i-C_5	0.18	0.99	0.00	0.00	0.00	0.00
n-C_5	0.27	0.36	0.00	0.00	0.00	0.59
$C_{5=+}$	1.59	0.41	1.21	1.71	0.94	1.11
i-C_6	1.99	3.43	2.32	2.87	3.34	2.44
n,$iC_{6=}$	3.52	5.28	6.66	6.11	6.93	6.87
C_7	6.00	5.10	3.48	2.47	2.58	3.43

Table A - 4.5d

Summary of n-hexane cracking reaction at 350 °C , over 1.01g Ak8-T catalyst at 1 atm, different flow rate of $16N_2$:$1nC_6$ feed

Flow rate (ml/min)	15.00	23.08	30.00	40.00	45.00	40.00
$WHSV^{-1}(g/gh^{-1})$	90.93	59.10	45.46	34.10	30.31	34.10
Conversion(%wt)	31.96	20.89	17.09	15.56	10.83	15.06
CMR	66.77	89.25	118.90	124.31	#DIV/0!	100.79
P/O	0.64	0.51	0.50	0.43	0.40	0.42
$iC_4/iC_{4=}$	0.10	0.05	0.04	0.04	0.00	0.03
iC_4/nC_4	0.15	0.11	0.08	0.08	0.00	0.09
Selectivity(%wt)						
C_1	2.02	1.74	1.58	1.55	1.45	1.54
C_2	11.14	9.77	8.94	8.84	8.32	9.22
$C_{2=}$	11.99	10.53	9.46	9.22	8.54	8.28
C_3	17.04	14.16	12.39	12.04	11.13	12.64
$C_{3=}$	35.83	41.32	41.93	46.11	46.94	45.63
i-C_4	0.38	0.25	0.17	0.16	0.00	0.19
n-C_4	2.57	2.27	2.00	1.94	1.89	2.06
T-$C_{4=}$	2.65	2.91	3.28	3.04	3.03	3.40
1-$C_{4=}$	1.38	1.60	1.75	1.73	1.78	1.98
i-$C_{4=}$	3.95	4.63	4.61	4.45	4.27	5.41
c-$C_{4=}$	1.99	2.07	2.12	2.09	2.17	2.44
i-C_5	0.00	0.00	0.00	0.00	0.00	0.00
n-C_5	0.00	0.00	0.00	0.00	0.00	0.00
$C_{5=+}$	1.64	1.57	2.22	1.66	1.92	1.44
i-C_6	0.06	0.32	0.17	0.46	0.89	0.58
n,i$C_{6=}$	1.41	1.48	1.14	1.84	2.95	1.70
C_7	5.96	5.37	8.22	4.89	4.74	3.51

Table A - 4.5e

Summary of n-hexane cracking reaction at 400 °C , over 1.01g Ak8-T catalyst at 1 atm, different flow rate of $16N_2$:$1nC_6$ feed.

TOS (min)	3.93	6.96	9.23	11.25	12.79
Flow rate (ml/min)	23.08	30.00	40.00	45.00	59.00
$WHSV^{-1}(g/gh^{-1})$	59.10	45.46	34.10	30.31	23.1
CMR	90.88	112.64	142.24	167.23	198.25
P/O	0.53	0.49	0.47	0.47	0.46
iC_4/nC_4	0.09	0.07	0.05	0.05	0.04
$iC_4/iC_{4=}$	0.00	0.00	0.00	0.00	0.00
Conversion(%wt)	49.12	43.23	36.05	35.73	27.63
Selectivity(%wt)					
C_1	2.24	2.13	2.01	1.97	1.91
C_2	12.03	11.74	11.55	11.53	11.29
$C_{2=}$	10.13	9.05	8.11	7.70	7.12
C_3	14.72	14.17	13.81	13.67	13.25
$C_{3=}$	38.03	38.65	39.34	39.57	39.79
i-C_4	0.27	0.20	0.15	0.13	0.10
n-C_4	2.86	2.83	2.81	2.74	2.69
T-$C_{4=}$	3.21	3.91	4.32	4.43	4.57
1-$C_{4=}$	1.93	2.45	2.82	2.98	3.15
i-$C_{4=}$	5.67	6.59	7.09	7.25	7.38
c-$C_{4=}$	2.41	2.95	3.25	3.32	3.45
i-C_5	0.00	0.00	0.00	0.00	0.00
n-C_5	0.00	0.00	0.00	0.00	0.00
$C_{5=+}$	2.87	2.37	2.11	2.00	1.97
i-C_6	0.18	0.12	0.05	0.10	0.08
n,$iC_{6=}$	1.09	1.05	1.00	0.88	1.01
C_7	2.34	1.81	1.58	1.74	2.23

Table A - 4.5f

Summary of n-hexane cracking reaction at 450 °C , over 1.01g Ak8-T catalyst at 1 atm, different flow rate of $16N_2$:$1nC_6$ feed

TOS (min)	3.03	5.3	7.32	8.89	10.35	13.38
Flow rate (ml/min)	30.00	40.00	45.00	59.00	65.00	30.00
$WHSV^{-1}(g/gh^{-1})$	45.46	34.10	30.31	23.12	20.98	45.46
CMR	172.03	179.38	178.92	208.56	238.68	151.19
P/O	11.89	29.43	35.98	17.74	12.04	58.30
iC_4/nC_4	0.00	0.00	0.00	0.00	0.00	0.00
$iC_4/iC_{4=}$	0.00	0.00	0.00	0.00	0.00	0.00
Conversion(%wt)	50.02	47.83	45.06	36.36	31.85	50.48
Selectivity(%wt)						
C_1	9.80	10.58	10.41	9.59	8.99	10.90
C_2	34.54	37.09	37.45	36.34	35.03	37.74
$C_{2=}$	1.82	0.53	0.40	0.74	1.04	0.24
C_3	35.44	38.19	38.55	37.74	37.15	38.50
$C_{3=}$	4.26	1.30	1.11	2.59	3.89	0.53
i-C_4	0.27	0.27	0.27	0.22	0.19	0.32
n-C_4	6.92	7.57	7.74	7.96	8.01	7.58
T-$C_{4=}$	0.14	0.13	0.06	0.17	0.28	0.07
1-$C_{4=}$	0.08	0.07	0.04	0.09	0.15	0.03
i-$C_{4=}$	0.47	0.22	0.18	0.50	0.79	0.10
c-$C_{4=}$	0.20	0.16	0.14	0.22	0.31	0.11
i-C_5	0.00	0.00	0.00	0.00	0.00	0.00
n-C_5	0.05	0.09	0.05	0.07	0.09	0.06
$C_{5=+}$	0.00	0.00	0.00	0.00	0.00	0.00
i-C_6	0.95	0.92	1.08	1.01	0.82	1.46
n,i$C_{6=}$	0.78	0.88	0.77	1.04	1.22	0.61
C_7	4.28	2.01	1.75	1.72	2.05	1.75

Table A - 4.6a

Summary of n-hexane cracking reaction at 300 °C , over 1.01g CR-ZSM 5 catalyst at , 1 atm different flow rate of $16N_2$:$1nC_6$ feed

Flow rate (ml/min)	23.08	30.00	40.00	45.00	59.00
$WHSV^{-1}(g/gh^{-1})$	59.10	45.46	34.10	30.31	23.12
CMR	1.09	1.60	1.29	1.69	2.14
P/O	1.96	1.72	1.68	1.43	1.22
iC_4/nC_4	0.61	0.56	0.53	0.50	0.46
$iC_4/iC_{4=}$	0.01	0.01	0.01	0.00	0.00
Conversion(%wt)	19.33	12.88	10.80	8.18	5.41
Selectivity(%wt)					
C_1	0.58	0.48	0.25	0.31	0.42
C_2	1.98	2.19	2.07	2.52	2.97
$C_{2=}$	6.23	7.82	5.93	6.32	6.16
C_3	31.88	30.91	30.18	29.67	28.22
$C_{3=}$	16.24	17.95	17.92	20.79	23.17
i-C_4	8.04	6.57	6.38	5.41	4.46
n-C_4	13.23	11.71	12.06	10.92	9.69
T-$C_{4=}$	2.68	2.95	3.06	3.45	3.59
1-$C_{4=}$	0.89	1.06	1.13	1.29	1.34
i-$C_{4=}$	4.64	5.18	5.55	6.05	5.97
c-$C_{4=}$	2.06	2.24	2.31	2.52	2.47
i-C_5	1.62	1.40	1.44	1.19	1.04
n-C_5	2.67	2.59	2.86	2.47	2.55
$C_{5=+}$	2.26	2.67	2.90	3.12	2.66
i-C_6	1.66	1.21	2.41	2.14	2.69
n,i$C_{6=}$	1.11	1.48	1.74	1.46	2.07
C_7	2.25	1.62	1.83	0.35	0.50

Table A - 4.6b

Summary of n-hexane cracking reaction at 350 °C , over 1.01g CR-ZSM 5 catalyst at , 1 atm different flow rate of $16N_2$:$1nC_6$ feed

Flow rate (ml/min)	23.08	30.00	40.00	45.00
$WHSV^{-1}(g/gh^{-1})$	59.10	45.46	34.10	30.31
CMR	3.95	5.11	6.08	6.99
P/O	1.28	1.08	0.97	0.89
iC_4/nC_4	0.58	0.49	0.43	0.40
$iC_4/iC_{4=}$	0.00	0.00	0.00	0.00
Conversion(%wt)	36.15	25.59	19.78	18.15
Selectivity(%wt)				
C_1	0.72	0.76	0.79	0.84
C_2	5.43	5.72	6.03	6.38
$C_{2=}$	11.08	10.83	10.51	10.24
C_3	30.86	29.10	27.90	26.96
$C_{3=}$	24.05	26.95	28.69	30.38
i-C_4	4.36	3.39	2.85	2.50
n-C_4	7.52	6.97	6.59	6.22
T-$C_{4=}$	2.92	3.08	3.18	3.16
1-$C_{4=}$	1.06	1.18	1.29	1.32
i-$C_{4=}$	4.54	4.87	5.02	5.15
c-$C_{4=}$	2.28	2.39	2.47	2.44
i-C_5	0.70	0.51	0.43	0.35
n-C_5	0.86	0.74	0.67	0.59
$C_{5=+}$	2.04	1.85	1.83	1.72
i-C_6	0.33	0.24	0.34	0.34
n,i$C_{6=}$	0.73	0.89	1.02	1.06
C_7	0.52	0.55	0.44	0.36

Table A - 4.6c

Summary of n-hexane cracking reaction at 400 °C , over 1.01g CR-ZSM 5 catalyst at 1 atm different flow rate of $16N_2 : 1nC_6$ feed

Flow rate (ml/min)	23.08	30.00	40.00	45.00	59.00
$WHSV^{-1}(g/gh^{-1})$	59.10	45.46	34.10	30.31	23.12
Conversion(%wt)	52.84	46.14	37.24	32.77	27.61
CMR	17.33	19.63	22.02	23.00	24.54
P/O	0.80	0.70	0.64	0.62	0.58
iC_4/nC_4	0.38	0.33	0.29	0.27	0.25
$iC_4/iC_{4=}$	0.46	0.35	0.28	0.25	0.21
Selectivity(%wt)					
C_1	1.68	1.60	1.52	1.48	1.45
C_2	9.88	9.74	9.62	9.57	9.60
$C_{2=}$	16.66	16.02	14.92	14.27	13.34
C_3	23.08	21.86	20.71	20.20	19.38
$C_{3=}$	28.07	30.90	33.12	33.96	35.57
$i\text{-}C_4$	1.63	1.39	1.18	1.10	0.99
$n\text{-}C_4$	4.29	4.25	4.15	4.11	4.01
$T\text{-}C_{4=}$	2.46	2.67	2.84	2.88	3.05
$1\text{-}C_{4=}$	1.03	1.25	1.42	1.51	1.66
$i\text{-}C_{4=}$	3.51	3.94	4.25	4.42	4.67
$c\text{-}C_{4=}$	1.91	2.05	2.18	2.24	2.33
$i\text{-}C_5$	0.16	0.13	0.12	0.10	0.09
$n\text{-}C_5$	0.17	0.16	0.15	0.14	0.17
$C_{5=+}$	1.12	1.15	1.17	1.17	1.18
$i\text{-}C_6$	0.02	0.03	0.03	0.04	0.09
$n,iC_{6=}$	0.87	1.00	1.10	1.19	1.33
C_7	3.45	1.87	1.52	1.60	1.08

Table A - 4.6d

Summary of n-hexane cracking reaction at 450 °C , over 1.01g CR-ZSM 5 catalyst at 1 atm different flow rate of $16N_2$:$1nC_6$ feed

Flow rate (ml/min)	30.00	40.00	45.00	59.00	65.00
$WHSV^{-1}(g/gh^{-1})$	45.46	34.10	30.31	23.12	20.98
CMR	44.85	49.67	50.32	57.70	58.62
P/O	0.57	0.51	0.49	0.44	0.43
iC_4/nC_4	0.00	0.00	0.00	0.00	0.00
$iC_4/iC_{4=}$	0.22	0.17	0.16	0.12	0.12
Conversion(%wt)	72.37	62.12	58.45	50.67	48.81
Selectivity(%wt)					
C_1	2.40	2.24	2.20	2.11	2.10
C_2	11.72	11.48	11.37	11.26	11.28
$C_{2=}$	20.24	18.94	18.53	16.99	16.51
C_3	17.68	16.81	16.35	15.67	15.56
$C_{3=}$	31.18	33.06	33.42	35.26	35.84
i-C_4	0.77	0.66	0.64	0.53	0.51
n-C_4	3.21	3.32	3.34	3.38	3.37
T-$C_{4=}$	2.56	2.79	2.88	3.02	3.15
1-$C_{4=}$	1.13	1.34	1.44	1.67	1.76
i-$C_{4=}$	3.44	3.83	3.97	4.29	4.39
c-$C_{4=}$	1.83	2.02	2.11	2.25	2.30
i-C_5	0.04	0.04	0.05	0.04	0.04
n-C_5	0.05	0.05	0.05	0.05	0.07
$C_{5=+}$	0.94	0.95	1.00	0.98	1.01
i-C_6	0.24	0.20	0.24	0.19	0.15
n,i$C_{6=}$	0.33	0.35	0.44	0.50	0.45
C_7	2.25	1.95	1.98	1.82	1.49

Table A - 4.7a

Summary of n-hexane cracking reaction at 300 °C , over 1.01g A-ZSM-5 catalyst at, 1 atm different flow rate of $16N_2$:$1nC_6$ feed.

Flow rate (ml/min)	15.00	23.08	30.00	40.00
$WHSV^{-1}(g/gh^{-1})$	90.90	59.10	45.46	34.10
CMR	3.63	4.25	5.63	#DIV/0!
P/O	1.48	1.39	1.41	1.35
iC_4/nC_4	0.35	0.38	0.30	0.00
$iC_4/iC_{4=}$	0.75	0.66	0.47	0.00
Conversion(%wt)	3.92	1.92	1.48	0.89
Selectivity(%wt)				
C_1	0.85	1.01	1.04	0.00
C_2	5.63	6.26	6.22	6.92
$C_{2=}$	4.95	4.14	4.00	3.93
C_3	31.85	25.45	23.24	22.49
$C_{3=}$	21.09	20.58	19.17	19.19
i-C_4	3.15	2.68	2.00	0.00
n-C_4	8.99	7.05	6.59	5.98
T-$C_{4=}$	2.89	3.75	3.26	2.36
1-$C_{4=}$	0.65	0.95	0.00	0.00
i-$C_{4=}$	4.18	4.08	4.22	2.83
c-$C_{4=}$	1.74	1.73	1.55	2.67
i-C_5	0.80	0.78	1.18	0.00
n-C_5	1.74	2.57	2.00	3.46
$C_{5=+}$	1.03	1.12	1.92	2.20
i-C_6	6.57	12.31	16.28	18.87
n,i$C_{6=}$	3.80	5.48	7.40	9.59
C_7	0.00	0.00	0.00	0.00

Table A - 4.7b

Summary of n-hexane cracking reaction at 350 °C , over 1.01g A-ZSM-5 catalyst at , varied flow rate of $16N_2 : 1nC_6$ feed.

Flow rate (ml/min)	23.08	30.00	40.00	45.00	59.00
$WHSV^{-1}(g/gh^{-1})$	59.10	45.46	34.10	30.31	23.12
CMR	19.46	20.56	20.89	22.42	25.22
P/O	0.65	0.61	0.59	0.58	0.58
iC_4/nC_4	0.25	0.24	0.24	0.22	0.19
$iC_4/iC_{4=}$	0.23	0.18	0.17	0.15	0.13
Conversion(%wt)	12.71	9.14	7.24	6.22	4.31
Selectivity(%wt)					
C_1	1.35	1.32	1.34	1.42	1.40
C_2	7.36	7.30	7.52	7.61	7.61
$C_{2=}$	10.72	9.53	8.82	8.48	7.96
C_3	19.53	17.69	16.52	16.07	15.30
$C_{3=}$	37.78	38.64	39.69	39.94	39.46
$i\text{-}C_4$	1.00	0.88	0.85	0.78	0.67
$n\text{-}C_4$	3.93	3.74	3.55	3.58	3.54
$T\text{-}C_{4=}$	3.29	3.69	3.82	3.87	3.92
$1\text{-}C_{4=}$	0.98	1.14	1.20	1.27	1.32
$i\text{-}C_{4=}$	4.41	4.80	4.97	5.06	5.21
$c\text{-}C_{4=}$	2.21	2.45	2.36	2.41	2.52
$i\text{-}C_5$	0.23	0.52	0.61	0.29	0.00
$n\text{-}C_5$	0.24	0.29	0.42	0.31	0.44
$C_{5=+}$	0.79	1.16	0.96	0.98	0.85
$i\text{-}C_6$	1.51	1.79	2.78	3.21	4.01
$n,iC_{6=}$	2.27	2.64	2.88	3.10	4.07
C_7	2.37	2.38	1.69	1.67	1.67

Table A - 4.7c

Summary of n-hexane cracking reaction at 400 °C , over 1.01g A-ZSM-5 catalyst at , 1 atm different flow rate of $16N_2$:$1nC_6$ feed

Flow rate (ml/min)	23.08	30.00	40.00	45	59.00
$WHSV^{-1}(g/gh^{-1})$	59.10	45.46	34.10	30.31	23.12
CMR	28.63	33.45	34.97	38.80	39.80
P/O	0.61	0.54	0.51	0.50	0.53
iC_4/nC_4	0.19	0.17	0.15	0.14	0.14
$iC_4/iC_{4=}$	0.16	0.12	0.10	0.09	0.09
Conversion(%wt)	21.48	17.70	12.22	12.03	10.37
Selectivity(%wt)					
C_1	1.62	1.66	1.51	1.60	1.58
C_2	9.55	9.48	9.07	9.35	9.09
$C_{2=}$	11.57	10.71	9.61	9.66	8.94
C_3	18.22	16.55	15.36	15.17	14.00
$C_{3=}$	36.59	39.11	39.50	40.29	39.78
i-C_4	0.79	0.65	0.58	0.53	0.49
n-C_4	4.11	3.83	3.76	3.68	3.44
T-$C_{4=}$	3.57	3.98	4.40	4.31	4.32
1-$C_{4=}$	1.19	1.36	1.51	1.53	1.56
i-$C_{4=}$	4.99	5.46	5.77	5.77	5.60
c-$C_{4=}$	2.47	2.56	2.97	2.93	2.80
i-C_5	0.18	0.14	0.22	0.13	0.00
n-C_5	0.48	0.33	0.32	0.29	0.34
$C_{5=+}$	0.88	0.94	1.13	0.91	0.89
i-C_6	0.58	0.74	1.16	1.20	4.15
n,$iC_{6=}$	0.99	0.94	1.34	1.17	1.53
C_7	2.21	1.55	1.77	1.48	1.50

Table A - 4.7d

Summary of n-hexane cracking reaction at 450 °C , over 1.01g A-ZSM-5 catalyst at , 1 atm varied flow rate of $16N_2$:$1nC_6$ feed

Flow rate (ml/min)	23.08	30.00	40.00	45	59.00
$WHSV^{-1}(g/gh^{-1})$	59.10	45.46	34.10	30.31	23.12
CMR	68.80	75.22	79.48	81.46	85.59
P/O	0.58	0.54	0.52	0.51	0.50
iC_4/nC_4	0.11	0.10	0.09	0.08	0.08
$iC_4/iC_{4=}$	0.09	0.07	0.06	0.06	0.05
Conversion(%wt)	44.77	34.70	28.69	25.78	21.46
Selectivity(%wt)					
C_1	2.17	2.06	1.97	1.94	1.92
C_2	11.06	10.79	10.66	10.61	10.52
$C_{2=}$	14.59	13.55	12.44	11.93	11.16
C_3	15.77	14.96	14.54	14.35	13.93
$C_{3=}$	35.73	37.20	38.82	39.19	39.72
i-C_4	0.40	0.35	0.32	0.30	0.28
n-C_4	3.77	3.68	3.62	3.62	3.56
T-$C_{4=}$	3.42	3.73	3.90	3.97	4.10
1-$C_{4=}$	1.28	1.42	1.54	1.61	1.69
i-$C_{4=}$	4.49	4.74	5.06	5.16	5.17
c-$C_{4=}$	2.36	2.57	2.68	2.74	2.81
i-C_5	0.06	0.06	0.06	0.06	0.11
n-C_5	0.39	0.34	0.40	0.44	0.66
$C_{5=+}$	0.81	0.90	0.84	0.85	0.88
i-C_6	0.10	0.10	0.25	0.40	0.62
n,$iC_{6=}$	0.56	0.67	0.75	0.89	1.15
C_7	3.04	2.86	2.19	1.96	1.74

Table A - 4.8

Selectivities of n-hexane cracking as a function of temperatures at WHSV-1(g/gh-1) 45.5, 1 atm, over 1.01g ZSM 5 catalyst

Temperature (oC)	180.00	200.00	250.00	300.00	350.00	400.00
CMR	0.03	0.30	0.57	2.80	8.13	16.99
P/O	8.68	5.53	3.75	1.73	1.37	0.86
iC_4/nC_4	1.19	1.15	0.86	0.74	0.62	0.63
$iC_4/iC_{4=}$	12.59	8.77	3.96	1.57	1.13	0.79
Conversion(%wt)	18.89	12.49	29.82	50.42	77.86	95.89
Selectivity(%wt)						
C_1	0.00	0.63	0.41	0.88	2.00	3.44
C_2	0.19	1.12	1.73	5.67	10.17	12.69
$C_{2=}$	0.58	4.05	5.24	10.71	14.84	21.19
C_3	17.63	20.79	32.19	33.16	27.27	20.39
$C_{3=}$	2.03	3.76	8.59	19.18	19.92	23.76
$i\text{-}C_4$	22.92	19.69	12.92	6.16	3.32	2.20
$n\text{-}C_4$	19.23	17.16	14.95	8.31	5.40	3.49
$T\text{-}C_{4=}$	0.86	1.21	1.70	2.28	1.87	1.75
$1\text{-}C_{4=}$	0.23	0.35	0.70	1.21	1.13	1.20
$i\text{-}C_{4=}$	1.82	2.24	3.27	3.91	2.93	2.78
$c\text{-}C_{4=}$	0.48	0.74	1.55	2.05	1.69	1.46
$i\text{-}C_5$	9.88	8.35	3.62	1.09	0.43	0.23
$n\text{-}C_5$	11.70	7.80	3.95	0.95	0.26	0.25
$C_{5=+}$	1.30	1.36	1.93	1.78	1.23	0.89
$i\text{-}C_6$	7.96	8.57	3.08	0.61	0.48	0.14
$n,iC_{6=}$	2.55	0.34	0.60	0.36	0.26	0.13
C_7	0.63	1.84	3.59	1.67	6.80	4.03

Table A - 4.9

Selectivity as a function of temperatures of n-hexane cracking at $WHSV^{-1}$(g/gh-1) 34.1, 1 atm over 1.01g Ak8-ZSM 5 catalyst

Temperature (oC)	180.00	200.00	250.00	300.00	350.00	400.00
CMR	0.08	0.21	1.51	3.62	7.06	15.69
P/O	2.51	2.04	1.69	1.08	0.97	0.77
iC_4/nC_4	1.08	0.97	0.72	0.58	0.58	0.46
$iC_4/iC_{4=}$	2.98	2.32	1.59	0.78	0.73	0.52
Conversion(%wt)	3.38	3.11	8.97	18.38	54.36	77.87
Selectivity(%wt)						
C_1	0.00	0.00	0.44	0.65	1.38	2.58
C_2	0.00	0.00	1.65	4.67	8.40	11.36
$C_{2=}$	1.17	2.74	8.97	8.96	13.31	17.34
C_3	12.53	14.42	24.14	26.72	25.51	20.68
$C_{3=}$	4.99	7.09	14.28	24.83	26.22	26.86
i-C_4	15.48	13.22	7.34	3.95	3.27	1.99
n-C_4	14.35	13.62	10.18	6.78	5.65	4.36
T-$C_{4=}$	2.99	2.49	2.55	2.91	2.60	2.32
1-$C_{4=}$	0.87	0.85	1.13	1.54	1.66	1.67
i-$C_{4=}$	5.20	5.69	4.62	5.05	4.47	3.80
c-$C_{4=}$	1.30	1.50	1.96	2.38	2.37	1.96
i-C_5	7.54	6.39	2.24	0.77	0.58	0.19
n-C_5	10.10	8.13	3.00	0.90	0.47	0.12
$C_{5=+}$	5.59	6.84	3.01	2.23	2.34	1.55
i-C_6	12.88	11.63	5.64	1.00	0.22	0.03
n,i$C_{6=}$	4.90	4.64	2.41	2.06	0.39	0.38
C_7	0.00	0.75	6.44	4.59	1.16	2.80

Table A - 4.10

Selectivities of n-hexane cracking as a function of temperatures at $WHSV^{-1}$(g/gh-1) = 45.5, 1 atm over 1.01g Theta-1 catalyst

Temp (oC)	180.00	200.00	250.00	300.00	350.00	400.00	450.00
CMR	0.42	1.57	#DIV/0!	28.47	73.25	148.37	192.29
P/O	2.25	1.53	0.52	0.49	0.46	0.38	0.36
iC_4/nC_4	0.41	0.33	0.00	0.19	0.11	0.08	0.11
$iC_4/iC_{4=}$	0.67	0.37	0.00	0.13	0.10	0.04	0.06
Conv.(%wt)	0.99	0.84	2.14	9.97	28.29	75.03	91.72
Selectivity(%wt)							
C_1	0.00	0.00	0.00	1.24	1.77	2.58	3.95
C_2	0.00	2.13	6.23	10.57	12.72	12.61	13.18
$C_{2=}$	2.15	1.77	3.99	5.61	9.37	13.19	20.50
C_3	19.31	20.37	19.44	19.30	17.82	14.44	12.60
$C_{3=}$	8.58	13.29	37.05	39.28	38.94	38.01	35.17
i-C_4	5.12	2.48	0.00	0.61	0.33	0.19	0.20
n-C_4	12.38	7.44	3.49	3.14	2.96	2.48	1.70
T-$C_{4=}$	4.79	2.83	3.49	3.73	2.69	3.19	1.98
1-$C_{4=}$	0.00	1.24	1.66	1.90	1.84	2.43	1.45
i-$C_{4=}$	7.59	6.73	6.48	4.57	3.43	5.24	3.37
c-$C_{4=}$	2.81	2.48	2.41	2.47	1.90	2.44	1.44
i-C_5	3.63	1.95	0.00	1.47	0.13	0.00	0.00
n-C_5	9.57	5.14	1.16	0.37	1.87	0.77	1.54
$C_{5=+}$	4.13	3.54	0.00	0.45	0.21	0.61	0.34
i-C_6	14.19	17.18	1.83	0.51	0.14	0.31	0.19
n,$iC_{6=}$	6.27	11.34	10.55	4.57	2.17	0.41	0.36
C_7	0	0	1.99	0.22	1.70	1.08	2.04

Table A - 4.11

Selectivity as a function of temperature of n-hexane cracking at $WHSV^{-1}$(g/gh-1) = 34.1, 1 atm over 1.01g Ak8-T catalyst.

Temperature (oC)	250.00	300.00	350.00	400.00	450.00
CMR	7.58		124.31	142.24	179.38
P/O	0.30	0.24	0.26	0.35	29.33
iC_4/nC_4	0.41	0.00	0.08	0.05	0.04
$iC_4/iC_{4=}$	0.25	0.00	0.04	0.02	1.22
Conversion(%wt)	1.45	5.08	15.56	36.05	47.83
Selectivity(%wt)					
C_1	0.00	1.14	1.55	2.01	10.58
C_2	3.63	6.60	8.84	11.55	37.09
$C_{2=}$	5.07	7.14	9.22	8.11	0.53
C_3	10.32	11.29	12.04	13.81	38.19
$C_{3=}$	34.51	47.68	46.11	39.34	1.30
i-C_4	1.15	0.00	0.16	0.15	0.27
n-C_4	2.77	1.59	1.94	2.81	7.57
T-$C_{4=}$	3.82	3.13	3.04	4.32	0.13
1-$C_{4=}$	1.53	1.65	1.73	2.82	0.07
i-$C_{4=}$	4.59	4.49	4.45	7.09	0.22
c-$C_{4=}$	2.10	2.16	2.09	3.25	0.16
i-C_5	1.63	0.00	0.00	0.00	0.00
n-C_5	2.58	0.00	0.00	0.00	0.09
$C_{5=+}$	1.43	1.71	1.66	2.11	0.00
i-C_6	11.85	2.87	0.46	0.05	0.92
n,$iC_{6=}$	11.28	6.11	1.84	1.00	0.88
C_7	1.53	2.47	4.89	1.58	2.01

Table A - 4.12

Selectivity as a function of temperatures of n-hexane cracking at $WHSV^{-1}$ (g/gh-1) = 34.1, 1 atm over 1.01g CR-ZSM 5 catalyst

Temperature (oC)	300.00	350.00	400.00	450.00
CMR	1.29	6.08	22.02	49.67
P/O	1.68	0.97	0.63	0.51
iC_4/nC_4	0.53	0.43	0.29	0.20
$iC_4/iC_{4=}$	1.15	0.57	0.28	0.17
Conversion(%wt)	10.80	19.78	37.24	62.12
Selectivity(%wt)				
C_1	0.25	0.79	1.52	2.24
C_2	2.07	6.03	9.62	11.48
$C_{2=}$	5.93	10.51	14.92	18.94
C_3	30.18	27.90	20.71	16.81
$C_{3=}$	17.92	28.69	33.12	33.06
i-C_4	6.38	2.85	1.18	0.66
n-C_4	12.06	6.59	4.15	3.32
T-$C_{4=}$	3.06	3.18	2.84	2.79
1-$C_{4=}$	1.13	1.29	1.42	1.34
i-$C_{4=}$	5.55	5.02	4.25	3.83
c-$C_{4=}$	2.31	2.47	2.18	2.02
i-C_5	1.44	0.43	0.12	0.04
n-C_5	2.86	0.67	0.15	0.05
$C_{5=+}$	2.90	1.83	1.17	0.95
i-C_6	2.41	0.34	0.03	0.20
n,i$C_{6=}$	1.74	1.02	1.10	0.35
C_7	1.83	0.44	1.52	1.95

Table A - 4.13

Selectivity as a function of temperatures of n-hexane cracking at WHSV (g/gh-1) =34.1, 1 atm over 1.01g A-ZSM 5 catalyst

Temperature (oC)	300.00	350.00	400.00	450.00
CMR	#DIV/0!	20.89	34.97	79.48
P/O	1.17	0.42	0.39	0.37
iC_4/nC_4	0.00	0.24	0.15	0.09
$iC_4/iC_{4=}$	0.00	0.17	0.10	0.06
Conversion(%wt)	0.89	7.24	12.22	28.69
Selectivity(%wt)				
C_1	0.00	1.34	1.51	1.97
C_2	6.92	7.52	9.07	10.66
$C_{2=}$	3.93	8.82	9.61	12.44
C_3	22.49	16.52	15.36	14.54
$C_{3=}$	19.19	39.69	39.50	38.82
i-C_4	0.00	0.85	0.58	0.32
n-C_4	5.98	3.55	3.76	3.62
T-$C_{4=}$	2.36	3.82	4.40	3.90
1-$C_{4=}$	0.00	1.20	1.51	1.54
i-$C_{4=}$	2.83	4.97	5.77	5.06
c-$C_{4=}$	2.67	2.36	2.97	2.68
i-C_5	0.00	0.61	0.22	0.06
n-C_5	3.46	0.42	0.32	0.40
$C_{5=+}$	2.20	0.96	1.13	0.84
i-C_6	18.87	2.78	1.16	0.25
n,i$C_{6=}$	9.59	2.88	1.34	0.75
C_7	0.00	1.69	1.77	2.19

Table A - 4.14

Summary of n-hexane cracking activity as a function of types of catalyst at (T= 300 °C),

Catalyst:	Ak3	Ak4	Ak5	Ak7	Ak8-P	Ak8-S	Ak4-P
100{whsv^{-1}]	10.20	8.08	9.81	9.81	6.75	9.00	10.20
Conv. (%)	1.43	1.66	3.07	5.01	2.02	2.73	3.26
CMR	5.09	2.24	4.13	3.34			
P/O	0.15	0.11	0.31	0.18			
iC_4/nC_4	1.10	2.10	0.83	2.57			
iC_5/nC_5	2.07	1.88	0.73	0.98	0.64	0.00	0.21
$iC_4/iC_{4=}$	0.00	0.00	0.00	0.00	0.00	0.00	0.00
Selectivity (wt %)							
C_1	3.27	1.64	1.73	2.46	0.00	3.19	0.58
C_2	1.33	0.78	2.41	1.31	0.00	0.00	0.00
$C_{2=}$	3.37	1.81	4.81	8.69	8.23	26.29	5.94
C_3	2.56	2.05	9.28	6.46	0.00	0.00	0.00
$C_{3=}$	17.02	18.23	30.19	36.04	8.74	15.52	6.23
i-C_4	1.56	1.89	2.17	3.74	0.00	0.00	0.00
n-C_4	1.42	0.90	2.61	1.45	0.00	0.65	0.00
T-$C_{4=}$	2.56	2.22	1.08	1.29	0.88	2.81	0.77
1-$C_{4=}$	0.81	1.56	0.54	0.59	0.71	1.08	0.60
i-$C_{4=}$	2.18	2.46	1.12	2.08	0.71	0.00	0.00
c-$C_{4=}$	0.81	1.48	0.68	0.73	0.00	1.46	0.39
i-C_5	2.75	2.46	1.73	1.96	0.38	0.00	0.34
n-C_5	1.33	1.31	2.37	2.00	0.59	1.51	1.64
$C_{5=+}$	0.00	4.27	0.00	0.00	0.00	0.00	0.00
i-C_6	1.94	4.60	6.51	4.28	11.37	4.44	7.78
n,i$C_{6=}$	15.03	23.48	12.47	8.36	13.67	4.65	23.43
C_7	42.06	29.89	20.43	18.64	54.59	38.24	52.41

REFERENCES

1. J. W. Mcbain; "The Sorption of Gases and Vapors by Solids", Rutledge and Sons, London (1932).
2. M. Richard and F. R. S Barrer; *Zeolites*, (1981), **1**, Oct. 130 – 140.
3. N. Y. Chen and T. F. Degnan; *Chemical Engineering Progress* (1988), **Feb.** 32 – 41.
4. K A. Cumming and B. W. Wojciechowski; *Catalysis Review-Sci. Eng.*, (1996) **38(1)**, 101 – 157.
5. J. Abbot and B. W. Wojciechowski; *J. Catal.*, (1987) **107**, 451.
6. J. Abbot and B. W. Wojciechowski; *J. Catal.*, (1988) **109**, 274.
7. J. Abbot and F. N. Guerzoni; *Appl. Catal.*, (1992) **85**, 173.
8. A. P. Bolton and R. L. Bojanski; *J. Catal.*, (1971) **23**, 331.
9. H. A. Benesi; *J. Catal.*, (1967) **8**, 368.
10. J. Abbot and B. W. Wojciechowski; *J. Catal.*, (1988) **113**, 353.
11. A. F. H. Wieleres, M. Vaar Kamp, and M. F. M. post; *J. Catal.*, (1991) **127**, 51.
12. D. B. Lukyanov, V. I. Shtral, and S. N. Khadzhiev; *J. Catal.*, (1994) **146**, 87.
13. D. H. Olson, W. O. Haag and R. M. Lago; *J. Catal.*, (1980) **61**, 390.
14. D. B. Lukyanov; *J. Catal.*, (1994) **145**, 54.
15. D. B. Lukyanov; *J. Catal.*, (1994) **147**, 494 – 499.

16. G. A. Olah, Y. Halpern, J. Shen, and Y. K. Mo; *J. Amer. Chem. Soc.* (a) (1973) **95**, 4960. (b) (1971) **93**, 1251.

17. D. M. Brouwer and H. Hogeveen; *Prog. Phys. Org. Chem.* (1972) **9**, 179.

18. W. O Haag, and R. M. Dessau; *Pro. 8th Int. Congr. Catal.,* Berlin, (1984) **2**, 305.

19. A. Corma, J. Planelles, J. Sanchez-Marin and F. Thomas; *J. Catal.,* (1985) **93**, 30.

20. G. Gianetto, S. Sansare and M. Guisnet; *J. Chem. Soc. Commun.* (1986) 1302.

21. B. C. Gates, J. R. Katzer, G. C. A. Schuit; "Chemistry of Catalytic Processes" McGraw-Hill New York, (1979) P.1.

22. C. L. Thomas; *Ind. Eng. Chem.* (1949) **41**, 2564.

23. B. S. Greensfelder, H. H. Voge and G. M. Good; *Ind. Eng. Chem.* (1949) **41**, 2573.

24. J. Abbot and B. W. Wojciechowski; *Canad. J. Eng.*, (1988) **66**, 825.

25. S. Jolly, J. Saussey, M. M. Bettahr, J.C. Lavalley, and E. Benazzi; *Appl. Catal. A: General* (1997) **156**, 71-96.

26. B. Sophie and M. L. Occelli; *Catal. Rev. Sci. Eng.,* (1998) **40(3)**, 329 – 407.

27. C. Klein and C. S. Hurlbut Jr; "Manual of Mineralogy", 20th Ed. John Wiley & Sons, New York (1985).

28. A. Corma; *Chem. Rev.* (1995), **95**, 559 – 614.

29. A. Corma; *Chem. Rev.* (1997), **97(6),** 2373 – 2419.

30. C. Mirodatos and D. Barthomeuf; *J. Catal.* (1985), **93**, 246.

31. W. Lowenstein; *Am. Mineral*, (1954), **39**, 92.

32. C. M. Zicovich-Wilson, A. Corma, P. Viruela; *J. Phys. Chem.* (1994), **98**, 10863 –10870.

33. J. S. Beck; USA patent 5057296, 1991;

34. C. T. Kresge, M. E. Leonowicz, W. J. Roth, J. C. Vartuli; USA patent 5098684, 1992

35. J. S. Beck, C. T. W. Chu, I. D. Johnson, C. T. Kresge, M. E. Leonowicz, W. J. Roth, J. C. Vartuli, USA patent 5108725. 1992.

36. J. S. Beck, J. C. Vartuli, J. W. Roth, M. E. Leonowicz, C. T. Kresge, K. D. Schmitt, Chu C. T. U, Oslon D. H, Sheppard E. W, McCullen S. B, Higgins J. B, and J. L. Schlenker; *J. Am. Chem. Soc.* (1992), **114**, 10834 - 10843.

37. J. S. Beck, C. T. Kresge, M. E. Leonowicz, W. J. Roth, J. C. Vartuli; *Nature* (1992), **359**, 710 – 712.

38. J. C. Vartuli, J. W. Roth, M. E. Leonowicz, C. T. Kresge, K. D. Schmitt, C. T. W. Chu, E. W Sheppard, S. B. McCullen; *Chem. Mater.* (1994), **6**, 2070.

39. J. S. Beck, G. J. Kennedy, C. T. Kresge, S. E. Schramm, W. J. Roth, J. C. Vartuli; *Chem. Mater.* (1994), **6**, 1816.

40. J. C. Vartuli, J. W. Roth, M. E. Leonowicz, C. T. Kresge, K. D. Schmitt, C. T. W. Chu, D. H. Olson, S. B. McCullen, S. D. Hellring, J. S. Beck, J. L. Schlenker, E. W. Sheppard; *Stud. Surf. Sci. Catal.* (1994), **84**, 53.

41. J. R. Anderson, K. Foger, T. Mole, R. A. Rajadhaksha, J. V. Sunders; *J. Catal.*, (1979) **58**, 114.

42. R. Szostack; "Molecular Sieves, Principles of Synthesis and Identification", Van Norstrand Reinhold, New York, 1989.

43. J. B. Uytterhoeven, L. G. Cristner and W. K. Hall; *J. Phys. Chem.,* (1965) **69**, 2117.

44. C. T. Chu and C. D. Chang; *J. Phys. Chem.,* (1985*)* **89**, 1569.

45. J. B. Uytterhoeven, P. A. Jacob, K. Mackay, and R. Schounheydt; *J. Phys. Chem.,* (1968) **72**, 1768.

46. W.O Haag, R. M. Lago and P. B. Weisz; *Nature* (1984) **309**, 589.

47. V. S. Nayak, and V. R. Chouldhary; *Appl. Catal. A: General* (1984) **10**, 137.

48. V. B. Kazansky; "Catalysis and Adsorption by Zeolites" G. Ohlmann et al., Elservier, Amsterdam (1991) p.117.

49. J. W. Ward; *J. Catal.,* (1971) **22**, 237.

50. M. B. Sayed, R. P. Cooney; *Aust. Chem.,* (1982) **35**, 2483.

51. M. B. Sayed, R. A. Kydd and R. P. Cooney; *J. Catal.,* (1984) **88**, 137.

52. B. W. Wojciechowski; *Catal. Rev. Sci. Eng.*, (1998) **40(3)**, 209 – 328.

53. F. H. Gayer; *Ind. Eng. Chem.*, (1933) **25**, 1122.

54. F. C. Whitmore; *Ind. Eng. Chem.*, (1934) **26**, 94.

55. R. C. Hansford; *Ind. Eng. Chem.*, (1947) **39**, 1122.

56. B. S. GreensFelder; *Ind. Eng. Chem.,* (1949) **41**, 1122.

57. C. L. Thomas; *Ind. Eng. Chem.,* (1949) **41**, 2564.

58. R. C. Hansford; "Development of the Theory of Catalytic Cracking", *ACS symposium series* No. **222**, American Chemical Society, Washington DC, 1983, p. 252.

59. V. Y. Borovkov, A. A. Alexeev and V. B. J. Kazansy; *J. Catal.,* (1983) **80**, 462.

60. A. Kogelbauer and J. A. Lercher; *J. Catal.,* (1990) **125**, 197.

61. H. A. Benesi and B. H. C. Winquist; *Adv. Catal.,* (1978) **27**, 97.

62. M. Lefrancois and G. malbois; *J. Catal.,* (1971) **20**, 350.

63. G. A. Olah; *J. Amer. Chem. Soc.,* (1977) **99**, 4379.

64. G. A. Olah, G. K. S. Prakash and J. Sommer; "Superacids" Wiley, New York, 1985.

65. G. A. Olah; *J. Amer. Chem. Soc.,* (1967) **89**, 2227.

66. G. A. Olah; *J. Amer. Chem. Soc.,* (1972) **94**, 808.

67. G. A. Olah, P. R. Clifford, Y. Halpern, and J. Johanson; *J. Amer. Chem. Soc.,* (1971) **93**, 4219.

68. Y. V. Kissin; *J. Catal.,* (1990) **126**, 600.

69. B. S. GreensFelder, H. H. Voge, and G. M. Goode; *Ind. Eng. Chem.,* (1949) **41**, 2572.

70. G. M. Mclellan, R. F. Howe, L. M. Parker, and D. M. Bibby; *J. Catal.,* (1986) **99**, 486.

71. G. A. Olah, P. V. R. Schleyer, and H. P. Leftin; *Carbonium ions*, Wiley Interscience, New York, (1968) **1**, 353.

72. G. Kortrum, J. Vogel, and W. Braum; *Angew. Chem.* (1958) **70**, 651.

73. H. P. Leftin and P. H. Hermana; *Proc. 3rd. Intern. Congr. Catalysis*, Amsterdam, North – Holland, New York (1965), p. 1064.

74. H. P. Leftin; *J. Phys. Chem.,* (1960) **64**, 1714.

75. R. G. Haldeman and P. H. Emmett; *J. Amer. Chem. Soc.,* (1956) **78**, 2917.

76. W. O. Haag, R. M. Lago, and P. B. Weisz; *Faraday Discuss. Chem. Soc.,* (1981) **72**, 317.

77. U. S. Patent, 3.702.886 to Mobil Oil (1972).

78. V. J. Frillette, W. O. Haag, and R. M. Lago; *J. Catal.,* (1981) **67**, 218.

79. M. Busio, J. Janchen, and J. H. C. Van Hooff; *Microporous Mater.,* (1995) 211.

80. W. O. Haag, R. M. Lago, and R. M. Dessau in: "Chemistry of Microporous Materials". *Stud. Surf. Sci. Catal.,* (1991) **60**, 255.

81. V. B. Kanzansky, M. V. Frash, R. A. Van Santen; *Catal. Lett.* (1994) **28**, 211.

82. S. R. Blaszkowski and R. A. Van Santen; *Topics Catal.*, (1997) **4**, 145.

83. B. A. Williams, S. M. Babitz, J. T. Miller, R. Q. Snurr and H. H. Kung; *Appl. Catal. A*, (1999) in press.

84. B. A. Williams, S. M. Babitz, J. T. Miller, R. Q. Snurr, W. O. Haag and H. H. Kung; *Appl. Catal. A*, (1999) **179**, 71 – 86.

85. L. A. Pine, P. J. Maher, and W. A. Wachter; *J. Catal.,* (1984) **85**, 466

86. G. Giannetto, S. Sansare, and M. Guisnet; *J. Chem. Soc., Chem. Commun.,* (1986) 1302.

87. A. Corma, M. Faraldos, A. Martinez, and A. Mifsud; *J. Catal.,* (1990) **122**, 230

88. D. B. Lukyanov; *Zeolites* (1991) **11**, 325

89. A. Corma, P. J. Miguel, and A. V. Orchilles; *J. Catal.,* (1994) **145**, 171

90. Y. Zhao, G. R. Bamwenda, and B. W. Wojciechowski; *J. Catal.,* (1993) **140**, 243

91. A. Corma, M. S. Grande, V. Gonzalez-Alfaro, and A. V. Orchilles; *J. of Catal.,* (1996) **159**, 375 - 382.

92. B. W. Wojciechowski; *Can. J. Chem. Eng.,* (1968) **46**, 48.

93. E. A Lombardo, T. R. Gaffney and K. W Hall; *Proceedings 9th Int. Conf. Catal.*. Calgary, (1988) **1**, 412.

94. E. G. Derouane, J. M. Andre and A. A. Lucas; *J. Catal.* (1988) **110**, 58.

95. E. G. Derouane; *J. Catal.* (1986) **100**, 541.

96. R. Beaumont and D. Barthomeuf; *J. Catal.,* (1972) **26**, 218.

97. P. O. Fritz and J. H. Lundsford; *J. Catal.,* (1989) **118**, 85.

98. T. F. Narbeshuber, H. Vinek and J. A. Lercher; J. Catal., (1995) **157**, 388

99. V. G. Malkin, V. V. Chesnokov, E. A. Paukshtis and G. M. Zhidomorov; J. Am. Chem. Soc., (1990) **112**, 666

100. M. Hunger, U. Schenk, M. Breuninger, R. Glaser and J. Weitkamp; *Microporous and Mesoporous Materials.,* (1999) **27** (2-3), 261 - 271

VITAE

In August 1991, I graduated from the University of Jos, Plateau state, Nigeria with a Bachelor of Science Honors degree in Chemistry and served as a Corp Liaison Officer, with Anka Local Government Area Council, Sokoto state on National Service in 1992. Between October 1992 to December 1995, I taught chemistry as a part-time instructor in the Air force Military School, Center for continue Education Plateau Polythenic, Government Secondary school Anglo-Jos, all in Jos, Plateau state, Nigeria. I served as a Quality Control Officer at Grand Cereal and Oil Mills Limited, a division of UAC Nigeria, from June 1994 to June 1997. I joined the Department of Chemistry, King Fahd University of Petroleum and Minerals as a graduate student on Research Assistantship in June 1997. The successful defense of this thesis in December 1999 earns me a Master of Science degree in Chemistry.